

1968

The effect of midspan diaphragms on load distribution in a prestressed concrete box-beam bridge - philadelphia bridge, June 1968

C. S. Lin

D. A. VanHorn

Follow this and additional works at: <http://preserve.lehigh.edu/engr-civil-environmental-fritz-lab-reports>

Recommended Citation

Lin, C. S. and VanHorn, D. A., "The effect of midspan diaphragms on load distribution in a prestressed concrete box-beam bridge - philadelphia bridge, June 1968" (1968). *Fritz Laboratory Reports*. Paper 232.
<http://preserve.lehigh.edu/engr-civil-environmental-fritz-lab-reports/232>

This Technical Report is brought to you for free and open access by the Civil and Environmental Engineering at Lehigh Preserve. It has been accepted for inclusion in Fritz Laboratory Reports by an authorized administrator of Lehigh Preserve. For more information, please contact preserve@lehigh.edu.

345.6
232.



Prestressed Concrete Box-Beam Bridges

Progress Report No. 5

**THE EFFECT OF MIDSPAN
DIAPHRAGMS ON LOAD DISTRIBUTION
IN A PRESTRESSED CONCRETE
BOX-BEAM BRIDGE**

PHILADELPHIA BRIDGE

FRITZ ENGINEERING
LABORATORY LIBRARY

by
Cheng-shung Lin
David A. VanHorn

Fritz Engineering Laboratory Report No. 315.6

U
N
I
V
E
R
S
I
T
Y
O
F
P
E
N
N
S
Y
L
V
A
N
I
A

I
N
S
T
I
T
U
T
E
O
F
R
E
S
E
A
R
C
H

Project 315

LATERAL DISTRIBUTION OF LOAD
IN PRESTRESSED CONCRETE BOX-BEAM BRIDGES

Progress Reports Completed to Date

Progress
Report No.

- 1 LATERAL DISTRIBUTION OF STATIC LOADS IN A PRE-STRESSED CONCRETE BOX-BEAM BRIDGE - DREHERSVILLE BRIDGE. Douglas, W. J. and VanHorn, D. A., F. L. Report 315.1, August 1966
- 2 LATERAL DISTRIBUTION OF DYNAMIC LOADS IN A PRE-STRESSED CONCRETE BOX-BEAM BRIDGE - DREHERSVILLE BRIDGE. Guilford, A. A. and VanHorn, D. A., F. L. Report 315.2, February 1967
- 3 STRUCTURAL RESPONSE OF A 45° SKEW PRESTRESSED CONCRETE BOX-GIRDER HIGHWAY BRIDGE SUBJECTED TO VEHICULAR LOADING - BROOKVILLE BRIDGE. Schaffer, Thomas and VanHorn, D. A., F. L. Report 315.5, October 1967
- 4 LATERAL DISTRIBUTION OF VEHICULAR LOADS IN A PRE-STRESSED CONCRETE BOX-BEAM BRIDGE - BERWICK BRIDGE. Guilford, A. A. and VanHorn, D. A., F. L. Report 315.4, October 1967
- 5 THE EFFECT OF MIDSPAN DIAPHRAGMS ON LOAD DISTRIBUTION IN A PRESTRESSED CONCRETE BOX-BEAM BRIDGE - PHILADELPHIA BRIDGE. Lin, Cheng-shung and VanHorn, D. A., F. L. Report 315.6, June 1968

THE EFFECT OF MIDSPAN
DIAPHRAGMS ON LOAD DISTRIBUTION
IN A PRESTRESSED CONCRETE BOX-BEAM BRIDGE
PHILADELPHIA BRIDGE

by

Cheng-shung Lin

David A. VanHorn

This work was conducted as part of the project Lateral Distribution of Load for Bridges Constructed with Prestressed Concrete Box-Beams, sponsored by the Pennsylvania Department of Highways, the U. S. Bureau of Public Roads, and the Reinforced Concrete Research Council. The opinions, findings, and conclusions expressed in this report are those of the authors, and not necessarily those of the sponsors.

Fritz Engineering Laboratory
Department of Civil Engineering
Lehigh University
Bethlehem, Pennsylvania

June 1968

Fritz Engineering Laboratory Report No. 315.6

TABLE OF CONTENTS

	<u>page</u>
ABSTRACT	1
1. INTRODUCTION	3
1.1 Background	3
1.2 Previous Research	5
2. TESTING	7
2.1 Test Bridge	7
2.2 Gage Sections and Locations	8
2.3 Loading Lanes	9
2.4 Timing and Position Indicators	10
2.5 Test Runs	10
3. DATA REDUCTION AND EVALUATION	11
3.1 Oscillograph Trace Reading	11
3.2 Evaluation of Oscillograph Data	12
3.2.1 Strains and Deflections	12
3.2.2 Neutral Axes, Effective Widths, Moment Coefficients, and Dis- tribution Coefficients	13
3.2.3 Distribution Factors	15
4. PRESENTATION OF TEST RESULTS	17
4.1 Moment Coefficients	17
4.2 Distribution Coefficients	17
4.3 Distribution Factors	18
4.4 Design and Experimental Live Load Moments	18

	<u>page</u>
4.5 Girder Deflections and Rotations	18
4.6 Neutral Axes and Transformed Effective Slab Widths	19
5. DISCUSSION OF RESULTS	20
5.1 Distribution Coefficients	20
5.2 Distribution Factors	21
5.3 Comparison of Design and Experimental Live Load Moments	22
5.4 Girder Deflections and Rotations	23
5.5 Strains, Neutral Axes, and Transformed Effective Slab Widths	23
5.6 Comparison of Test Results and Guyon-Massonnet Load Distribution Theory	25
6. SUMMARY AND CONCLUSIONS	28
6.1 Summary	28
6.2 Conclusions	30
7. ACKNOWLEDGMENTS	32
8. APPENDIX	34
8.1 Instrumentation	34
8.2 Test Vehicle	35
9. TABLES	36
10. FIGURES	55
11. REFERENCES	99

ABSTRACT

This report describes the field testing of an existing beam-slab bridge constructed with prestressed concrete spread box girders. The main purpose of this study was to experimentally investigate the effect of midspan diaphragms on distribution of vehicular loads to each of the longitudinal beams. The bridge was tested first with the diaphragms in place, and then again after the diaphragms had been removed.

It was found that the midspan diaphragms did transmit load laterally. The distribution coefficients and deflections for girders directly under the vehicular loads were slightly reduced by the use of the diaphragms, when the bridge was loaded with one truck. However, owing to the compensating effects when several lanes were loaded simultaneously, the distribution factors were not appreciably affected by the use of the diaphragms. It was also found that the experimentally determined distribution factors for interior girders were considerably less than the PDH design values, while for exterior girders, the experimental values were greater than the design values.

The effect of girder spacing was studied by comparing the test results with those from the study of another bridge of similar construction (Dreherstown Bridge - 1965). In addition, an evaluation of the applicability of the Guyon-Massonnet load distribution theory was investigated by comparing the results with the values predicted by the theory.

1. INTRODUCTION

1.1 Background

The first prestressed concrete bridge in the United States, the Walnut Lane Bridge in Philadelphia, was constructed in 1950. Since that time has come a succession of improvements and new concepts that make the growth of this type of bridge possible. One of the most recent developments was the design of the spread box girder bridges, in which the box girders are spread apart and act compositely with the slab as T-beams.

For the spread box girder bridges, current design procedures adopted by the Pennsylvania Department of Highways are presented in the PDH Bridge Division Standards ST-200 through ST-208.¹ These standards specify the use of a live load distribution factor of $S/5.5$ for interior beams, where S is the average girder spacing in feet. This factor is identical to that given in the AASHO Specifications,² Section 3, governing the distribution of wheel loads to interior steel I-beam stringers and prestressed concrete girders, topped with a concrete floor. The distribution of live load for the exterior beams is based on the assumption that the slab acts as a simple span between girders, in transmitting wheel loads laterally. This

procedure, which is identical to that set forth in the AASHO Specifications, is believed to be overly conservative.

In 1964, the Structural Concrete Division of the Fritz Laboratory, Department of Civil Engineering, at Lehigh University, initiated a research project to investigate the actual structural behavior of bridges of the spread box-beam type, and to develop design procedure which reflects the actual behavior.⁷

The overall investigation consists of the field testing of five existing bridges, and a related analytical study. In the summer of 1964, the first bridge was tested to serve as a pilot study. Three bridges were tested in the summer of 1965 to study the effects of beam width and skew. Finally, during August 1966, a fifth bridge was tested, particularly in order to study the effect of the midspan diaphragms. All of the experimental data from these five bridges will be used in the development of a method of analysis.^{3, 4, 5, 6}

The use and the effect of midspan diaphragms in highway bridges is a somewhat controversial subject. Their function is generally believed to aid in the lateral distribution of load, and hence, to reduce the deflections and maximum moment carried by each individual beam. Current practice, as stated in the PDH Bridge Division Standards,¹ specifies the use of intermediate

diaphragms for spread box-beam bridges with spans of over 45 feet. Similar requirements are stated in the AASHO Specifications² for other types of concrete bridges. Neither of the two specifications provide for revision of load distribution factors when diaphragms are used.

The purpose of the Philadelphia Bridge study was to experimentally investigate the effect of midspan diaphragms on load distribution. The bridge was first tested with diaphragms in place, and then the same tests were repeated after the diaphragms had been removed. This report describes the results of these field tests.

1.2 Previous Research

Much of the description of the previous field work was covered in Reports No. 315.1,³ 315.2,⁴ 315.4,⁵ and 315.5.⁶ Nearly all of the previous work contributed in some way to the planning of the field tests conducted by Lehigh University. The testing procedures adopted in the test of the Philadelphia Bridge were based on the following findings found in the Dreher-ville Bridge studies:³

1. At least four strain gages should be applied to each face of the girder, so that the location of the neutral axis can be accurately established.

2. For testing at crawl speed, the superimposing of single truck loading to determine the effects of multi-truck loading is a valid procedure.
3. For a symmetrical cross-section, the strain measurements taken with half of the girders gaged can be combined to accurately represent measurements taken with all girders gaged.

2. TESTING

2.1 Test Bridge

A bridge under construction near Philadelphia was selected so that joints between the diaphragms and slab could be fabricated to enable diaphragm removal without damage to the slab. This bridge, located on Bristol Road (Legislative Route 09006), crossed over U.S. 1, which is Legislative Route 281 PAR. The middle span of the three-span bridge, as illustrated in Fig. 1, was chosen as the test span. The test span was simply supported with a length of 71 feet, 9 inches, center-to-center of bearings. The skew was 87° .

The cross-section of the bridge, as shown in Fig. 2, consists of five identical pre-cast prestressed hollow box girders, covered with a cast-in-place reinforced concrete deck. The five box girders, which are 48 inches wide and 42 inches deep, are equally spaced at 9 feet, 6 inches, center-to-center. Cast-in-place concrete diaphragms were initially placed between the beams at the ends of the span and at midspan. The diaphragms were 10 inches in thickness, while the end diaphragms were 12 inches. The reinforced concrete deck provides a roadway 40 feet in width. The specified minimum thickness

of the slab was 7-1/2 inches. However, measurements taken near midspan showed that actual slab thickness varies from 8.4 to 10.3 inches, with an average of 9.2 inches. The safety curb consists of a 15-in. wide parapet on top of a 33-in. wide curb section. The joint between the slab and the curb was a construction joint with a raked finish. Vertical reinforcement for the curb section extended through the joint into the slab. Further typical details are given in the PDH Bridge Division Standards for prestressed concrete bridges.¹

The girders were designed for AASHO HS 20-44 loading. A distribution factor of $S/5.5 = 1.727$ was used for the interior girders, while the factor of 1.158 was used for the exterior girders. The impact factor was 0.255. The specified minimum 28-day cylinder strength of the girder concrete was 5500 psi. Each of the girders was pre-tensioned with 52-7/16-in. seven-wire strands.

2.2 Gage Sections and Locations

A cross-section, located 3.55 feet east of midspan, was selected for strain gage application. Theoretically, maximum girder moments would occur at this section as the drive axle passed over the section with the load vehicle moving eastward.

Deflectometers were installed either at the above-mentioned maximum moment section, or at the east end of the test span.

As shown in Fig. 5, four strain gages were applied on each side of each gaged girder. One was located at the bottom face, and the others were installed 6 inches, 15 inches, and 40 inches, respectively from the bottom face of the beam. Of the five girders, only Girders A, B, and C were gaged as shown in Fig. 5.

One pair of deflection gages was applied at the edges of the bottom face of each gaged beam. The deflectometers at the east end were clamped close to the pier cap face, with sufficient clearance to allow for anchor wires.

2.3 Loading Lanes

Seven loading lanes were located on the roadway such that the centerline of the truck would coincide with a girder centerline, or a centerline of the girder spacing. As shown in Fig. 2, the centerlines of the loading lanes were spaced at 57 inches. When the vehicle was running in the two outer lanes, (Nos. 1 and 7), the centerline of a wheel group was located 31.5 inches from the curb face.

2.4 Timing and Position Indicators

Three air hoses were used as position indicators. They were placed at the test section, 40 feet east of the test section, and at the west end of the middle span, respectively. The distances were measured along the roadway centerline, and the hoses were placed normal to that centerline. An abrupt offset from the oscillograph trace was produced as each axle passed over one of these hoses. The offsets were then used to correlate the truck position with strain values in the data reduction. A pair of timer hoses, 100 feet apart, was used to monitor the speed of the testing vehicle. A timer was actuated as the front axle of an approaching vehicle passed over one of the timer hoses, and was shut off as the front axle passed over the other hose.

2.5 Test Runs

A total of 63 test runs were conducted. Crawl runs at a speed of 2 to 3 mph were considered to represent the static loading condition. As listed in Table 1, these test runs were divided into eight sets. Each set corresponded to a different combination of three factors: direction, diaphragm existence, and location of deflectometers. Before and after each set of test runs, the gages were calibrated with no load on the bridge to relate the deviation of the oscillograph traces to base values. Twelve separate calibrations were made.

3. DATA REDUCTION AND EVALUATION

3.1 Oscillograph Trace Reading

To begin with, the trace numbers, each of which represented a specific strain gage, were correlated with the traces on the test record. The correlation was achieved by observing the relative position of trace breaks on the sixteen active gage traces and two inactive reference traces on each of the three oscillograph records from each test run. This procedure of identifying the traces on the oscillograph records was termed editing.

After the editing was completed, the calibration values were read. The trace deviations due to added resistances in the Wheatstone bridge circuits with no truck on the bridge are the calibration values. These values were measured with an accuracy of 0.01 inch from the oscillograph traces of the calibration runs. For some gages, the calibration values varied slightly during a series of test runs. In those instances, the average of calibration values immediately preceding and following the test runs was used.

After determining the calibration values, the trace amplitudes of the actual test runs were evaluated. No-load

readings at the left side of the record were taken. Also taken were load readings corresponding to the drive axle passing over the test section. The vehicle position was vividly indicated by the offset from the oscillograph trace caused as the drive axle hit the air hose at the test section. All of the measurements of these trace readings were made with an accuracy of 0.01 inch.

3.2 Evaluation of Oscillograph Data

3.2.1 Strains and Deflections

In order to convert oscillograph trace readings to strains and deflections, a WIZ computer program, used with a GE 225 computer, was written to determine strain coefficients. The program input consisted of gage resistance, gage factor, lead cable length correction factor, operation attenuation, and calibration attenuation. Strains and deflections were calculated by another WIZ program which required strain coefficients, calibration values, load trace readings, no-load trace readings, and deflection multipliers as input. The output of the computer, consisting of strains and deflections, was listed on a prepared cross-section of the bridge, so that sizable errors could be easily recognized.

With four strains obtained for each girder face, a WIZ program was written to plot the strains along each girder face. Then, a straight line was drawn through the strain points to pinpoint poor strain readings. Consistent linear strain distribution was found, while very few poor strain readings were discarded in the later calculation of neutral axes.

3.2.2 Neutral Axes, Effective Widths, Moment Coefficients and Distribution Coefficients

A comprehensive computer program, evolved from programs used for the Dreherstown Bridge,³ was used to evaluate neutral axes, effective slab widths, moment coefficients, and distribution coefficients in one operation. The input of the computer program consisted primarily of the number of data points to be used, the strain for each gage point, the vertical location of the gage on the girder face, constants, and dimensions of the cross-section.

In the first step, a linear strain distribution along each girder face was fitted by the method of least squares. Neutral axes and the fiber strains at the bottom surfaces of the girders were calculated on the basis of the fitted linear strain distributions. With the neutral axes determined, the computer program then calculated effective widths of slab, curb,

and parapet by equating the first moments of the compression area and the tension area thereby balancing the compressive and tensile forces. Then, using the previously computed bottom fiber strain, the moment carried by each of the girders could be calculated in terms of the modulus of elasticity of the concrete. The moment coefficient, which was equal to the moment divided by the modulus of elasticity, was used to represent the moment carried by each girder. In these calculations, full composite behavior between the girder, slab, curb, and parapet was assumed. In the case of the exterior girder, the effective width of the adjacent interior beam extended beyond the midway point between the girders, the maximum effective slab width for the exterior beam was the portion of the slab left above the exterior girder; otherwise, it was limited to half the distance between the girder centerlines.

The last step of the computer program was to determine the percentage of total resisting moment distributed to each girder. The distribution coefficient of a girder was equal to the moment coefficient for that girder divided by the sum of the moment coefficient for all five girders, while the test vehicle ran in a particular lane. Since only Girders A, B, and C were gaged, moment coefficients for Girders D and E were taken as values from Girders A and B when the truck was located in a

symmetric lane on the opposite side of the bridge. For instance, the moment coefficients in Girders C, D, and E with the truck running in Lane 1 were equivalent to the moment coefficients in Girders C, B, and A, respectively, with the truck running in Lane 7. A detailed description of the computer program is included in Fritz Engineering Laboratory Report No. 315.5.⁶

The effective values of modulus of elasticity were obtained by equating the externally applied moment to the internal resisting moment at the cross-section.

3.2.3 Distribution Factors

Lateral load distribution provided in the AASHO Specification² is expressed in terms of distribution factors. The distribution factor is defined as the fraction of a line of wheel loads applied to a girder in calculating the live load bending moment. The AASHO Specifications also specify that for the design of girders, the centerline of a wheel or wheel group shall be assumed to be at least 24 inches from the face of the curb. Moreover, the Specifications state that the lane loadings, or standard trucks, shall be assumed to occupy any position within their individual design traffic lane which will produce the maximum stress. In order to make the experimental load distribution comparable with the AASHO provisions, distribution

coefficients with the test truck in various test lanes were superimposed to approximate the specified design loading. The roadway of 40 feet of the test bridge was designed for three traffic lanes, each having a width of 13 feet 4 inches. Therefore, a close approximation of the AASHO design loading was produced when the trucks were located in Lanes 1, 4, and 7. The experimental distribution factor for a girder was obtained by summing the distribution coefficients for that girder with the truck in Lanes 1, 4, and 7, and multiplying by two, since distribution factors are given in terms of wheel loads rather than axle loads.

4. PRESENTATION OF TEST RESULTS

4.1 Moment Coefficients

The moment coefficients are presented in Table 2. Each set of the values is headed by loading keys consisting of a diagram showing truck location and direction. These loading keys are widely used in the succeeding presentation of test results. Each of the moment coefficients represents the moment coefficient carried by a particular girder for the designated load lane with the truck location and direction shown by the loading key. Average values of two or three sets of test runs are used. An experimental value for the modulus of elasticity for each loading lane was determined by dividing the theoretical total moment by the summation of moment coefficients.

4.2 Distribution Coefficients

Distribution coefficients, which are defined as the percentages of total resisting moment distributed to individual girders, are presented in Table 3 and Fig. 7-20. Table 3 lists the distribution coefficients for the truck traveling in either direction with the diaphragms in place or removed. To illustrate the effect of diaphragms on distribution

coefficients, these values are plotted in Figs. 7 through 14. Load lane, truck position, and direction of travel are indicated by the loading key. Figures 15 through 20 are influence lines for the distribution coefficients. Each curve shows the distribution coefficients for a particular girder with the truck in various load lanes.

4.3 Distribution Factors

Distribution factors were determined as explained in Section 3.2.3. The experimental distribution factors for the bridge with and without diaphragms, as well as PDH design values, are tabulated in Tables 5 and 6, for eastbound and westbound runs, respectively. In the last two columns, the ratios of experimental value divided by design value are given.

4.4 Design and Experimental Live Load Moments

A vivid comparison of the design and experimental moments is shown in Figs. 21 and 22 for eastbound runs and westbound runs, respectively.

4.5 Girder Deflections and Rotations

Girder deflections at the test section are listed in Tables 9 and 10. Deflections at the end of the span are listed

in Tables 11 and 12. Since only Girders A, B, and C were gaged, deflections for Girders D and E were obtained as deflections for A and B when the truck was located in a symmetric lane on the opposite side of the bridge. Similar procedures have been used in finding moment coefficients, as explained in Section 3.2.2. Deflections are also plotted in Figs. 23 through 27. Figure 23 is intended to show the relative magnitudes of the deflections at the end as compared with the deflections at the test section. Figures 24 through 27 show the comparisons of deflections with and without diaphragms. Girder rotations are tabulated in Tables 13 through 16.

4.6 Neutral Axes and Transformed Effective Slab Widths

Figure 28 shows typical examples of neutral axis location for various lane loadings. Tables 17 and 18 list transformed effective slab widths, which are average values of two or three similar test runs. The effective width of 102 inches, which often appears in the values for the exterior girder, is the maximum slab width available. The effective slab width for the interior girders, in line with the provisions of the AASHO Specifications, is 114 inches.

5. DISCUSSION OF RESULTS

5.1 Distribution Coefficients

Referring to Figs. 7 through 14, comparisons of distribution coefficients with and without diaphragms indicated that the midspan diaphragms did have an effect on the lateral transmission of single-vehicle loads. As would be expected, load distribution was more uniform with diaphragms than without diaphragms. However, the actual variation between the distribution coefficients was relatively small for cases with and without diaphragms.

In Figs. 15 through 20, influence lines for distribution coefficients are compared for cases with and without diaphragms. It was observed that with diaphragms, influence lines were less fluctuating than in the case without diaphragms. This also indicated the load distribution effect of the diaphragms.

The total external moment at the test section was greater with the truck traveling eastward than with the truck traveling westward. Comparisons of distribution coefficients for the eastbound runs and westbound runs showed that the distributions of load for the former were slightly less uniform than for the latter.

5.2 Distribution Factors

As shown in Table 4, the experimental distribution factors with and without diaphragms appear to be extremely close. This phenomenon resulted from the compensation of the effects of diaphragms when loads in three test lanes were superimposed. The design values are also listed in Tables 4 and 5. It is observed that the design value for the interior girders is substantially greater than the experimental values, whereas the design value for the exterior girders is less than the experimental values. Consequently, it appears that the design value for the interior girders is considerably over-conservative. However, the exterior beams are by no means under-designed, since in the design procedure, the extra strength contributed by the curbs and parapets is not considered.

By comparing the results of the Dreherstown³ and Philadelphia bridges, the effect of girder spacing can be examined. The Dreherstown Bridge also consists of five identical box-girders, equally spaced at 7 feet 2 inches. A comparison of distribution factors for these two bridges is shown in Table 8. The ratios of experimental distribution factor to design values for interior girders are reasonably close for the two bridges. This indicates that the current design method for interior girders reasonably reflects the influence of girder spacing. However,

there is a considerable variation in the ratios for the exterior girders. Therefore, the design method for estimating distribution factors for exterior girders does not reflect the actual behavior.

5.3 Comparison of Design and Experimental Live Load Moments

A comparison of the design and experimental live load moments is shown in Figs. 21 and 22. It is clearly shown in Fig. 21 that the effects of the diaphragms on girder moments were compensating when truck loads in Lanes 1, 4, and 7 were superimposed. Consequently, extremely close experimental live load moments were obtained for the bridge with and without mid-span diaphragms. Therefore, it appears that the use of diaphragms is not necessary.

For exterior girders, the ratio of experimental moment to design moment is greater than one. This does not mean that the girders were over-stressed under design loading since the strength contributed by the curbs and parapets was not considered in the design of exterior girders. For the interior girders, the ratios range from 0.657 to 0.672, which consistently indicate that the interior girder is over-designed.

5.4 Girder Deflections and Rotations

Girder deflections were quite small. The maximum deflection measured at the test section was only 0.115 inch, while the maximum deflection measured at the end was 0.0117 inch. The deflections at the end were very small in comparison with the deflections at the test section, as shown in Fig. 23. Figures 24 through 27 show that deflections, both at the test section and at the end, for girders directly under the truck load, were slightly reduced by the use of the midspan diaphragms.

Girder rotations at the test section were extremely small; the rotations at the end were even smaller. A comparison of the girder rotations with and without diaphragms indicates that the rotations were affected by the use of diaphragms, but no apparent definite increase or decrease can be observed.

5.5 Strains, Neutral Axes, and Transformed Effective Slab Widths

Plots of strains along the side faces of interior girders consistently indicated a linear relationship of strains along the girder faces and into the deck. Figure 29 is a typical example of the plots. Similar plots for the exterior girders showed that the linear strain relationship also existed along the girder faces and up to the curb sections, while relatively

low strains were found in the parapets. Figure 30 is a representative plot of the strains for the exterior girder. It is concluded that full composite action existed between the girder, slab, and curb; while only partial composite action occurred between the curb and the parapet.

Figure 28 shows typical examples of neutral axis locations for various lane loadings. It was found that the neutral axis of the girder tended to incline when the load was not applied directly above the girder. The inclination of the neutral axis indicated the occurrence of biaxial bending in the girders. The vertical location of the neutral axes with respect to the bottom girder face also shifted slightly. In general, the location was highest when the truck was positioned directly above the girder, and progressively lower as the truck transferred to lanes farther away from the girder.

Tables 17 and 18 list transformed effective slab widths. The values listed are averages of two or three identical runs. There is some variation between identical runs, especially when the girder strains are small. The variation is primarily due to the sensitivity of the computed effective slab width to small changes in neutral axis location, and the neutral axis location cannot be accurately computed when the girder strains are relatively small. Fortunately, moment

coefficients are in good agreement for identical runs. This indicates that the moment coefficients are relatively insensitive to the variation of transformed effective slab widths.

5.6 Comparison of Test Results and Guyon-Massonnet Load Distribution Theory

One of the best known analytical methods for beam-slab type and grid type bridges is the Guyon-Massonnet method. The method was first developed by M. Y. Guyon¹⁰ for the case of zero torsional stiffness of the supporting members, and was further developed and extended to the case of torsionally stiff members by C. Massonnet.^{11,12} In order to evaluate the applicability of this method to the spread box-girder type of bridges, a comparison was made between the Guyon-Massonnet theory and the test results.

The theory is based on the following two assumptions:

1. The actual bridge may be replaced by an equivalent orthotropic plate which has the same average flexural and torsional stiffness as the actual bridge.
2. The actual wheel loads are assumed to be distributed sinusoidally along the length of the bridge. Massonnet reasons that this loading is more representative of the actual distribution of truck wheel loads arranged on the bridge to produce

maximum moment, than would be either uniform loading or concentrated loads. Owing to these assumptions, the method yields the same distribution coefficients for bending moments and deflections in the longitudinal girders. A detailed description of the theory is contained in Refs. 7, 8, and 9.

In this report, the theoretical distribution coefficients are compared with experimental distribution coefficients for both moments and deflections. The distribution coefficient for moments has been defined in Section 3.2.2. The distribution coefficient for deflections is analogously defined as the ratio of the vertical deflection of a girder to the sum of the deflections of all five girders. Two difficulties were encountered in applying the theory to the Philadelphia Bridge. First, the effect of the curbs and parapets was difficult to take into account. Second, the effective slab width for the midspan diaphragms could not be accurately estimated. In the calculations included in this report, the curb and parapet effect is considered only in determining the effective bridge width. In the Berwick Bridge study,⁵ strains measured in the diaphragms indicated that the neutral axes of the midspan diaphragms varied around the vicinity of the joints between the diaphragms and the slab. Therefore, the effective slab width for the diaphragms was estimated by assuming

that the neutral axis was located at the joint. In addition, other effective slab widths for the diaphragms were assumed. It was found that the resulting distribution coefficients were relatively insensitive to the effective slab width assumed.

The calculated distribution coefficients and distribution factors by the Guyon-Massonnet theory are listed in Tables 4 and 7, respectively. A comparison of experimentally determined distribution coefficients with the theoretical values is presented for the bridge with diaphragms in Figs. 31 to 34, and in Figs. 35 to 38 for the bridge without diaphragms. Figures 39 through 44 present the comparison in the form of influence lines. It can be seen that the theoretical distribution coefficients are in fair agreement with the experimental values for deflections, but are not as consistent with the experimental distribution coefficients for moments. This disagreement arose from the fact that the extra stiffness in the interior beams, contributed by the curbs and parapets, created some difficulty in replacing the actual structure by a uniform orthotropic plate. As shown in Table 7, a comparison of the distribution factors based on the Guyon-Massonnet theory with those determined from the experimental values indicates that the theory can give only a fair estimation of the distribution factors.

6. SUMMARY AND CONCLUSIONS

6.1 Summary

The main objective of the Philadelphia Bridge study was to experimentally investigate the effects of midspan diaphragms on load distribution in highway bridges constructed with prestressed concrete box girders. A secondary objective is to provide part of the experimental data needed in the development of a reasonable design procedure which closely reflects the actual behavior of bridges of the spread box-beam type.

This report presents the results of the field test of an existing bridge located near Philadelphia. The bridge was first tested with midspan diaphragms, and then the same tests were repeated after the diaphragms had been removed. The cross-section of the bridge consists of five identical precast prestressed concrete box girders, a composite cast-in-place reinforced concrete deck, and reinforced concrete curbs and parapets. Strain gages were applied at a test section where maximum moments would occur as the drive axle of the test truck passed over the section. Deflectometers were installed either at the test section, or at the east end of

the test span. A truck simulating AASHO HS 20-44 loading was used as the test vehicle. All of the tests were conducted with the test vehicle moving at crawl speed, in seven loading lanes. Strain and deflection measurements were recorded with continuous recording equipment provided and operated by the U.S. Bureau of Public Roads.

The data recorded in the field was reduced to strains and deflections. From the strains, moment coefficients, experimental live load moments, distribution coefficients, distribution factors, and effective slab widths were determined. An evaluation of the effects of midspan diaphragms was made by comparing the test results for the cases with diaphragms in place and with diaphragms removed. A comparison of the test results with those from the Drehersville Bridge was made.

In an evaluation of the applicability of the Guyon-Massonnet theory to spread box-girder bridges, experimentally determined distribution coefficients for moment and deflection were compared with theoretical values. The distribution factors for moments developed from these coefficients, as compared with values based on field test results, ranged from 6 to 15% on the low side for exterior beams, and from 4 to 15% on the high side for interior beams.

6.2 Conclusions

The following conclusions were made based on the test results of the field study of the Philadelphia Bridge.

1. The diaphragms did transmit loads laterally, but owing to compensating effects when various lanes were loaded, the experimentally determined distribution factors were not appreciably affected. Based on the testing of the Philadelphia Bridge, the necessity of the use of mid-span diaphragms is questionable.
2. The deflections of the girders directly under the truck load were slightly reduced by the use of the diaphragms.
3. The distribution factors currently utilized in the PDH Bridge Division Standards did not adequately reflect the actual load distribution in the bridge. For interior girders, the experimental distribution factor was considerably less than the PDH design value; while the experimental value for exterior girders was greater than the design value.
4. It would be desirable to include the effects of at least the curbs in future design procedures.
5. The current distribution factor for interior girders reasonably reflects the influence of

girder spacing on distribution factors, although the experimentally determined values were considerably less than design values. However, the design method for estimating distribution factors for exterior girders does not yield a satisfactory representation.

6. The distribution based on the Guyon-Massonnet theory was a fair qualitative representation of distribution coefficients for individual runs of the test vehicle and for the influence lines. However, the combination of these values to form distribution factors yielded values which did not adequately reflect the actual behavior of the Philadelphia Bridge.

7. ACKNOWLEDGMENTS

This study was conducted in the Department of Civil Engineering at Fritz Engineering Laboratory, under the auspices of the Lehigh University Institute of Research, as part of a research investigation sponsored by the Pennsylvania Department of Highways, the U.S. Bureau of Public Roads, and the Reinforced Concrete Research Council.

The field test equipment was made available through the cooperation of Mr. C. F. Scheffey, Chief, Structures and Applied Mechanics Division, Office of Research and Development, Bureau of Public Roads. The instrumentation and operation of the test equipment were accomplished by Messrs. R. F. Varney, W. Armstrong, and H. Laatz, all of the Bureau of Public Roads.

The basic planning in this investigation was in cooperation with Mr. K. H. Jensen, formerly Bridge Engineer, and Mr. H. P. Koretzky, Engineer in Charge of Prestressed Concrete Structures, both of the Bridge Engineering Division, Pennsylvania Department of Highways.

The following Lehigh University staff attended the field testing: Mr. A. A. Guilford, Principal Investigator,

and Messrs. T. W. Schaffer and S. H. Cowen. The advice and help of Mr. A. A. Guilford are deeply appreciated. Thanks are extended to Mrs. Carol Kostenbader for typing the manuscript, and to Mr. J. M. Gera, Jr. for tracing the figures.

8. APPENDIX

8.1 Instrumentation

All strain gages used in the testing were of the SR-4 electrical resistance type manufactured by the Baldwin-Lima-Hamilton Corporation. Initially, each gage location was ground smooth, cleaned with acetone, and sealed with diluted SR-4 cement. The strain gages were then mounted with undiluted SR-4 cement after the initial coat had cured. Gages applied to the rain-exposed surfaces of the roadway, curb, and parapet were waterproofed.

Each deflectometer consisted of strain gages bonded to a flexible, triangular aluminum plate. The aluminum plate was attached to a bar which was clamped along the bottom surface of a girder. The apex of the plate was connected by a wire to a weight resting on the ground. The wire was adjusted to impose a downward deflection on the plate. Each deflectometer was calibrated so that changes of flexural strain in the plate, occurring when the girder deflected, could be converted to deflections. Girder rotations were measured by using two deflectometers mounted on the two edges of the bottom surface of a girder as shown in Fig. 3.

Corresponding to each active strain gage and deflection gage, temperature compensation gages were located near each gage location. Each active gage and temperature compensation gage was connected to one of the 48 channels of monitoring equipment in the equipment trailer provided by the Bureau of Public Roads. Each channel formed a Wheatstone bridge composed of an active gage, temperature compensating gage, power supply, amplifier, oscillator, and galvanometer. As the galvanometer responded to the changes in resistance of the active strain gage, thin-line traces produced by beams of light were recorded on light-sensitive oscillograph paper. Three variable-speed recorders were used to record the responses of the 48 gages.

8.2 Test Vehicle

The vehicle used for testing was a diesel-powered tractor and semi-trailer provided by the Bureau of Public Roads. The truck was loaded with crushed stone to approximate the AASHO HS 20-44 design loading.² A photograph of the test vehicle, along with the wheel spacings and axle loads is shown in Fig. 6.

9. TABLES

Table 1 Listing of Test Runs

Direction	Diaphragms	Position of Deflectometers	Lanes	Number
West	In	At Test Section	1 through 7	14*
East	In	At Test Section	1 through 7	7
West	In	At End	1 through 7	7
East	In	At End	1 through 7	7
West	Out	At End	1 through 7	7
East	Out	At End	1 through 7	7
East	Out	At Test Section	1 through 7	7
West	Out	At Test Section	1 through 7	7

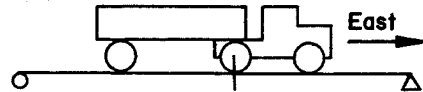
* Two runs per lane

Table 2 Moment Coefficients (10^{-3} ft-in²)

-38-

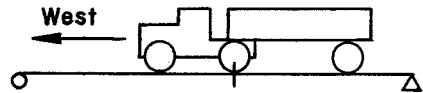
Midspan Diaphragms in Place

GIRDER	GIRDER					Modulus of Elasticity (10^6 psi)
	A	B	C	D	E	



T.M.* = 951.3 (kip-ft)

Lane 1	78.6	50.4	26.1	14.4	8.1	5.36
Lane 2	50.3	54.9	33.0	20.6	13.3	5.53
Lane 3	36.9	48.6	43.0	26.5	17.9	5.50
Lane 4	26.4	35.8	47.2	35.8	26.4	5.55

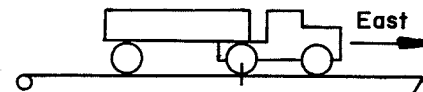


T.M.* = 902.9 (kip-ft)

Lane 1	66.3	46.8	24.4	12.8	8.2	5.70
Lane 2	46.3	51.3	31.0	17.7	11.4	5.72
Lane 3	33.3	44.3	40.8	25.4	17.3	5.60
Lane 4	23.4	33.5	47.3	33.5	23.4	5.60

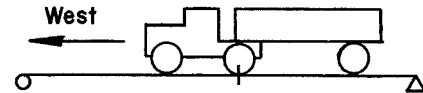
Midspan Diaphragms Removed

GIRDER	GIRDER					Modulus of Elasticity (10^6 psi)
	A	B	C	D	E	



T.M.* = 951.3 (kip-ft)

Lane 1	89.4	56.1	24.8	13.1	11.6	4.88
Lane 2	53.6	63.9	35.6	16.5	10.8	5.27
Lane 3	36.6	56.9	49.5	25.4	16.1	5.16
Lane 4	21.7	37.0	56.8	37.0	21.7	5.46



T.M.* = 902.9 (kip-ft)

Lane 1	68.9	51.4	23.2	10.4	7.5	5.59
Lane 2	46.3	58.8	33.0	16.3	11.7	5.44
Lane 3	30.9	51.8	48.0	23.0	14.7	5.36
Lane 4	21.3	36.9	55.0	36.9	21.3	5.27

* T.M. = Theoretical Total Moment

Table 3 Distribution Coefficients

$$\text{DISTRIBUTION COEFFICIENT} = \frac{\text{Moment Coefficient}}{\Sigma \text{ Moment Coefficients}} (100)$$

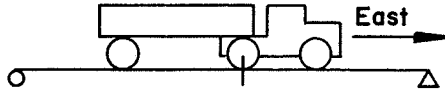
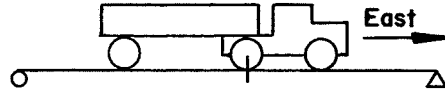
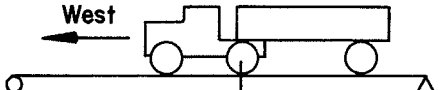
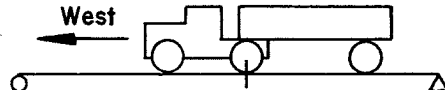
	With Diaphragm					Without Diaphragm				
	GIRDER					GIRDER				
	A	B	C	D	E	A	B	C	D	E
										
Lane 1	44.22	28.38	14.74	8.10	4.56	45.86	28.78	12.69	6.73	5.94
Lane 2	29.23	31.91	19.16	11.96	7.74	29.71	35.43	19.71	9.15	6.00
Lane 3	21.33	28.10	24.89	15.30	10.38	19.84	30.83	26.82	13.78	8.73
Lane 4	15.36	20.88	27.52	20.88	15.36	12.47	21.23	32.60	21.23	12.47
										
Lane 1	41.85	29.53	15.37	8.05	5.20	42.69	31.86	14.38	6.43	4.64
Lane 2	29.35	32.53	19.66	11.21	7.25	27.86	35.40	19.88	9.81	7.05
Lane 3	20.67	27.49	25.31	15.78	10.75	18.33	30.77	28.51	13.65	8.74
Lane 4	14.54	20.78	29.36	20.78	14.54	12.41	21.54	32.10	21.54	12.41

Table 4 Distribution Coefficients by Guyon-Massonnet Theory

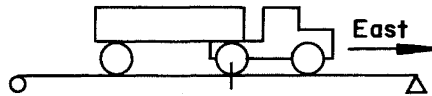
$$\text{DISTRIBUTION COEFFICIENT} = \frac{\text{Girder Moment}}{\Sigma \text{ Girder Moments}} (100) = \frac{\text{Girder Deflection}}{\Sigma \text{ Girder Deflections}} (100)$$

-0h-

Midspan Diaphragms in Place						
GIRDER						
	A	B	C	D	E	Σ
Lane 1	38.17	29.16	19.28	10.38	2.22	99.21
Lane 2	30.52	27.37	21.65	14.24	6.58	100.36
Lane 3	23.56	24.66	23.40	18.00	11.68	101.30
Lane 4	17.33	21.52	24.00	21.52	17.33	101.70

Midspan Diaphragms Removed						
GIRDER						
	A	B	C	D	E	Σ
Lane 1	40.20	32.60	17.21	7.19	2.56	99.76
Lane 2	28.66	34.28	23.96	11.04	4.08	102.02
Lane 3	19.17	30.08	30.08	17.10	7.16	103.59
Lane 4	12.10	23.87	32.08	23.87	12.10	104.02

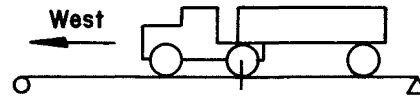
Table 5 Distribution Factors, Eastbound



Girder	Experimental Distr. Factor		PDH Design Value	Experimental Design	
	With Diaphragms	Without Diaphragms		With Diaphragms	Without Diaphragms
A	1.283	1.286	1.158	1.108	1.111
B	1.147 $\frac{S}{8.28}$	1.135 $\frac{S}{8.37}$	1.727 $\frac{S}{5.5}$	0.664	0.657
C	1.140 $\frac{S}{8.33}$	1.160 $\frac{S}{8.19}$	1.727 $\frac{S}{5.5}$	0.661	0.672

S is the girder spacing

Table 6 Distribution Factors, Westbound



Girder	Experimental Distr. Factor		PDH Design Value	Experimental Design	
	With Diaphragms	Without Diaphragms		With Diaphragms	Without Diaphragms
A	1.232	1.195	1.158	1.065	1.032
B	1.167 $\frac{S}{8.14}$	1.197 $\frac{S}{7.94}$	1.727 $\frac{S}{5.5}$	0.675	0.693
C	1.202 $\frac{S}{7.90}$	1.217 $\frac{S}{7.80}$	1.727 $\frac{S}{5.5}$	0.696	0.704

S is the girder spacing

Table 7 Distribution Factors by Guyon-Massonnet Theory

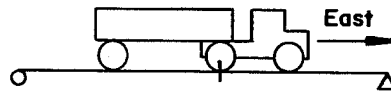
GIRDER	Experimental Values		PDH Design Value	Guyon-Massonnet Value
	Eastbound	Westbound		
Midspan Diaphragms in Place				
A	1.283	1.232	1.158	1.154
B	1.147	1.167	1.727	1.221
C	1.140	1.202	1.727	1.251
Midspan Diaphragms Removed				
A	1.286	1.195	1.158	1.097
B	1.135	1.197	1.727	1.273
C	1.160	1.217	1.727	1.330

Table 8 Comparison of Distribution Factors
for Drehersville Bridge and Philadelphia Bridge

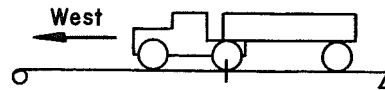
Bridge	Beam Spac.	BEAM A			BEAM B			BEAM C		
		Experi- mental	Design	<u>Exper.</u> <u>Design</u>	Experi- mental	Design	<u>Exper.</u> <u>Design</u>	Experi- mental	Design	<u>Exper.</u> <u>Design</u>
Drehersville	7'-2	1.13	0.81	1.393	0.85	1.30	0.654	0.69	1.30	0.53
Philadelphia (with diaph.)	9'-6	1.283	1.158	1.108	1.147	1.727	0.664	1.140	1.727	0.661
Philadelphia (without diaph.)	9'-6	1.286	1.158	1.111	1.135	1.727	0.657	1.160	1.727	0.672

Table 9 Girder Deflections at Test Section, With Diaphragms in Place
(All values in inches)

GIRDER A B C D E



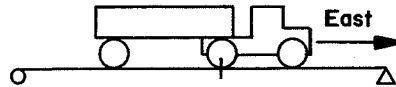
Lane 1	0.108	0.105	0.093	0.080	0.058	0.045	0.032	0.024	0.015	0.011
Lane 2	0.078	0.083	0.090	0.086	0.068	0.056	0.041	0.033	0.021	0.016
Lane 3	0.055	0.061	0.076	0.082	0.076	0.068	0.055	0.045	0.031	0.024
Lane 4	0.038	0.045	0.061	0.070	0.078	0.078	0.070	0.061	0.045	0.038



Lane 1	0.095	0.093	0.082	0.070	0.051	0.041	0.029	0.022	0.014	0.009
Lane 2	0.066	0.073	0.082	0.080	0.063	0.056	0.039	0.032	0.021	0.016
Lane 3	0.049	0.056	0.070	0.076	0.072	0.065	0.049	0.040	0.028	0.023
Lane 4	0.034	0.041	0.054	0.063	0.074	0.074	0.063	0.054	0.041	0.034

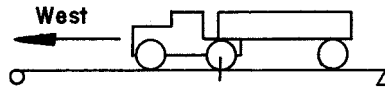
Table 10 Girder Deflections at Test Section, With Diaphragms Removed
(All values in inches)

GIRDER A B C D E



- 94 -

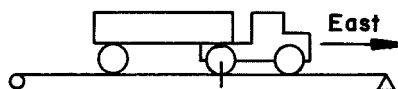
Lane 1	0.115	0.113	0.097	0.082	0.059	0.046	0.028	0.022	0.013	0.011
Lane 2	0.077	0.084	0.097	0.094	0.077	0.063	0.037	0.029	0.018	0.014
Lane 3	0.053	0.060	0.080	0.089	0.090	0.080	0.053	0.042	0.027	0.022
Lane 4	0.034	0.040	0.059	0.073	0.095	0.095	0.073	0.059	0.040	0.034



Lane 1	0.099	0.098	0.087	0.075	0.054	0.041	0.024	0.018	0.011	0.009
Lane 2	0.068	0.075	0.087	0.088	0.076	0.060	0.039	0.029	0.018	0.015
Lane 3	0.045	0.053	0.072	0.085	0.089	0.076	0.049	0.037	0.023	0.019
Lane 4	0.031	0.036	0.054	0.068	0.092	0.092	0.068	0.054	0.036	0.031

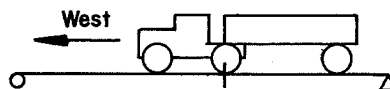
Table 12 Girder Deflections at End, With Diaphragms Removed
(All values in inches)

GIRDER A B C D E



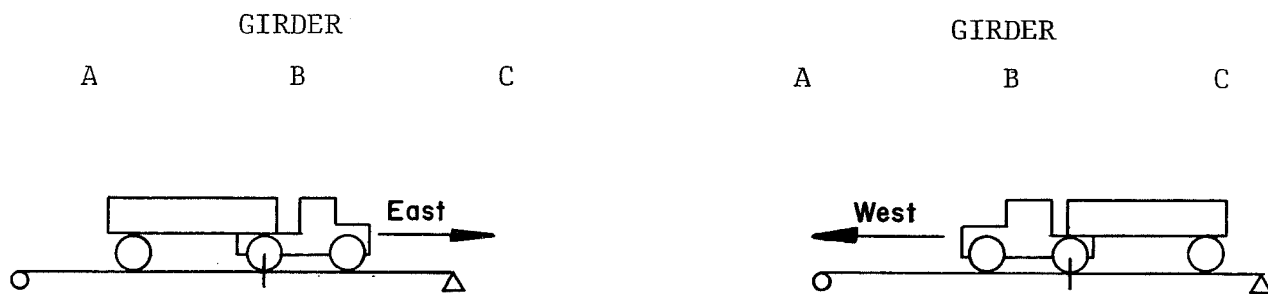
- 8 ft -

Lane 1	0.0081	0.0065	0.0091	0.0037	0.0055	0.0006	0.0020	-0.0001	0.0006	-0.0003
Lane 2	0.0015	0.0056	0.0068	0.0058	0.0064	0.0008	0.0028	0.0001	0.0008	-0.0008
Lane 3	0.0006	0.0045	0.0042	0.0081	0.0077	0.0032	0.0047	0.0015	0.0021	-0.0003
Lane 4	-0.0013	0.0011	0.0013	0.0064	0.0044	0.0044	0.0064	0.0013	0.0011	-0.0013



Lane 1	0.0092	0.0098	0.0117	0.0050	0.0056	0.0007	0.0023	0.0003	0.0011	0.0005
Lane 2	0.0016	0.0069	0.0100	0.0099	0.0082	0.0012	0.0031	0.0002	0.0008	-0.0004
Lane 3	-0.0010	0.0037	0.0053	0.0112	0.0104	0.0036	0.0055	0.0009	0.0017	-0.0003
Lane 4	-0.0005	0.0024	0.0021	0.0087	0.0085	0.0085	0.0087	0.0021	0.0024	-0.0005

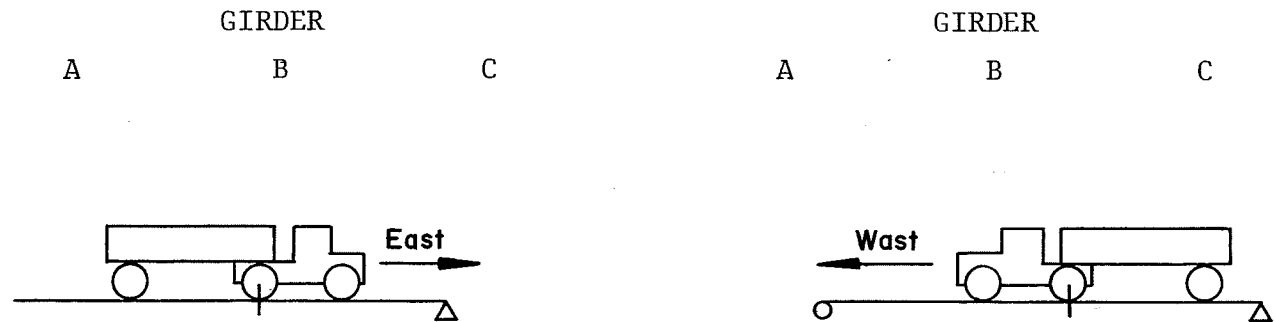
Table 13 Girder Rotations at Test Section, With Midspan Diaphragms in Place
(All values in radians)*



	GIRDER			GIRDER		
	A	B	C	A	B	C
Lane 1	-0.000068	-0.000274	-0.000165	-0.000046	-0.000237	-0.000108
Lane 2	+0.000097	-0.000092	-0.000163	+0.000146	-0.000046	-0.000053
Lane 3	+0.000127	+0.000125	-0.000018	+0.000142	+0.000130	+0.000012
Lane 4	+0.000141	+0.000196	+0.000143	+0.000139	+0.000188	+0.000130
Lane 5	+0.000135	+0.000203	+0.000336	+0.000120	+0.000181	+0.000259
Lane 6	+0.000111	+0.000182	+0.000358	+0.000106	+0.000162	+0.000279
Lane 7	+0.000093	+0.000155	+0.000351	+0.000100	+0.000154	+0.000294

* Positive rotation is clockwise (see Fig. 2)

Table 14 Girder Rotations at Test Section, With Midspan Diaphragms Removed
(All values in radians)*

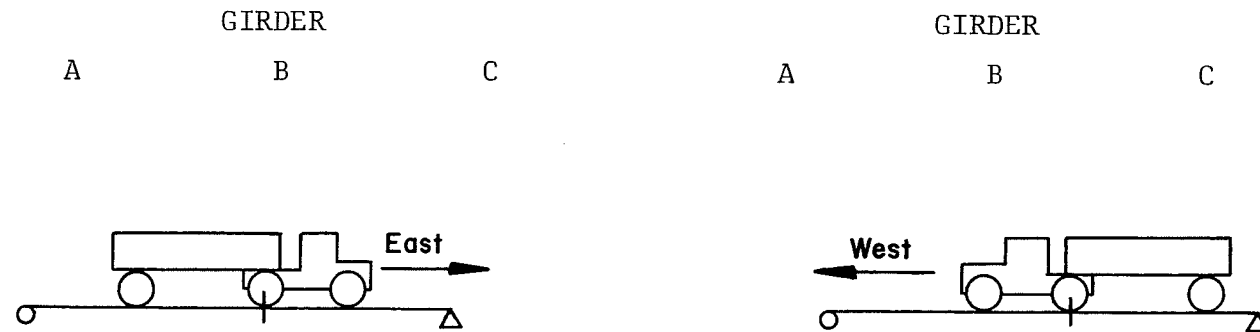


	GIRDER			GIRDER		
	A	B	C	A	B	C
Lane 1	-0.000043	-0.000318	-0.000269	-0.000024	-0.000245	-0.000267
Lane 2	+0.000134	-0.000060	-0.000304	+0.000148	+0.000019	-0.000341
Lane 3	+0.000148	+0.000185	-0.000189	+0.000147	+0.000268	-0.000280
Lane 4	+0.000116	+0.000280	-0.000007	+0.000115	+0.000289	-0.000001
Lane 5	+0.000093	+0.000229	+0.000230	+0.000085	+0.000233	+0.000257
Lane 6	+0.000069	+0.000171	+0.000303	+0.000067	+0.000193	+0.000321
Lane 7	+0.000041	+0.000137	+0.000256	+0.000039	+0.000139	+0.000278

* Positive rotation is clockwise (see Fig. 2)

Table 15 Girder Rotations at End, With Midspan Diaphragms in Place
(All values in radians)*

-51-

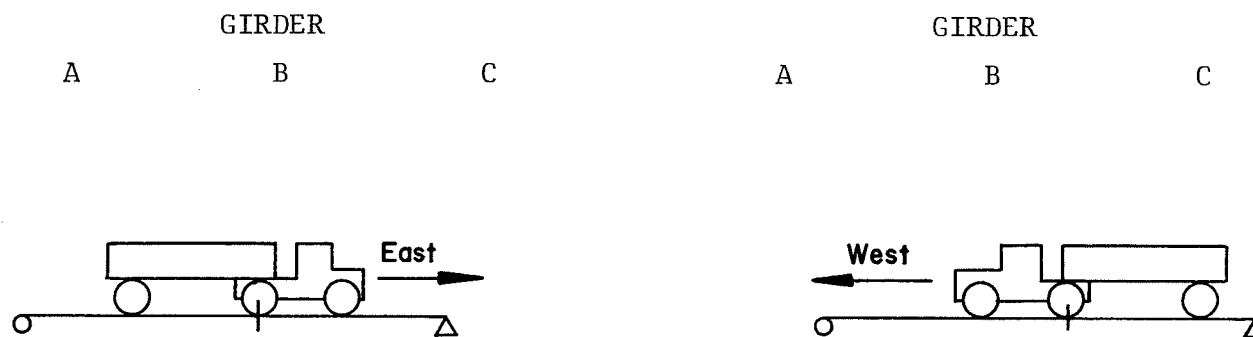


	GIRDER			GIRDER		
	A	B	C	A	B	C
Lane 1	-0.000084	-0.000087	-0.000092	-0.000055	-0.000110	-0.000087
Lane 2	+0.000022	-0.000012	-0.000096	+0.000057	-0.000007	-0.000111
Lane 3	+0.000049	+0.000053	-0.000081	+0.000056	+0.000096	-0.000123
Lane 4	+0.000059	+0.000064	-0.000020	+0.000050	+0.000099	-0.000021
Lane 5	+0.000055	+0.000068	+0.000051	+0.000048	+0.000068	+0.000114
Lane 6	+0.000045	+0.000015	+0.000083	+0.000055	+0.000062	+0.000102
Lane 7	+0.000042	+0.000057	+0.000075	+0.000021	+0.000047	+0.000097

* Positive rotation is clockwise (see Fig. 2)

Table 16 Girder Rotations at End, With Midspan Diaphragms Removed
(All values in radians)*

-52

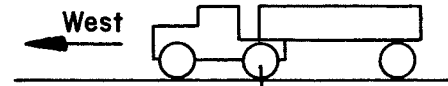
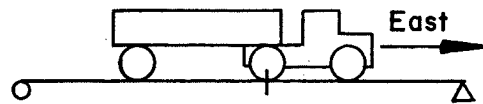


	GIRDER			GIRDER		
	A	B	C	A	B	C
Lane 1	-0.000033	-0.000111	-0.000106	+0.000012	-0.000140	-0.000105
Lane 2	+0.000085	-0.000020	-0.000128	+0.000111	-0.000003	-0.000150
Lane 3	+0.000080	+0.000080	-0.000108	+0.000096	+0.000121	-0.000153
Lane 4	+0.000050	+0.000108	-0.000010	+0.000059	+0.000138	-0.000009
Lane 5	+0.000051	+0.000068	+0.000082	+0.000041	+0.000095	+0.000131
Lane 6	+0.000033	+0.000056	+0.000108	+0.000025	+0.000060	+0.000141
Lane 7	+0.000017	+0.000043	+0.000095	+0.000013	+0.000042	+0.000100

* Positive rotation is clockwise (see Fig. 2)

Table 17 Transformed Effective Slab Widths, With Midspan Diaphragms in Place
(All values in inches)

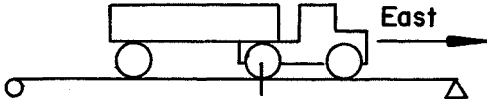
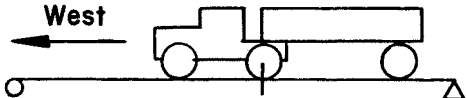
GIRDER			GIRDER		
A	B	C	A	B	C



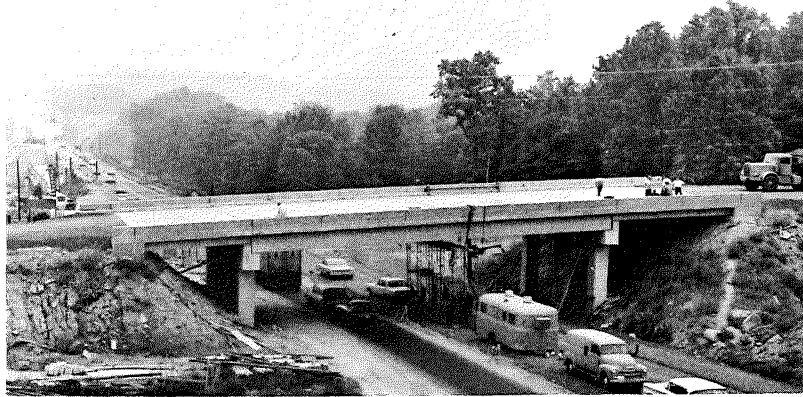
Lane 1	85.88	146.24	76.18	99.78	118.39	81.74
Lane 2	85.56	146.89	113.44	90.06	137.88	105.71
Lane 3	81.11	155.79	134.51	89.81	138.38	129.53
Lane 4	100.68	113.90	143.40	92.55	121.03	147.10
Lane 5	93.46	89.84	113.99	102.00	97.06	125.37
Lane 6	102.00	82.23	88.48	102.00	73.10	89.38
Lane 7	100.33	63.83	73.20	98.71	63.44	79.65

Table 18 Transformed Effective Slab Widths, With Midspan Diaphragms Removed
(All values in inches)

-54-

	GIRDER			GIRDER		
	A	B	C	A	B	C
						
Lane 1	78.18	161.64	81.68	96.25	125.51	80.42
Lane 2	71.76	174.48	109.68	87.36	143.28	102.15
Lane 3	72.16	173.69	128.55	83.46	151.09	137.83
Lane 4	99.41	115.55	140.87	90.97	136.07	145.43
Lane 5	102.00	96.36	124.69	98.70	93.16	132.10
Lane 6	102.00	66.14	105.10	102.00	65.16	93.62
Lane 7	102.00	72.50	82.51	102.00	65.28	78.04

10. FIGURES



-56-

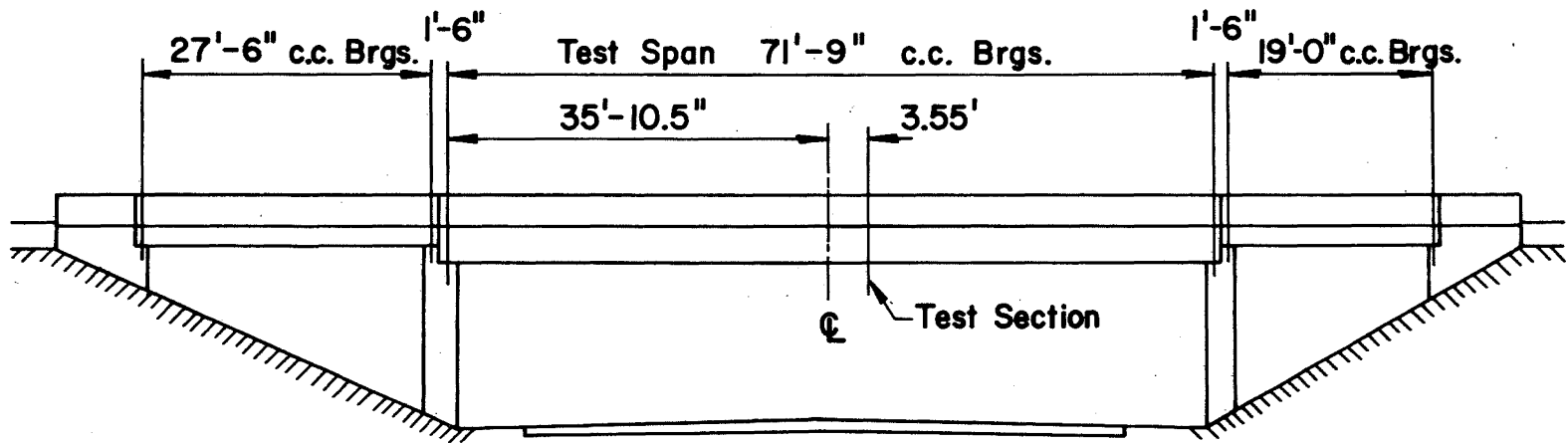


Fig. 1 Elevation of the Test Bridge

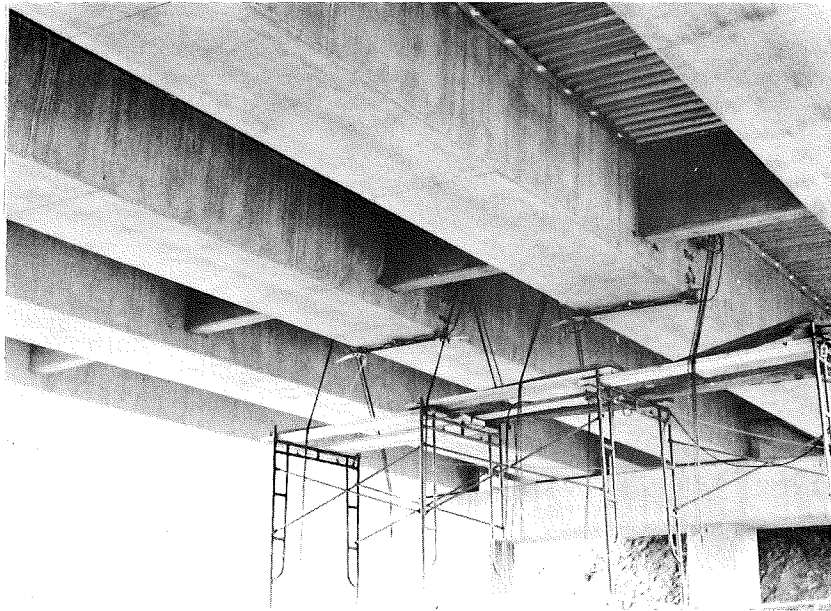


Fig. 3 Underside of Test Bridge,
Showing Instrumentation and Midspan Diaphragms

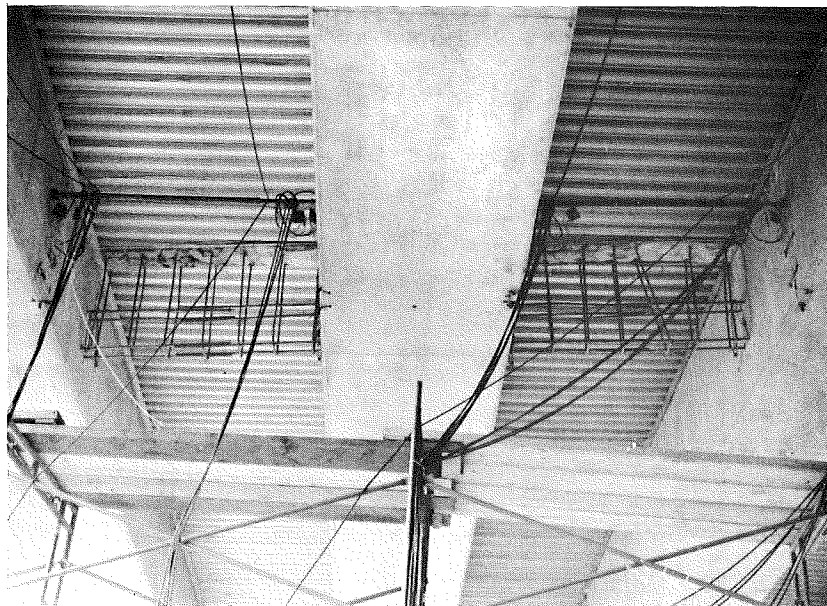
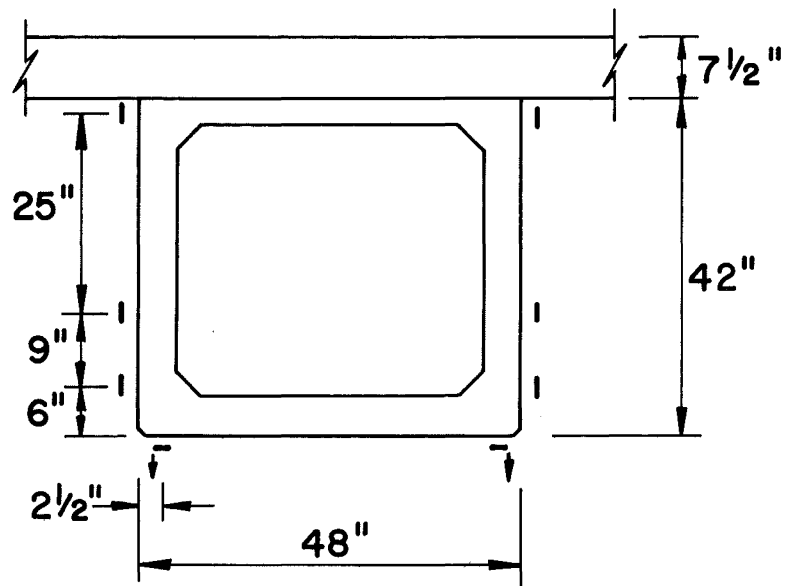
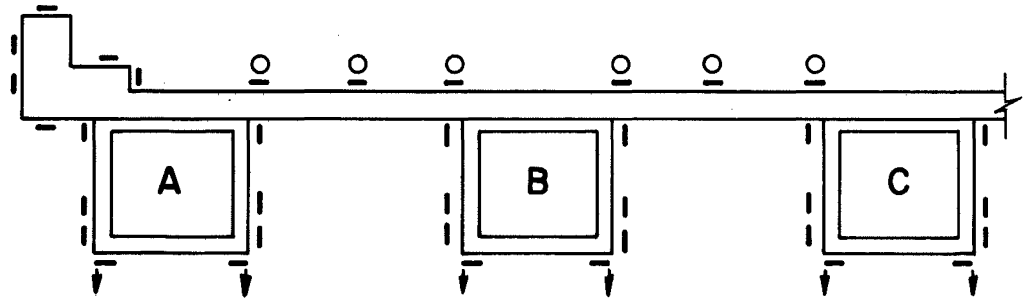


Fig. 4 Underside of Test Bridge
After Midspan Diaphragms Were Removed



SINGLE BEAM

- Longitudinal Gages
- o Transverse Gages
- ↓ Deflection Gages



BRIDGE CROSS-SECTION

Fig. 5 Location of Gages

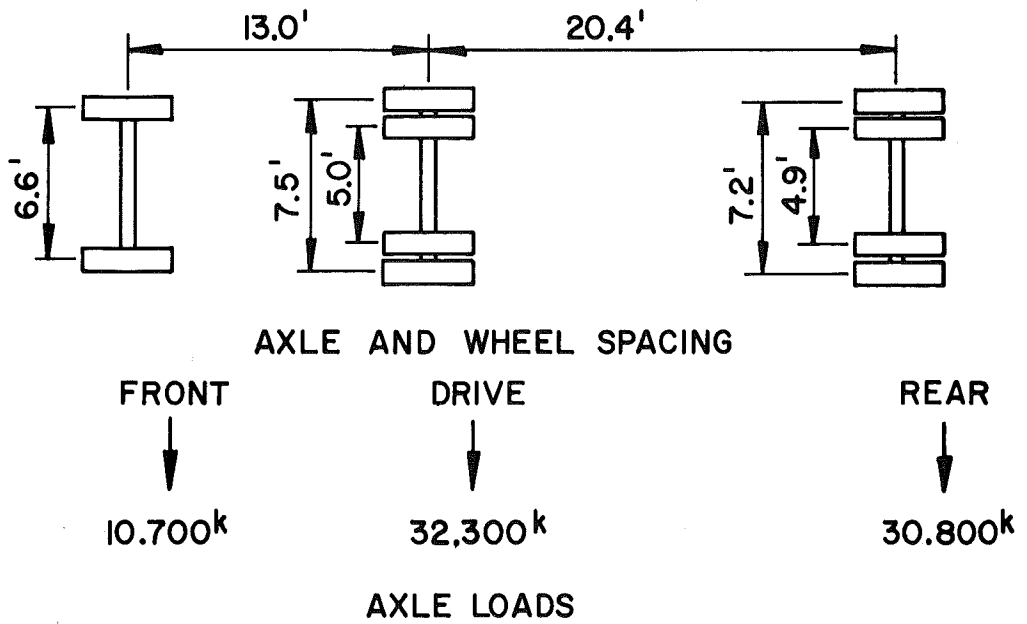
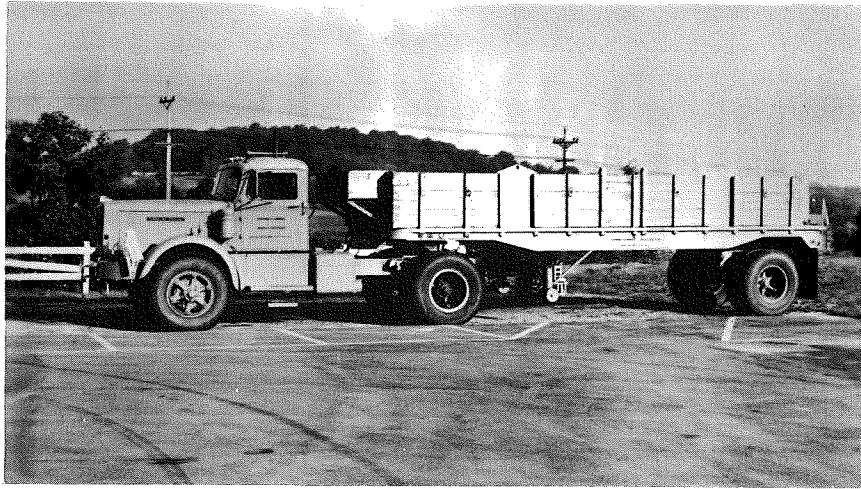


Fig. 6 Test Vehicle

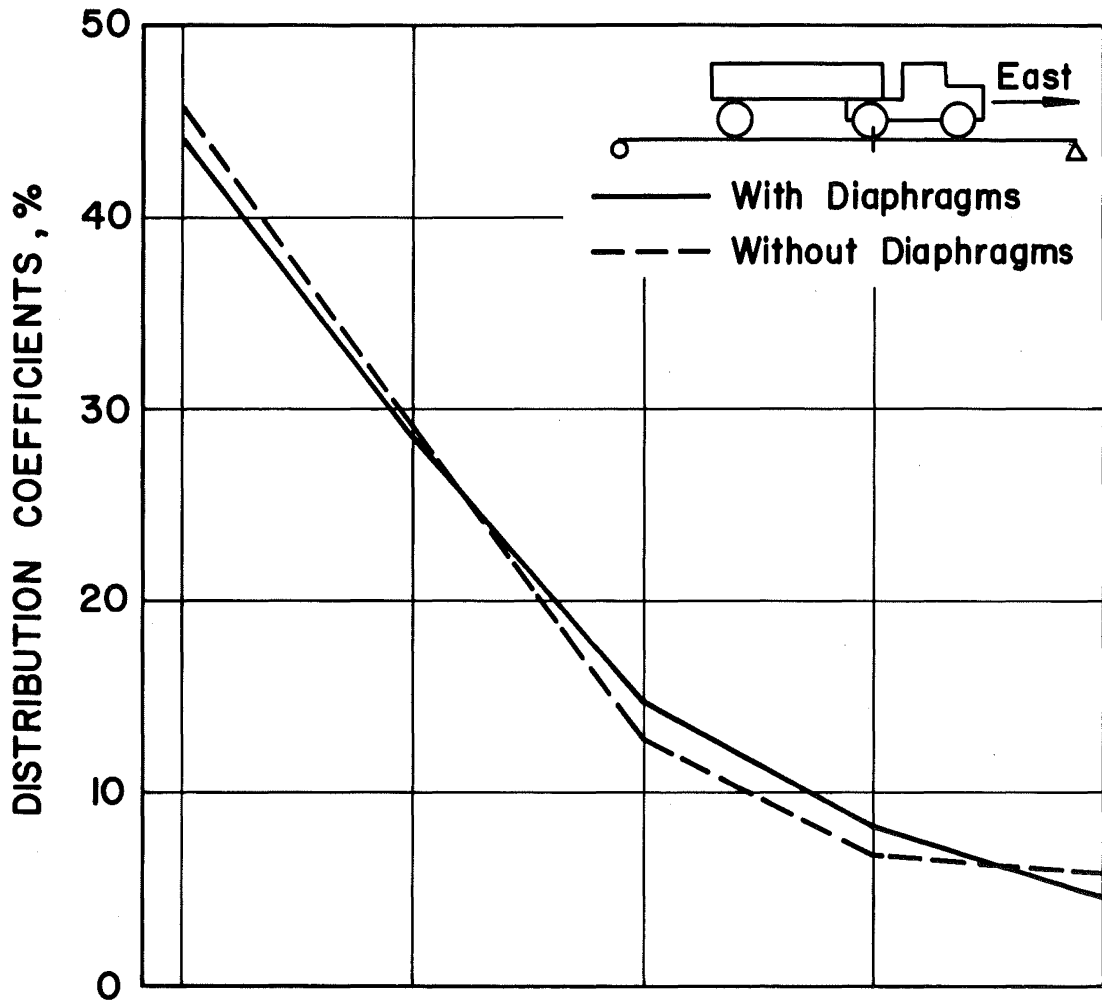
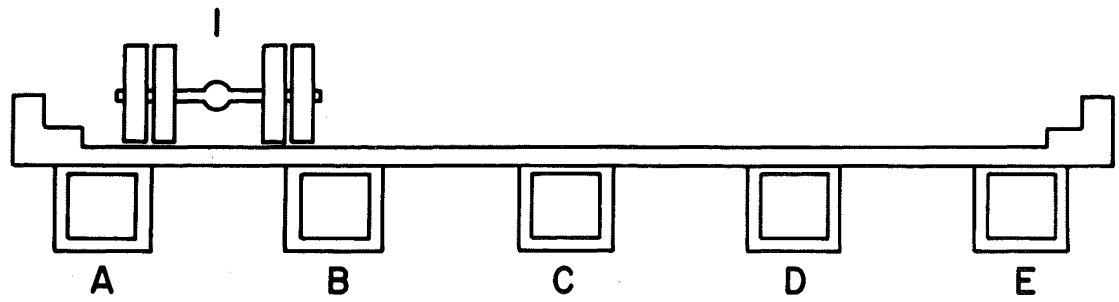


Fig. 7 Distribution Coefficients - Lane 1, Eastbound

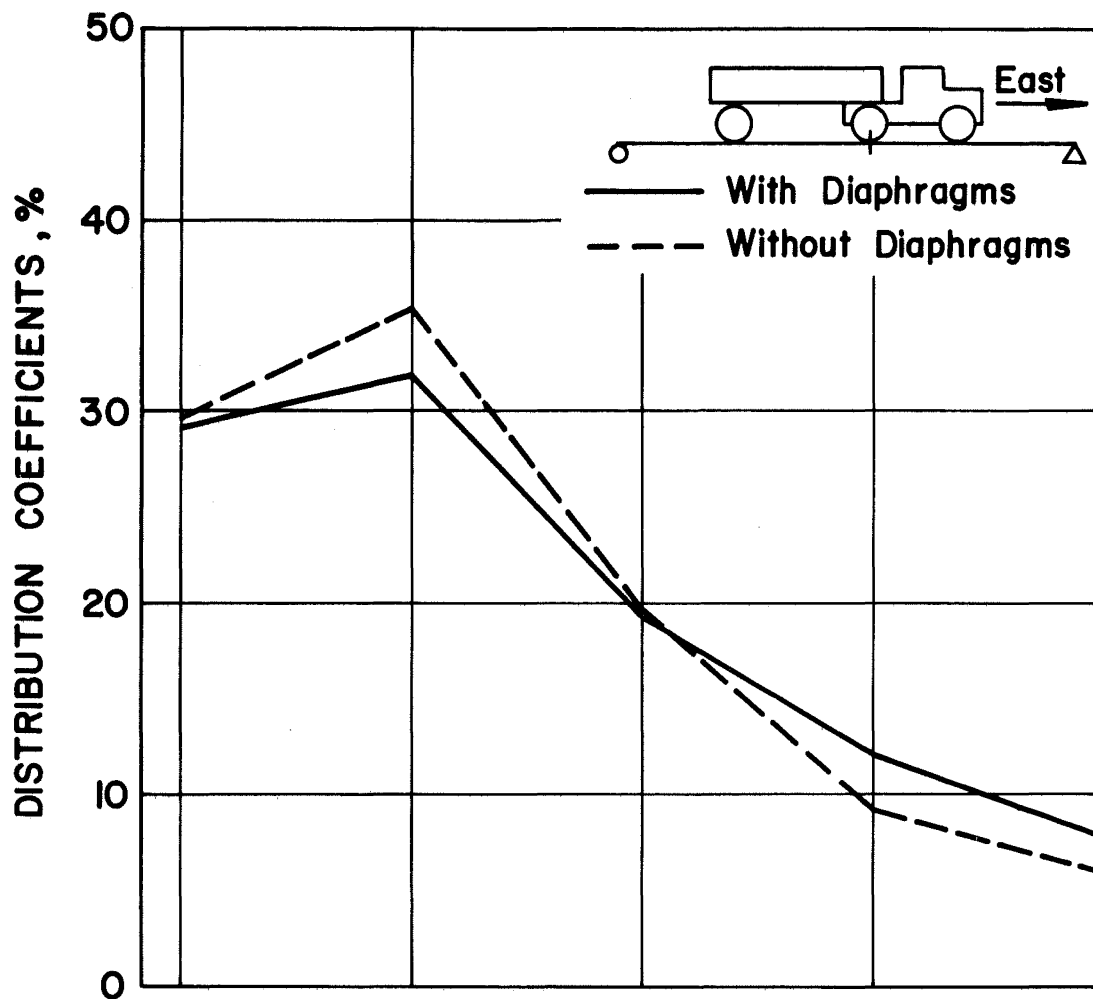
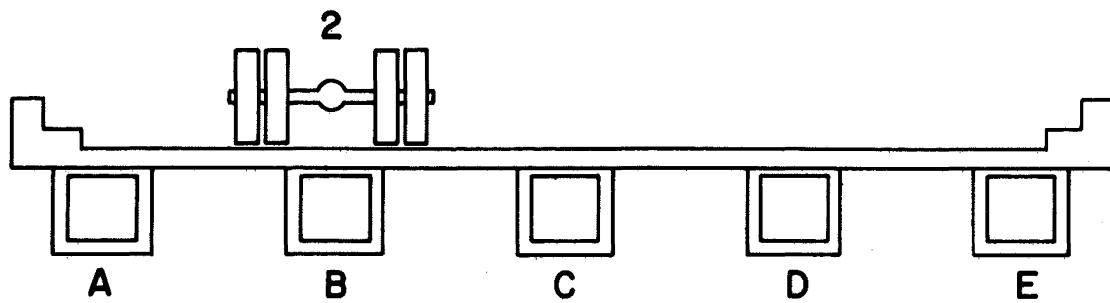


Fig. 8 Distribution Coefficients - Lane 2, Eastbound

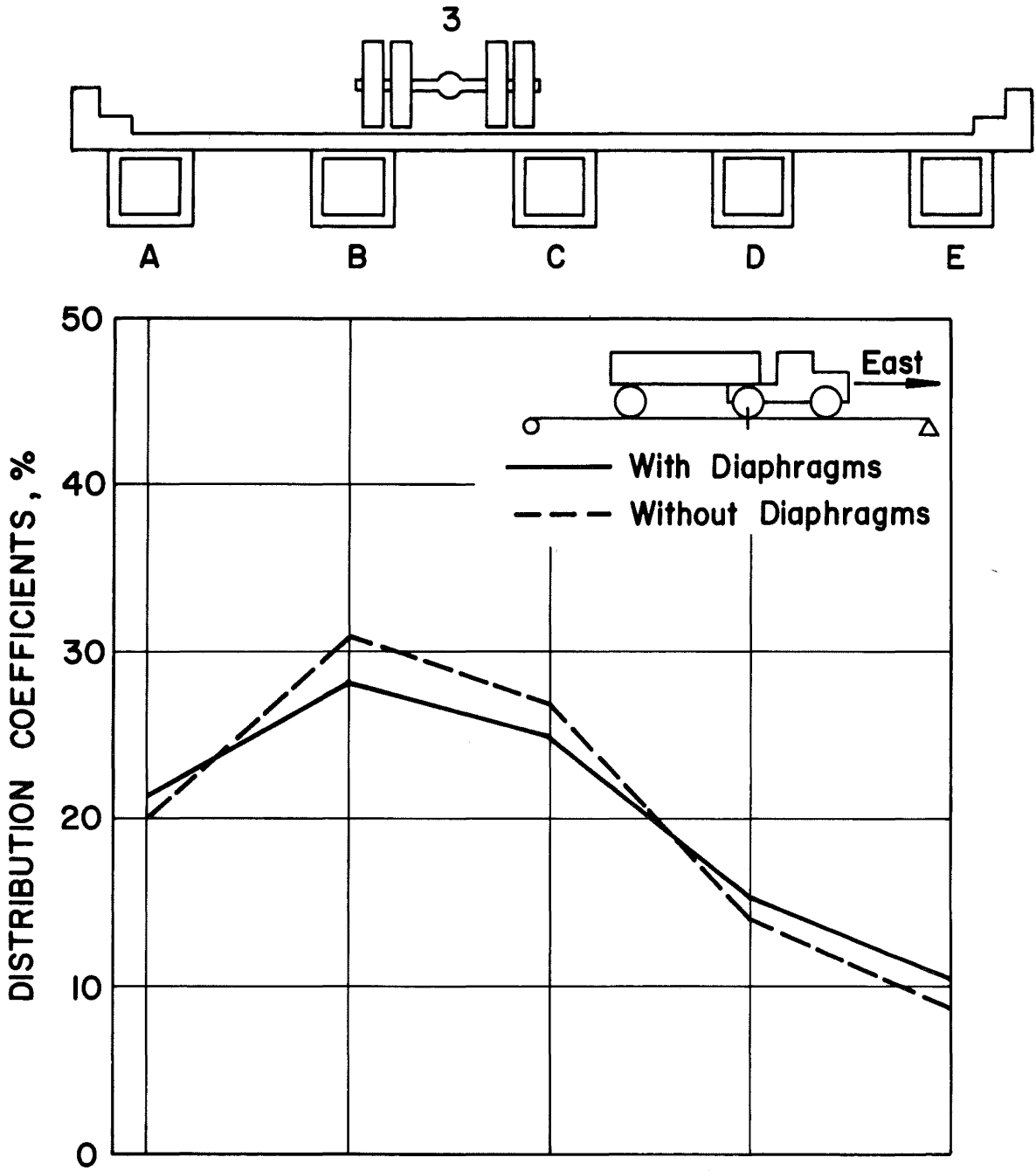


Fig. 9 Distribution Coefficients - Lane 3, Eastbound

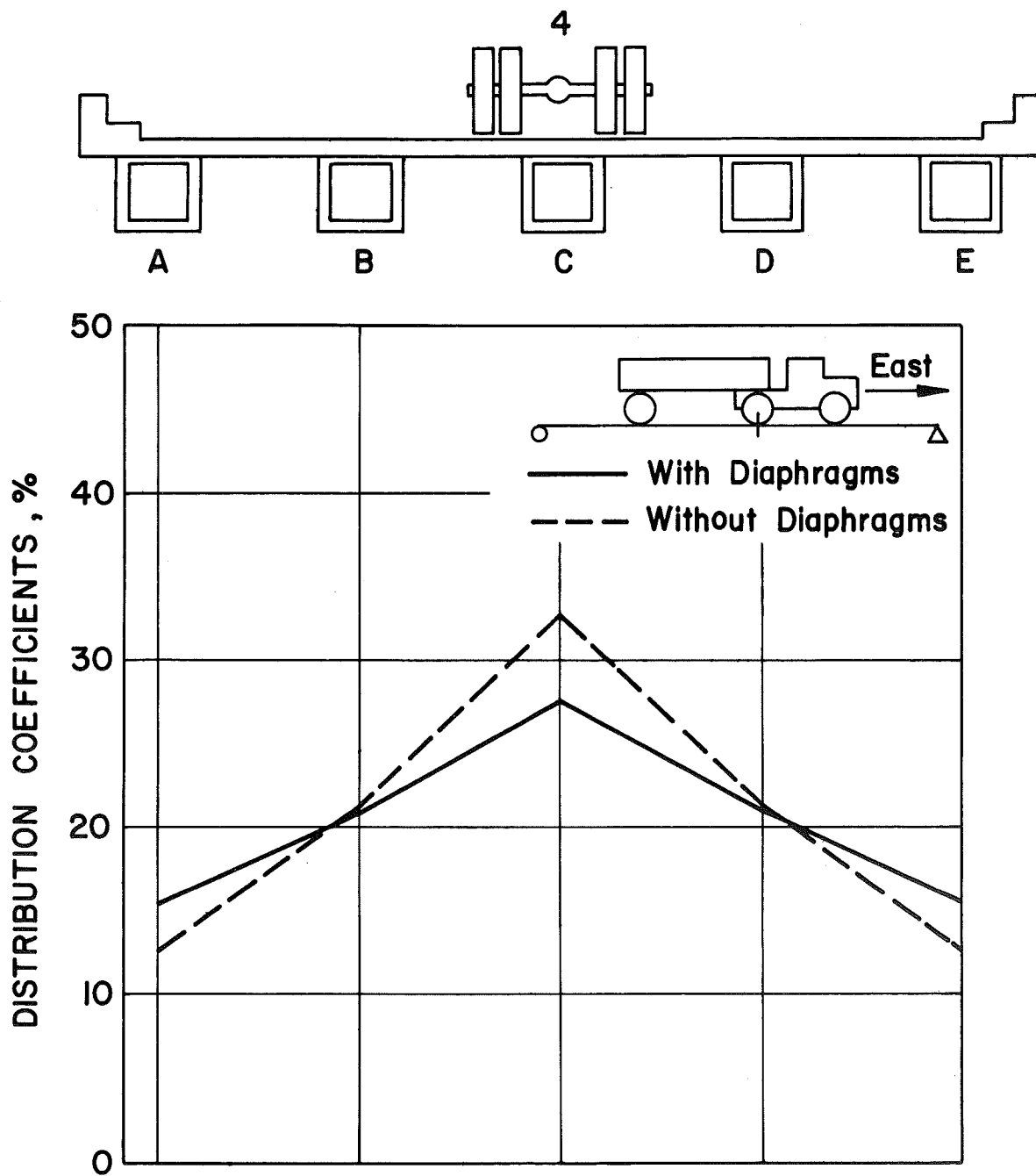


Fig. 10 Distribution Coefficients - Lane 4, Eastbound

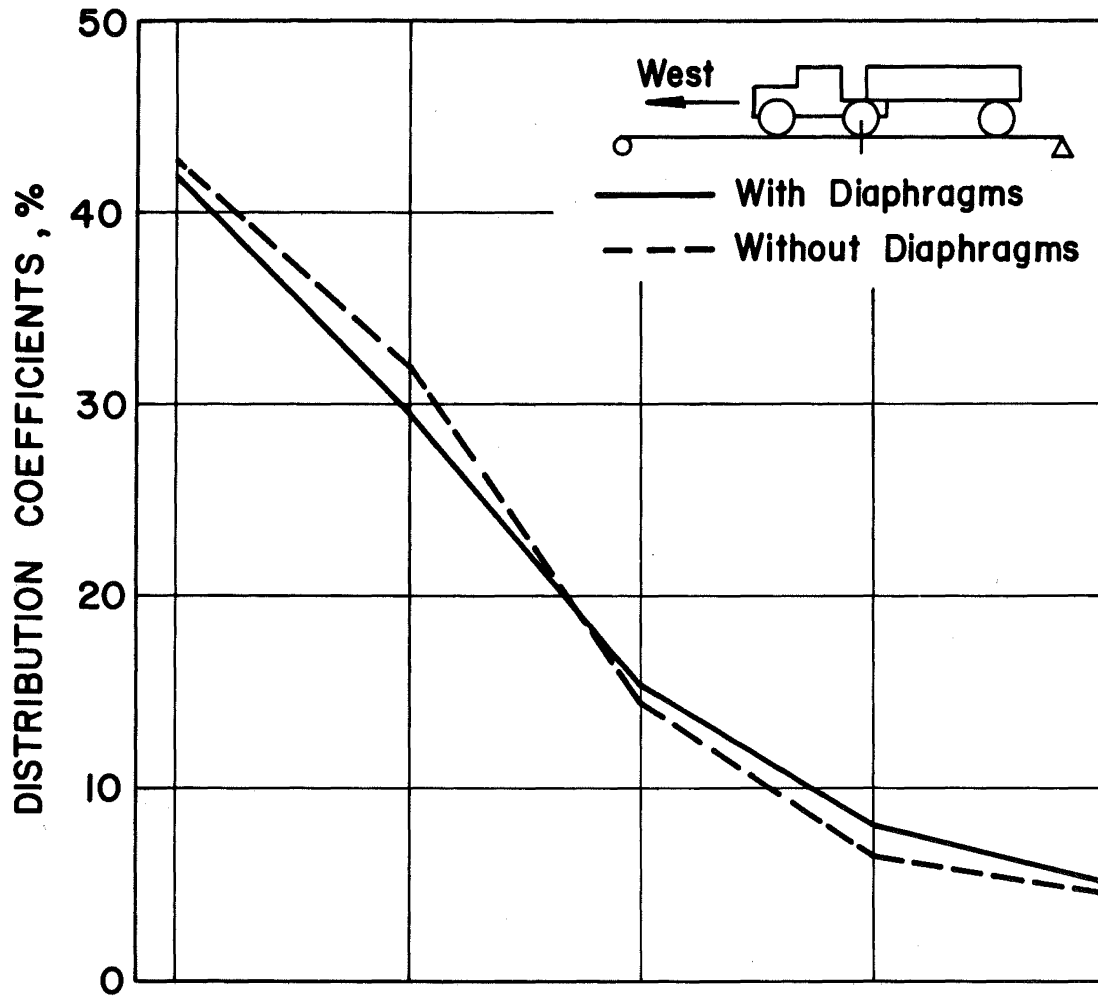
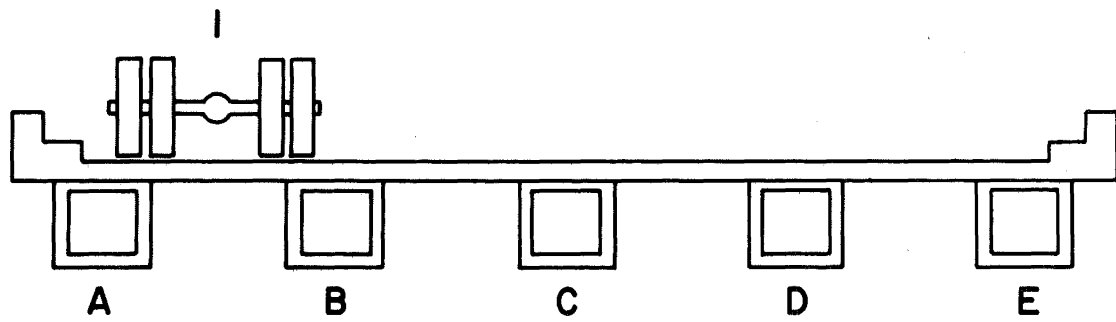


Fig. 11 Distribution Coefficients - Lane 1, Westbound

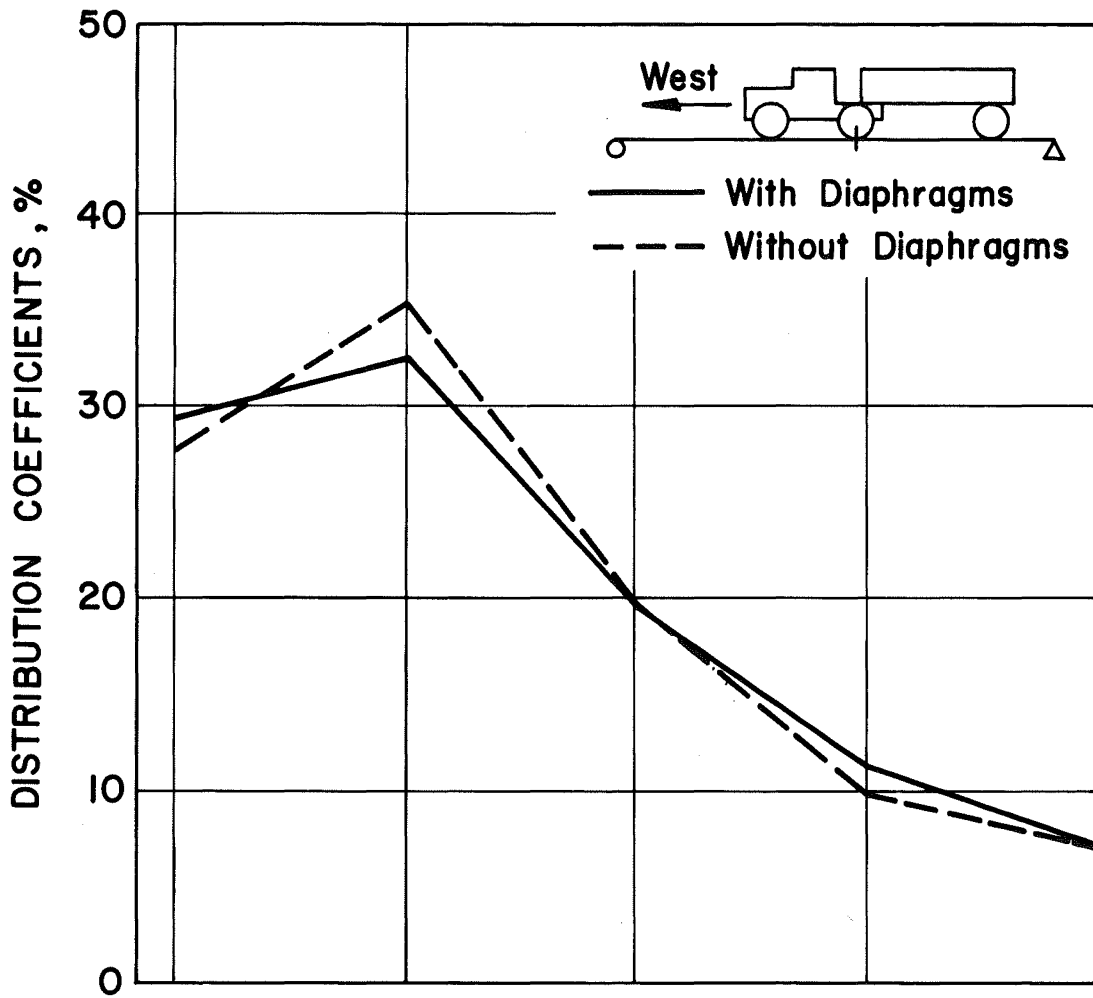
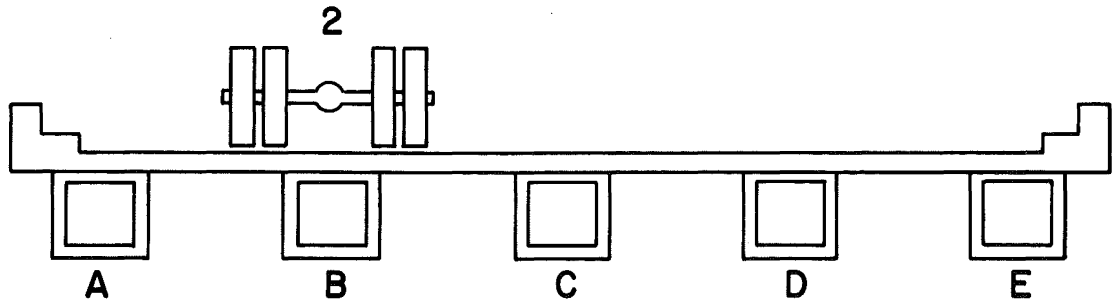


Fig. 12 Distribution Coefficients - Lane 2, Westbound

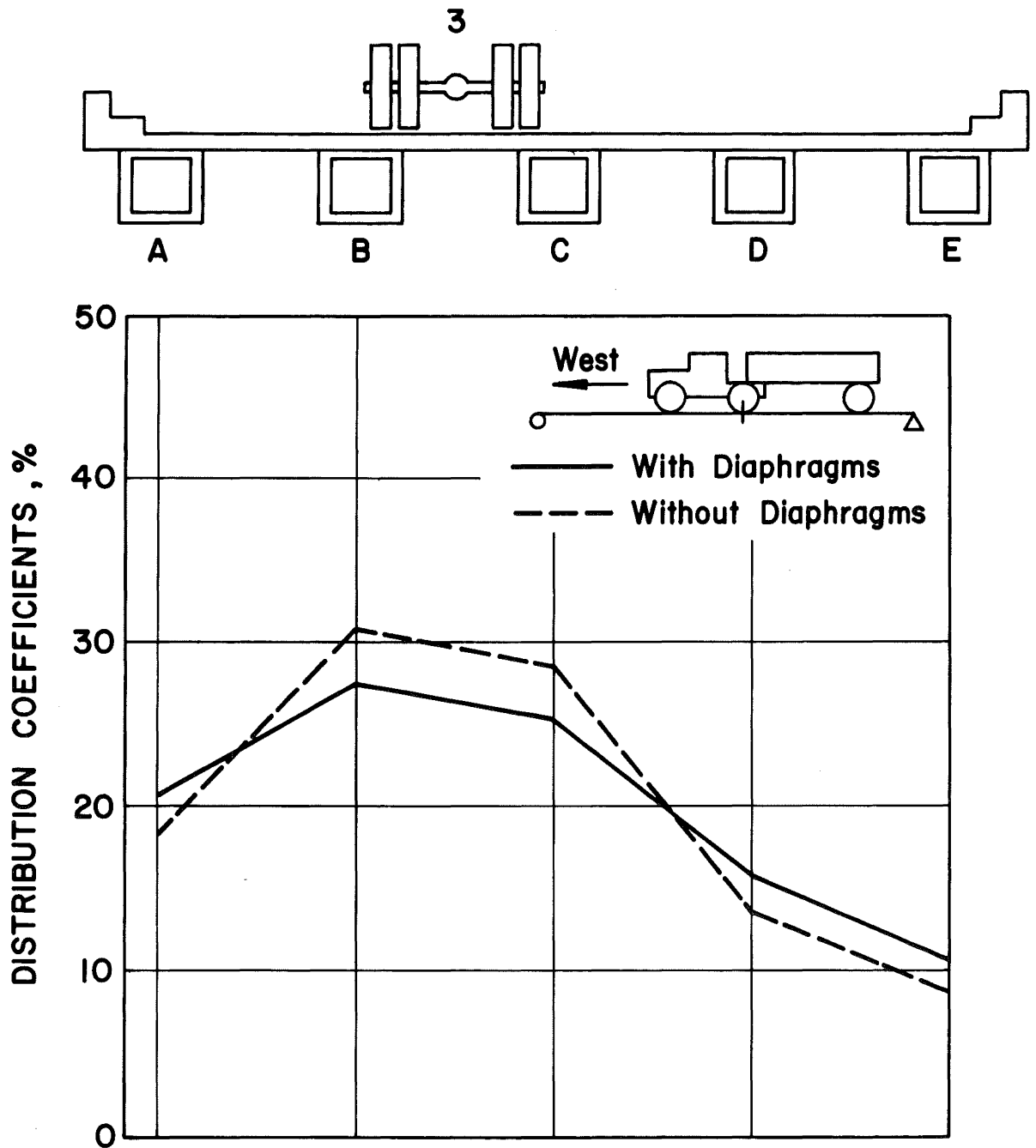


Fig. 13 Distribution Coefficients - Lane 3, Westbound

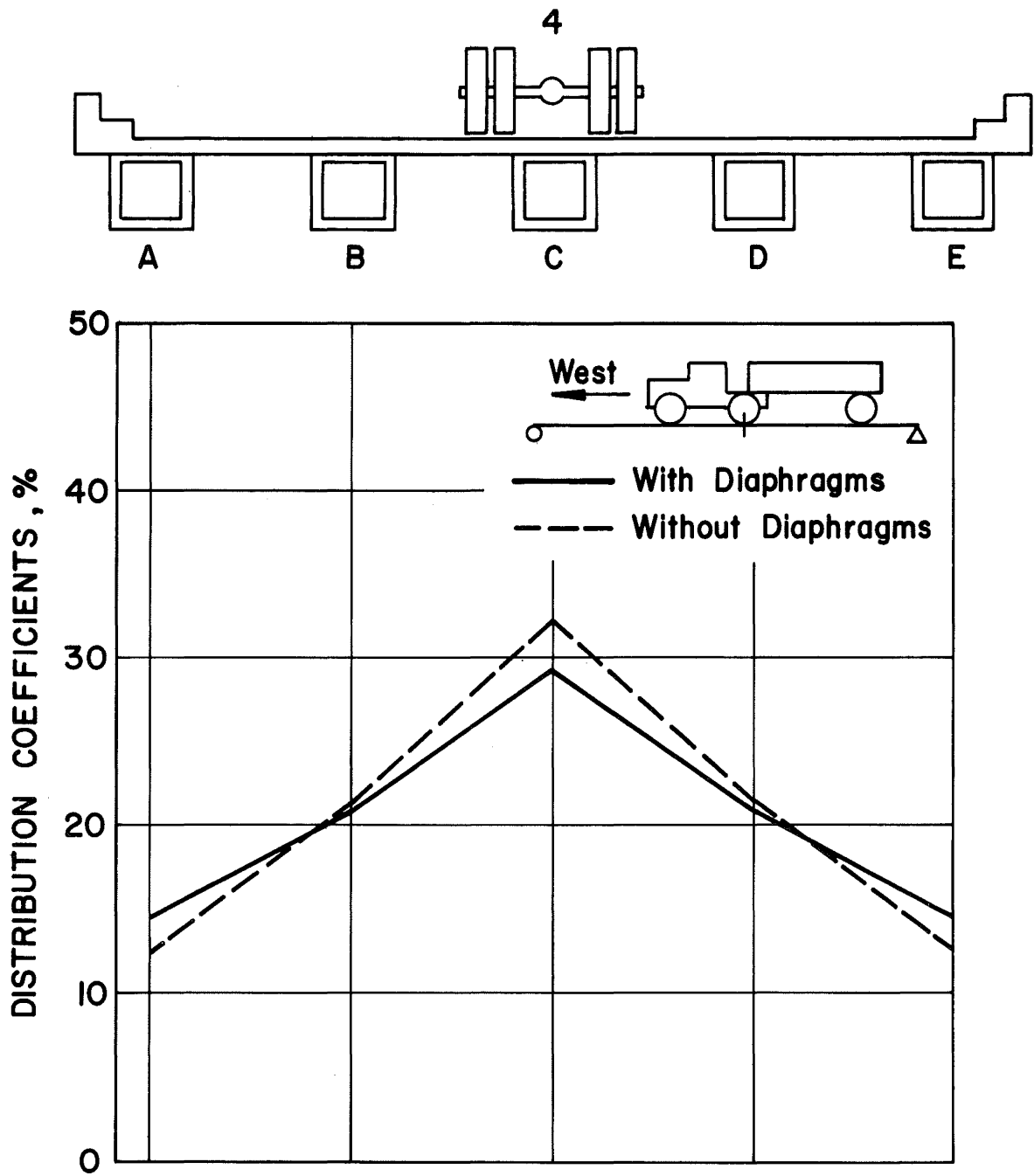


Fig. 14 Distribution Coefficients - Lane 4, Westbound

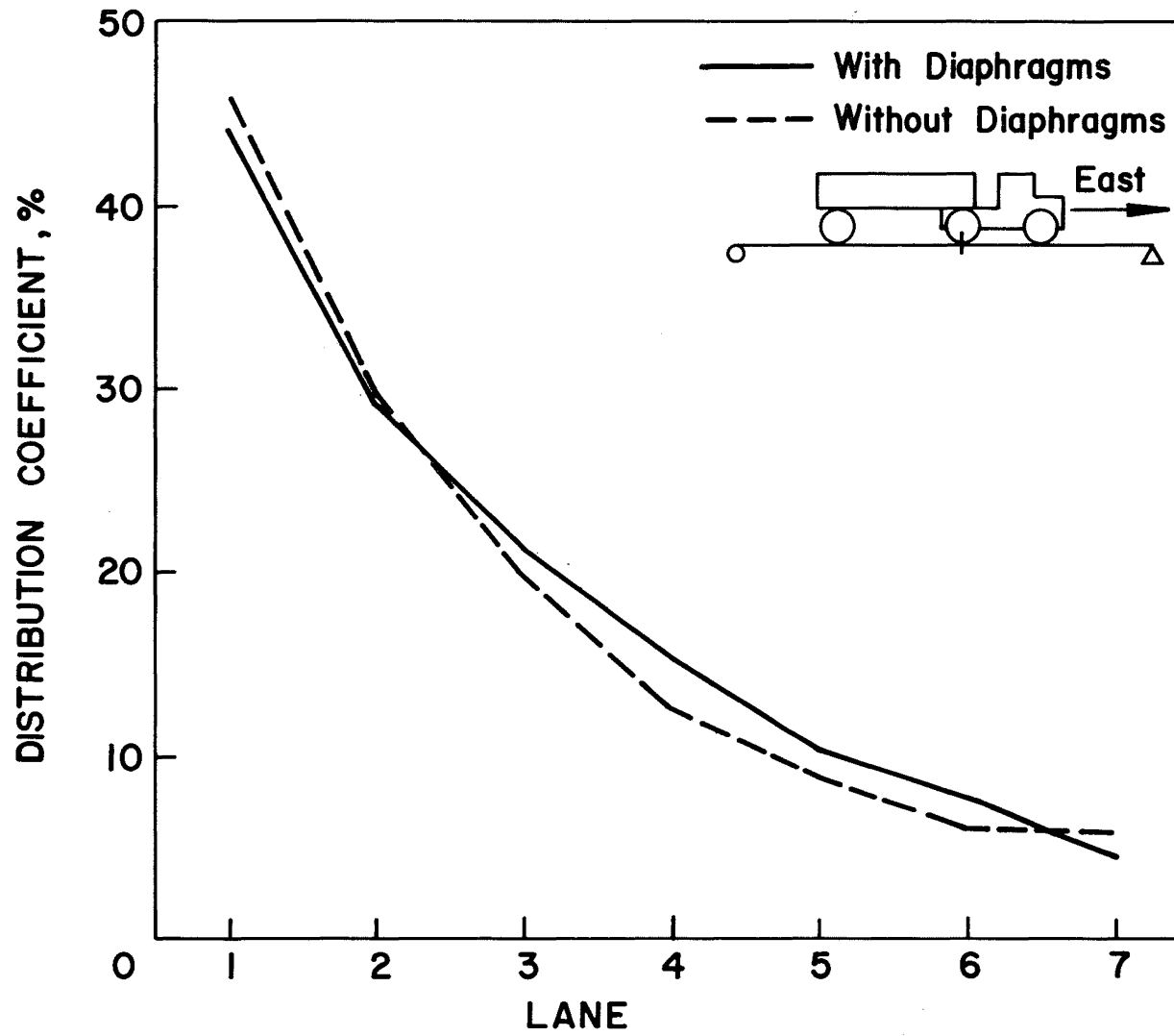


Fig. 15 Influence Line for Distribution Coefficients -
Beam A, Eastbound

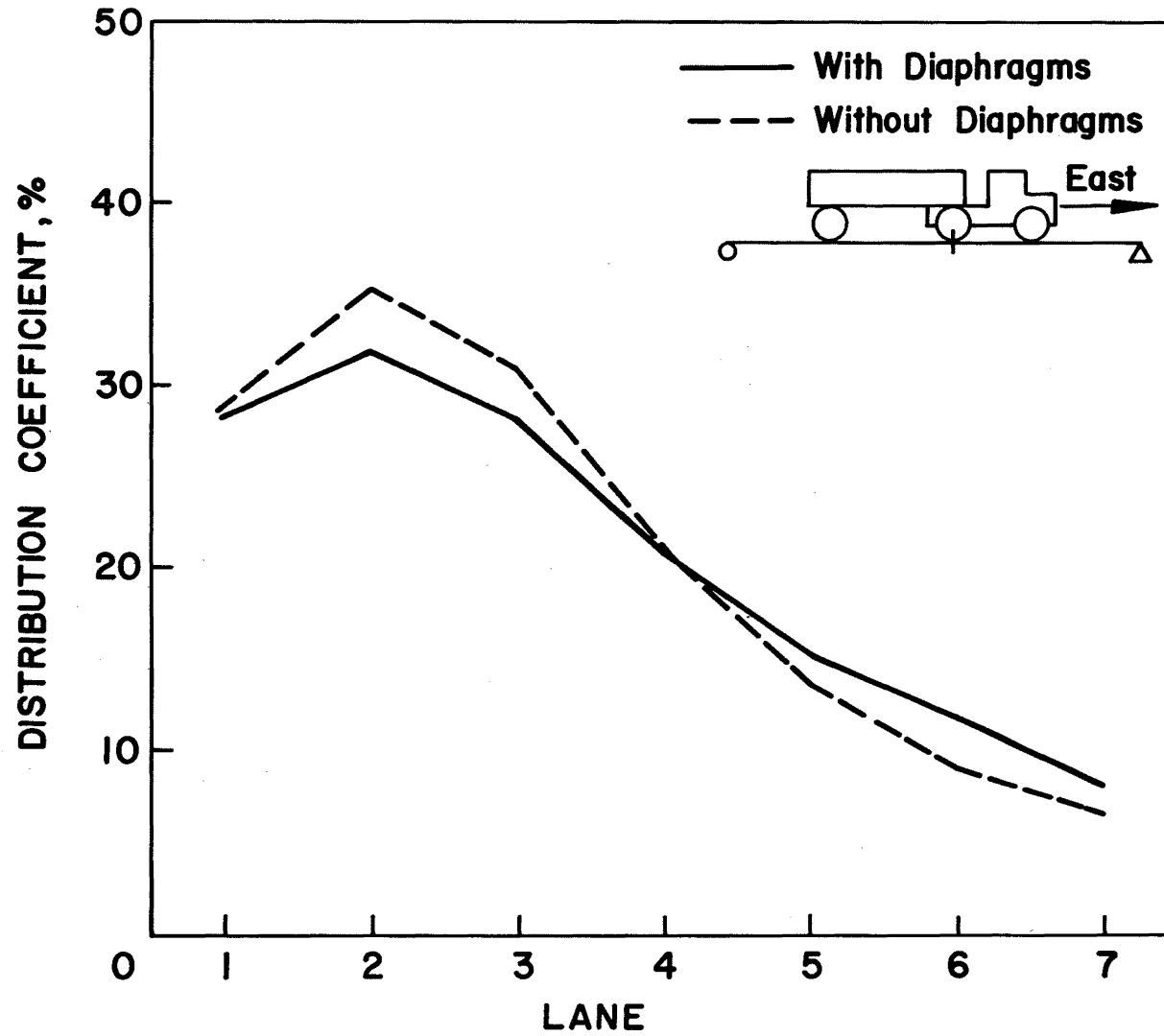


Fig. 16 Influence Line for Distribution Coefficients -
Beam B, Eastbound

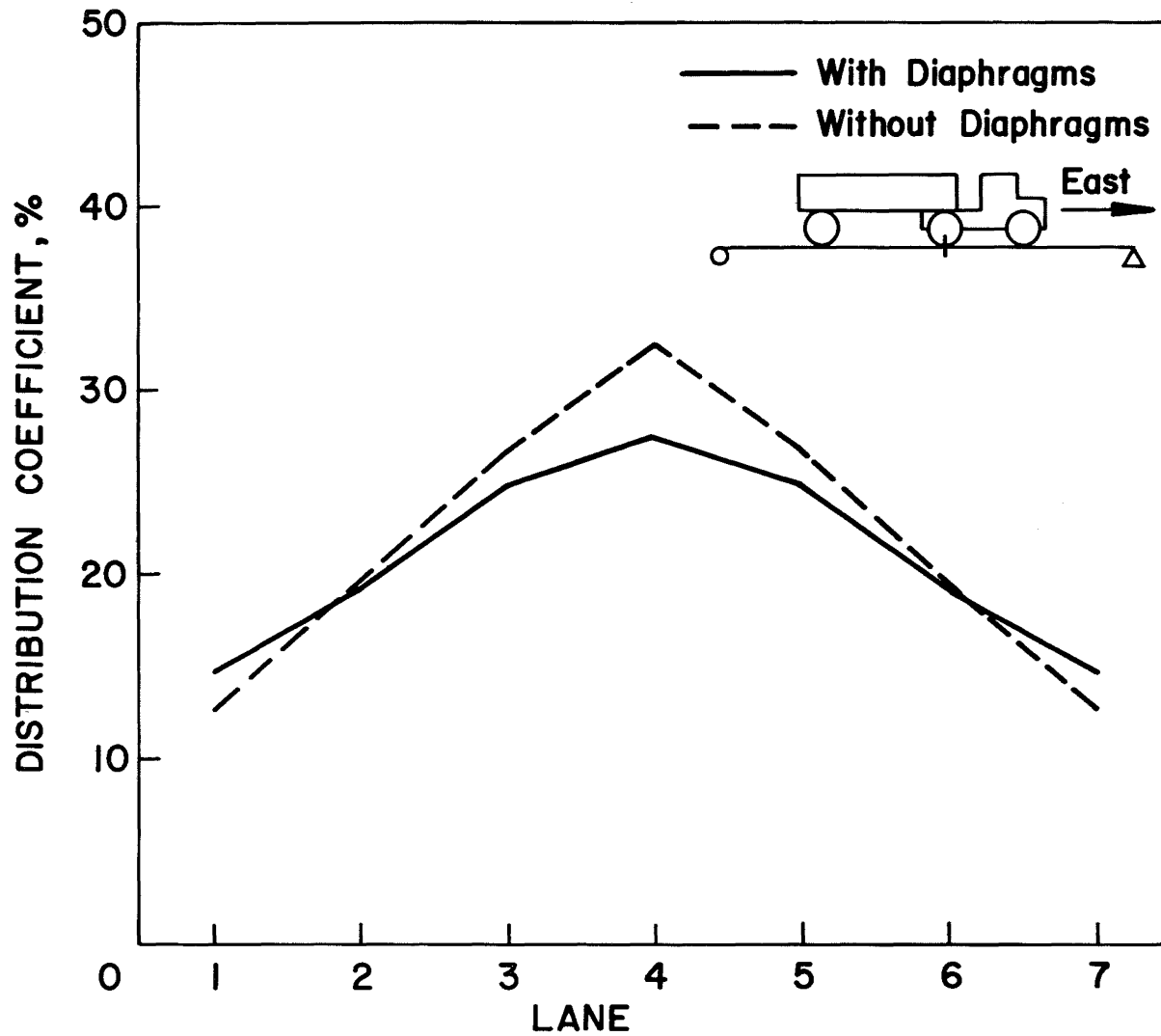


Fig. 17 Influence Line for Distribution Coefficients -
Beam C, Eastbound

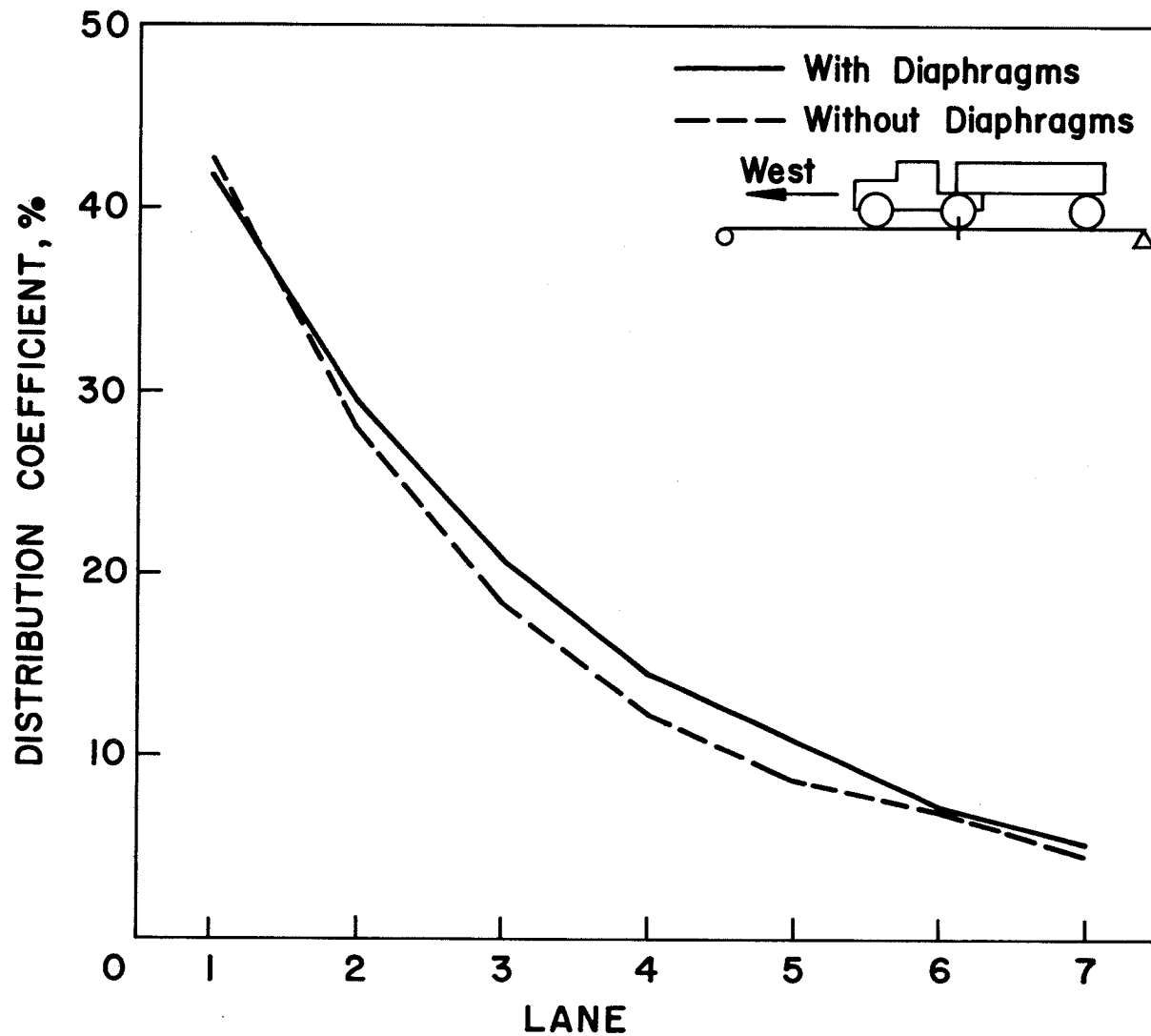


Fig. 18 Influence Line for Distribution Coefficients -
Beam A, Westbound

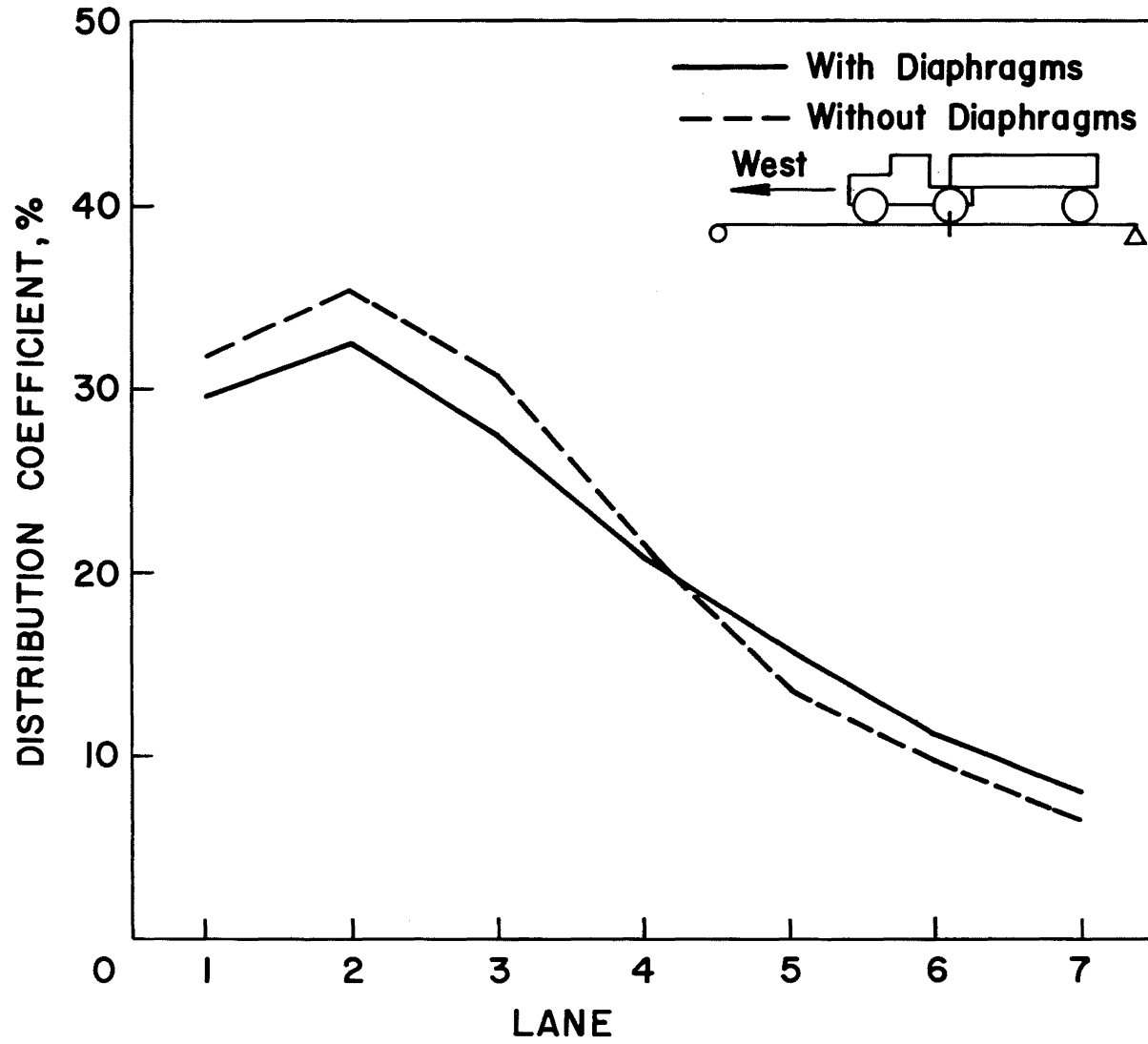


Fig. 19 Influence Line for Distribution Coefficients -
Beam B, Westbound

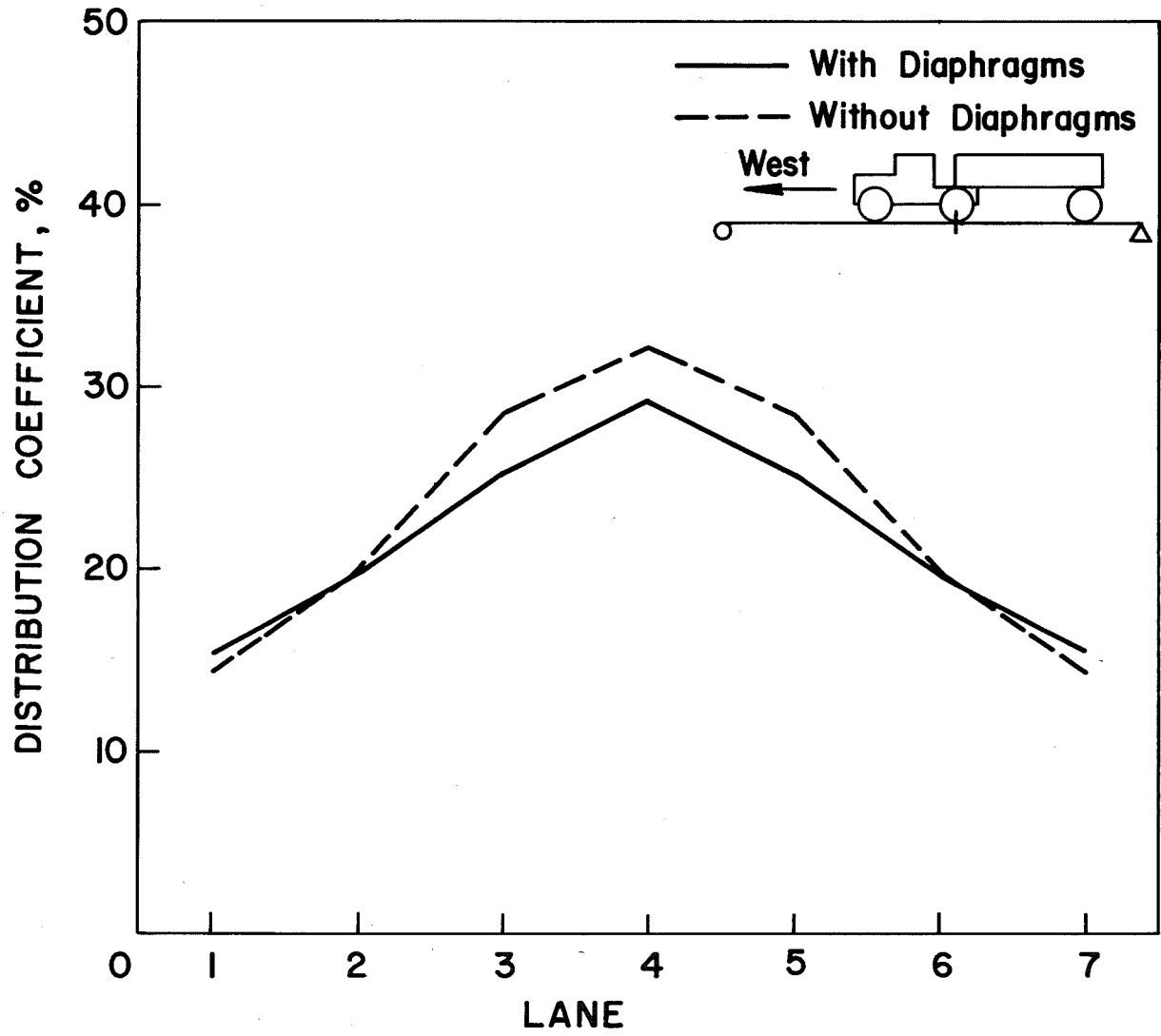


Fig. 20 Influence Line for Distribution Coefficients -
Beam C, Westbound

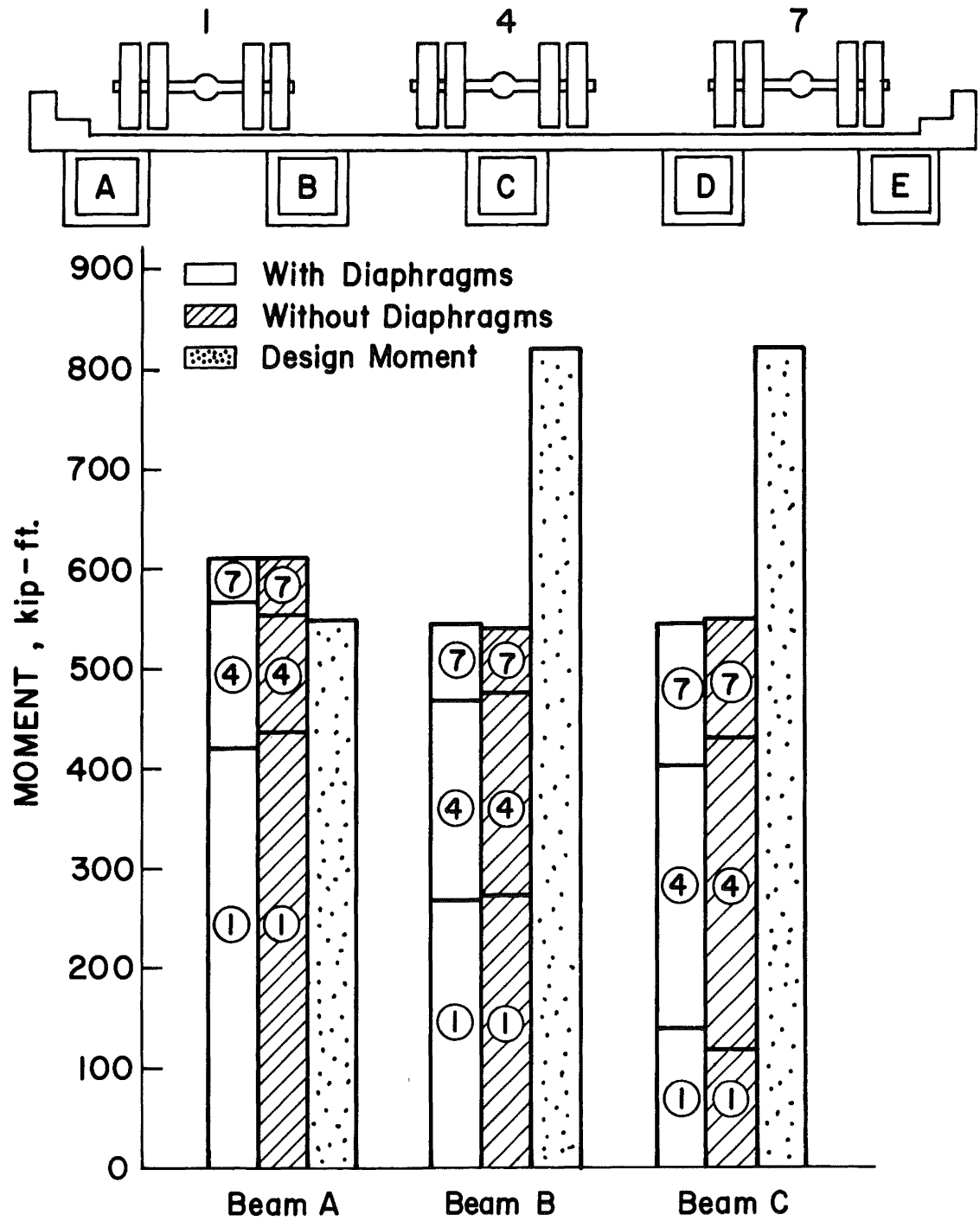


Fig. 21 Design and Experimental Live Load Moments - Eastbound

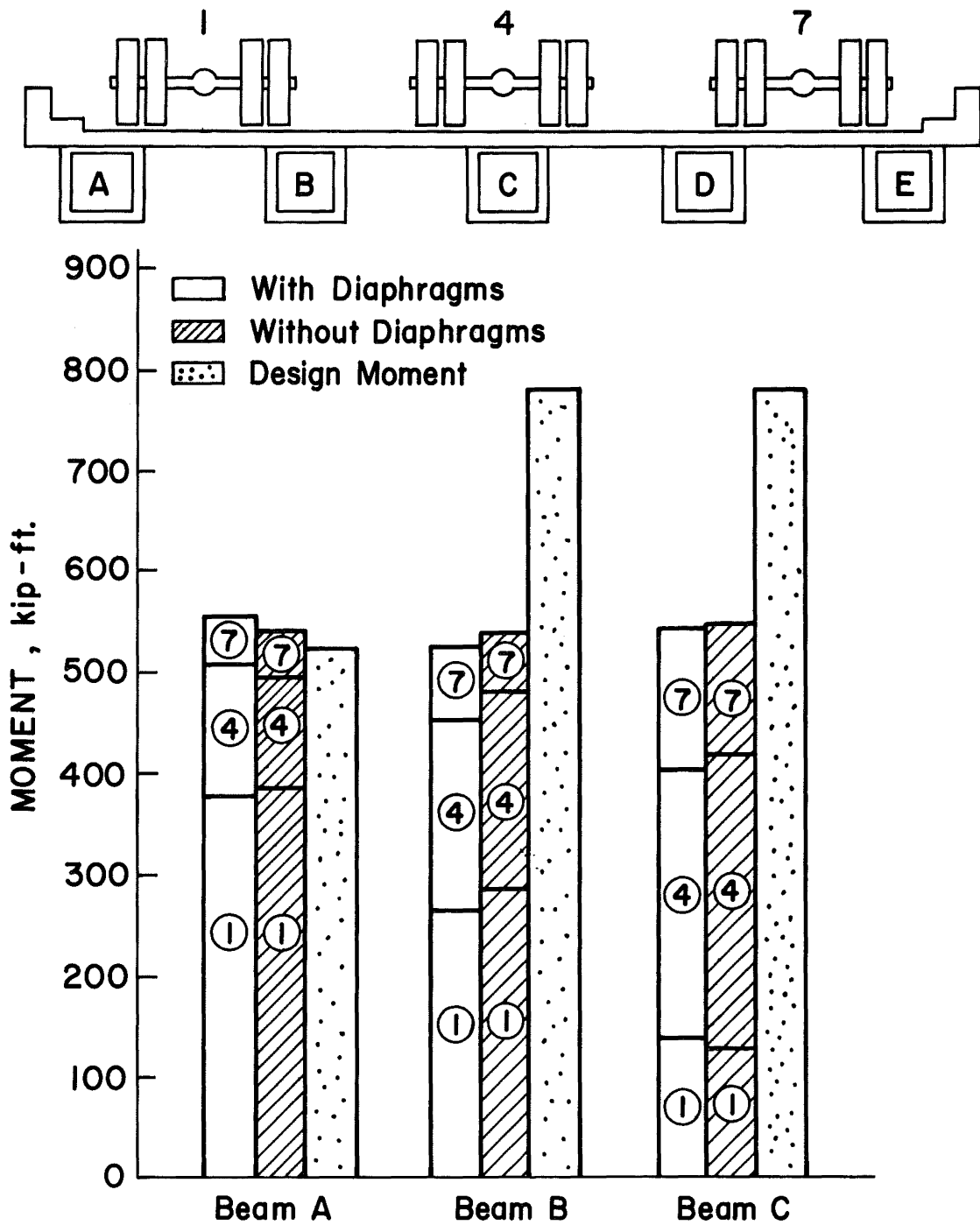


Fig. 22 Design and Experimental Live Load Moments - Westbound

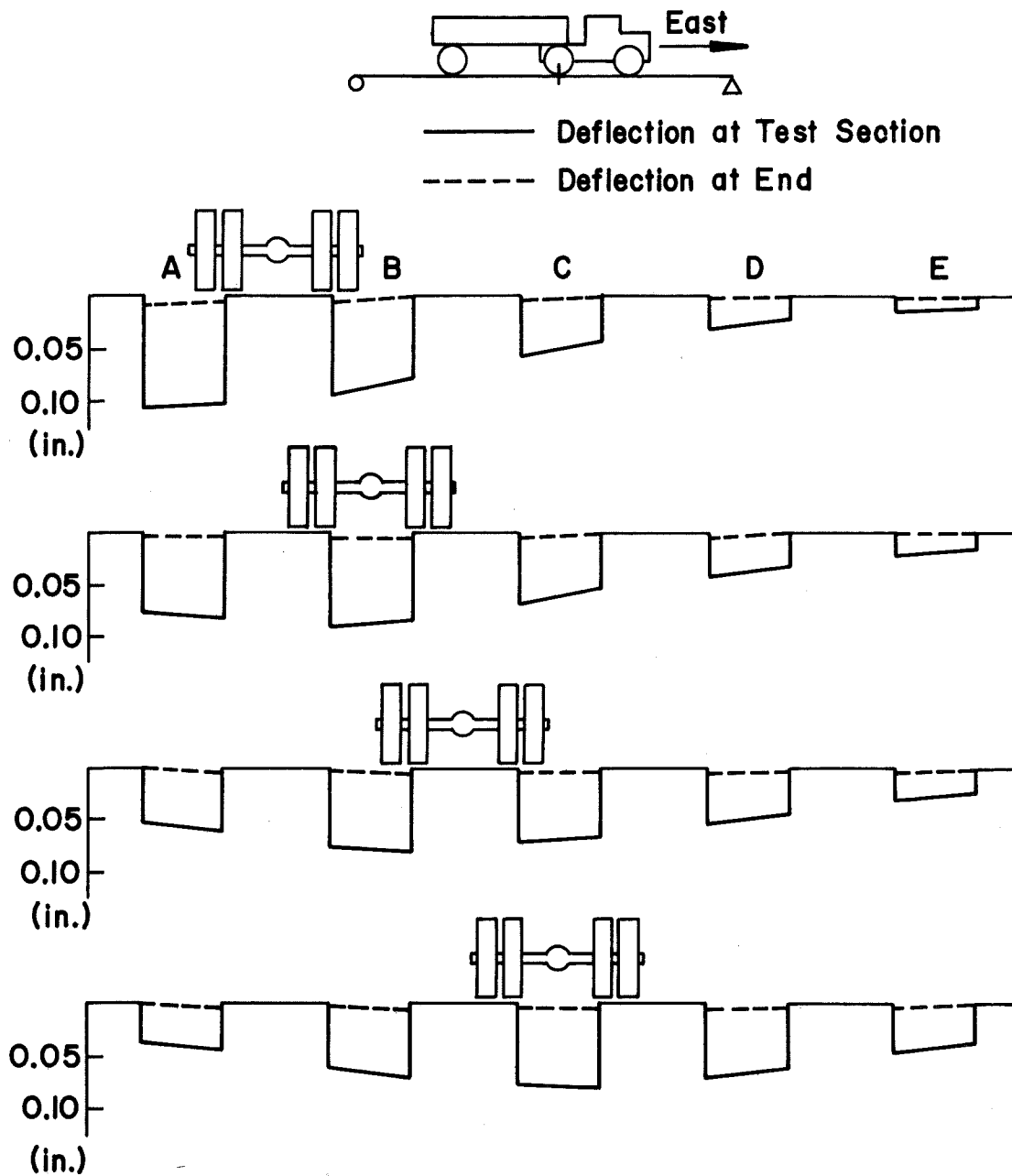


Fig. 23 Deflections at Test Section and End - With Diaphragms, Eastbound

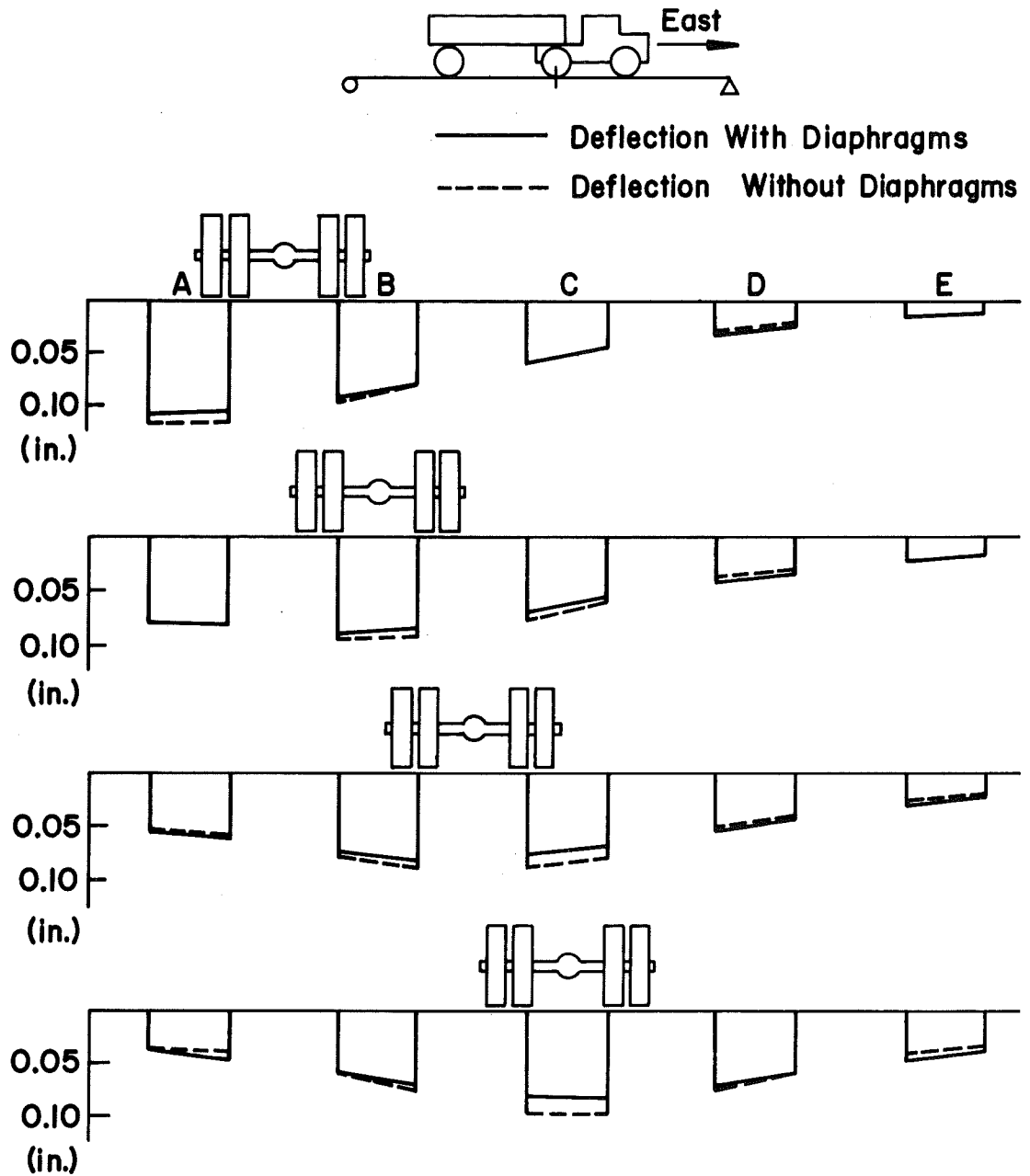


Fig. 24 Deflections at Test Section - Eastbound

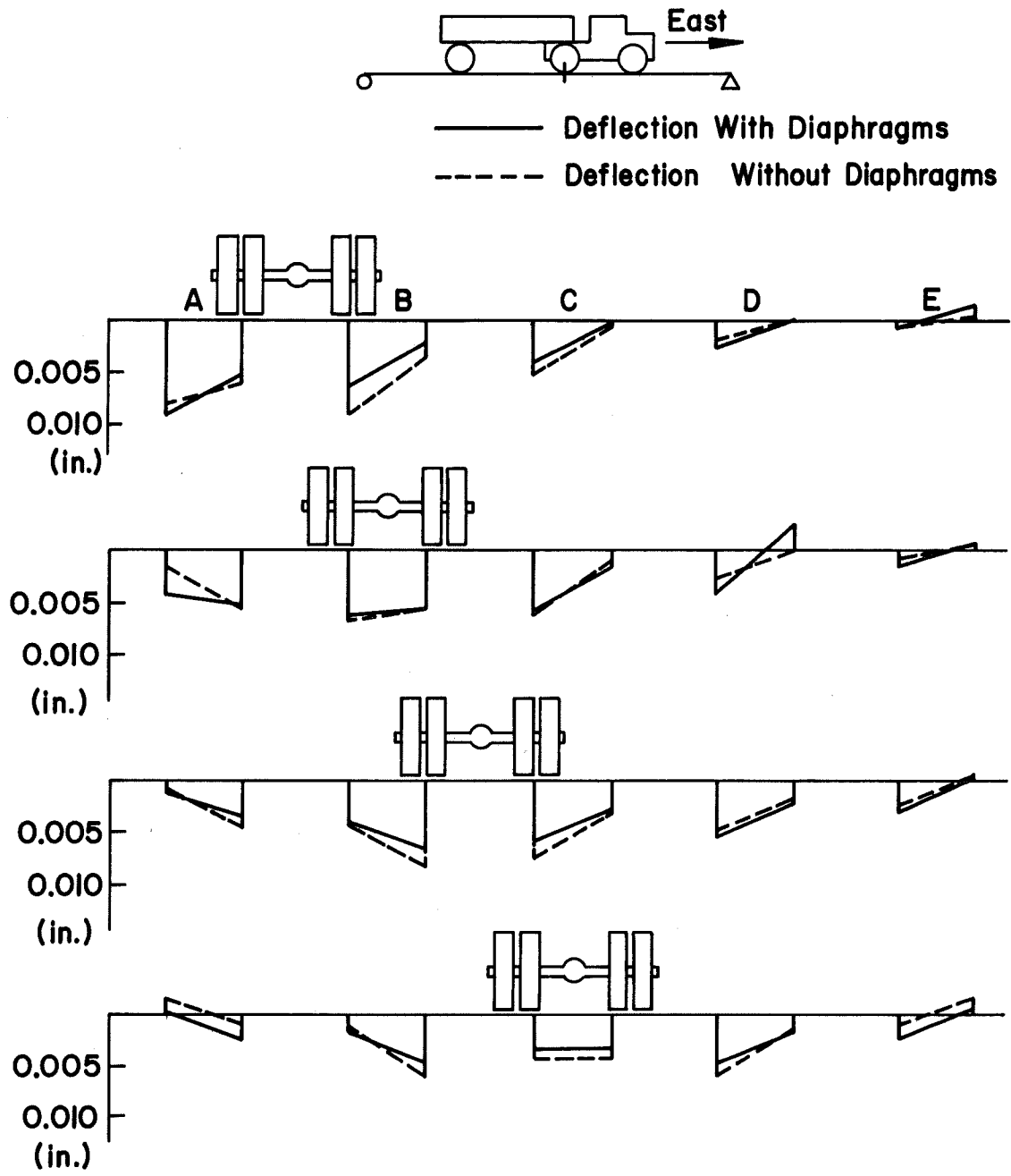


Fig. 25 Deflections at End - Eastbound

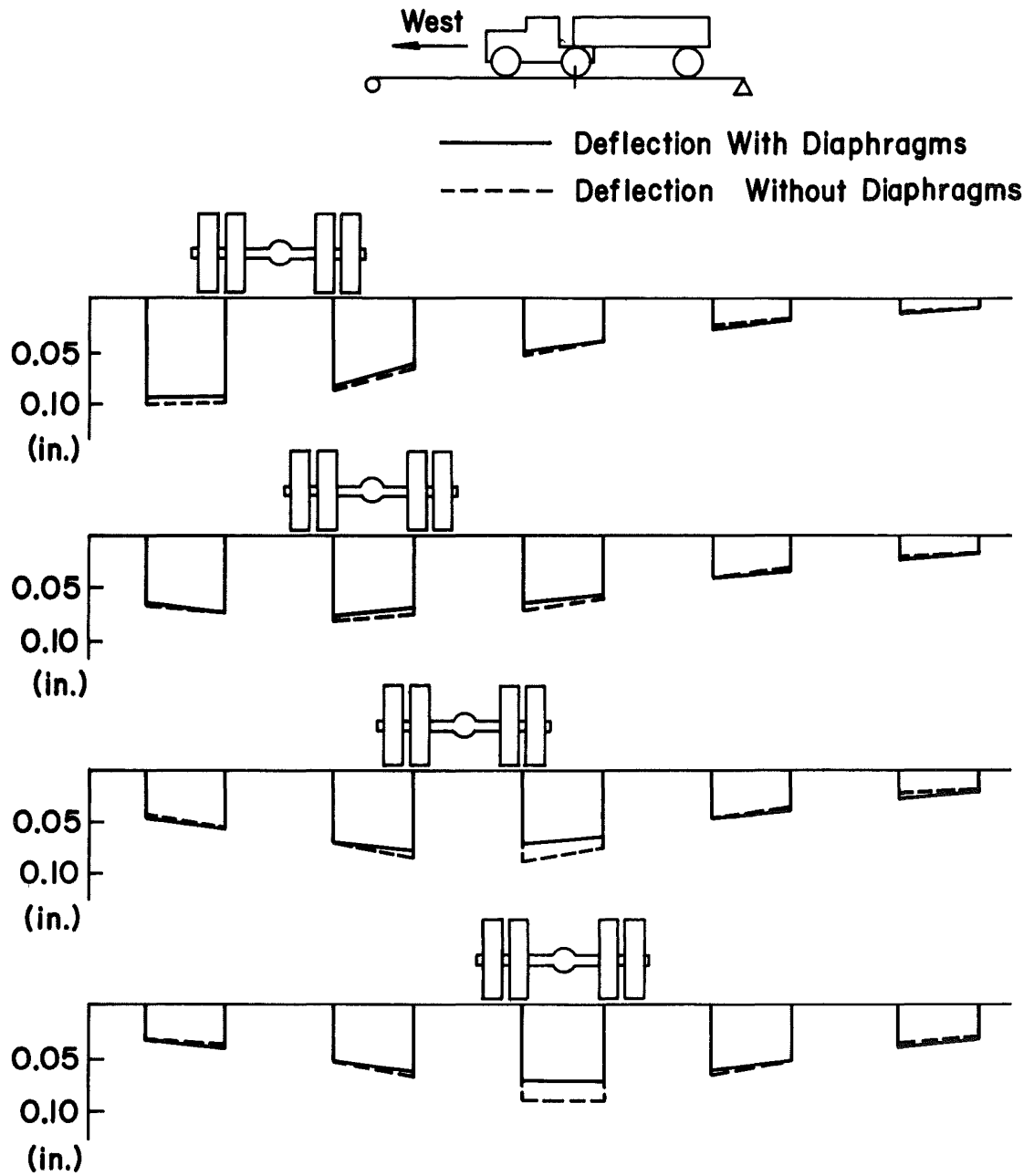


Fig. 26 Deflections at Test Section - Westbound

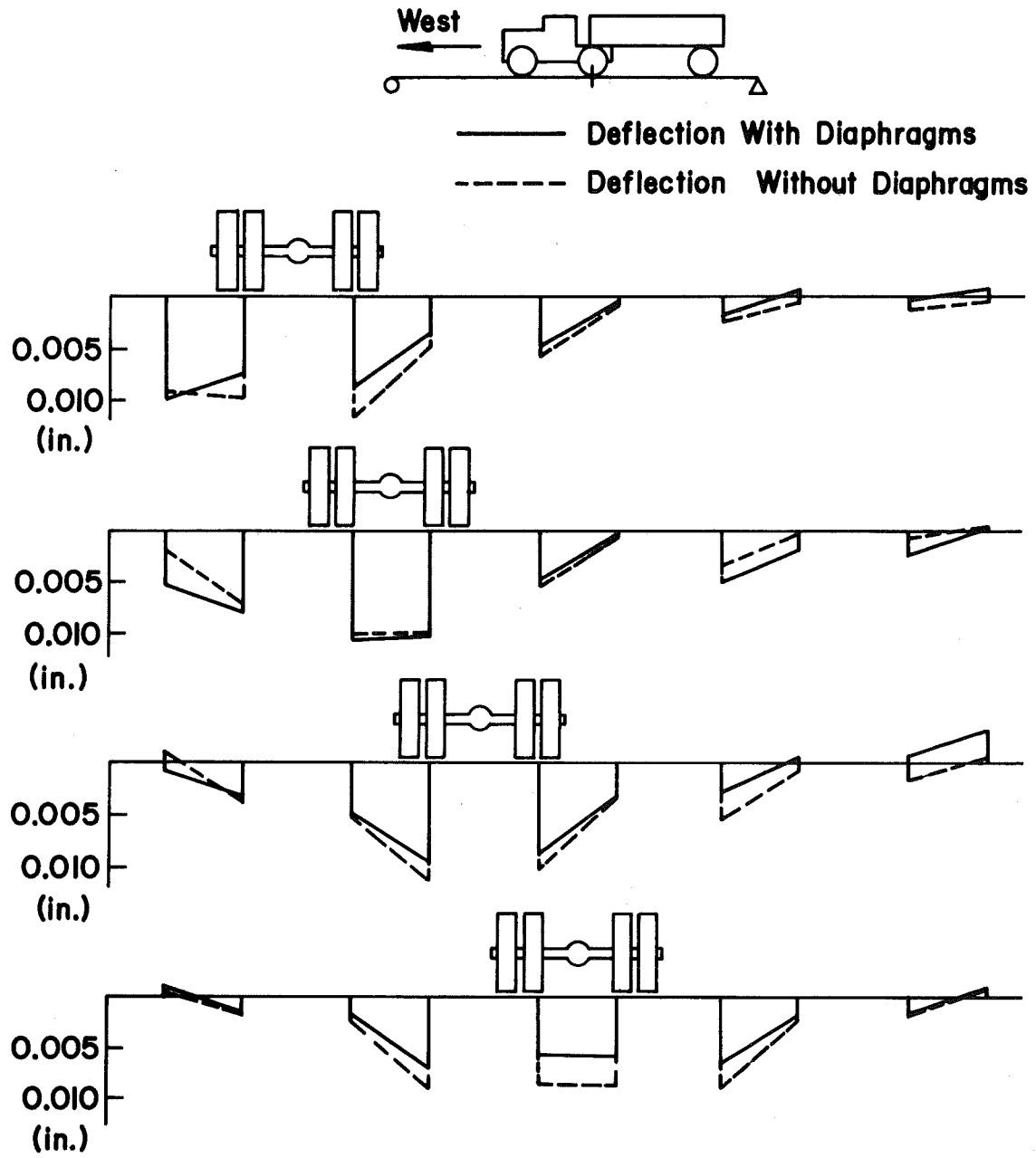


Fig. 27 Deflections at End - Westbound

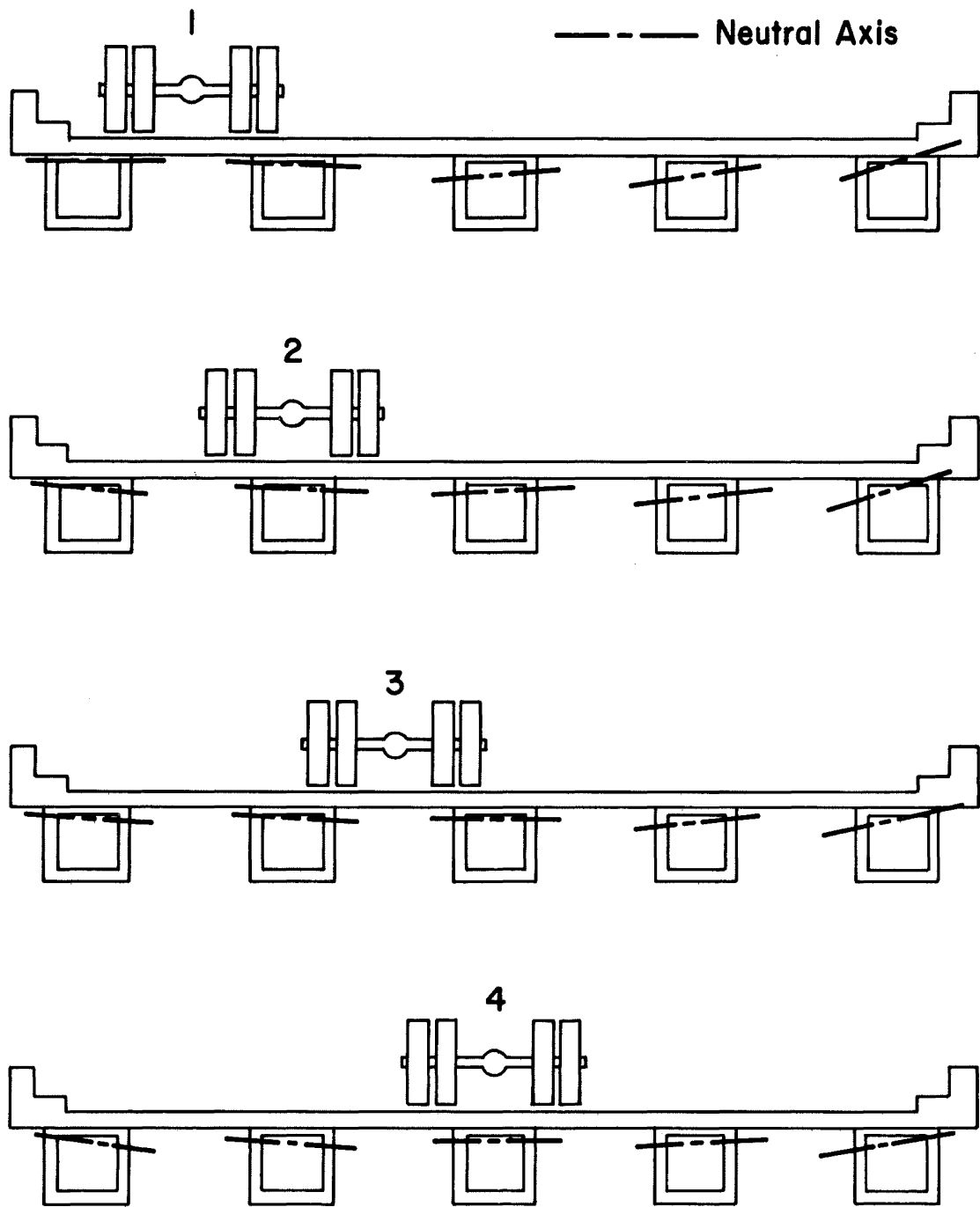


Fig. 28 Typical Examples of Neutral Axis Locations for Various Lane Loading

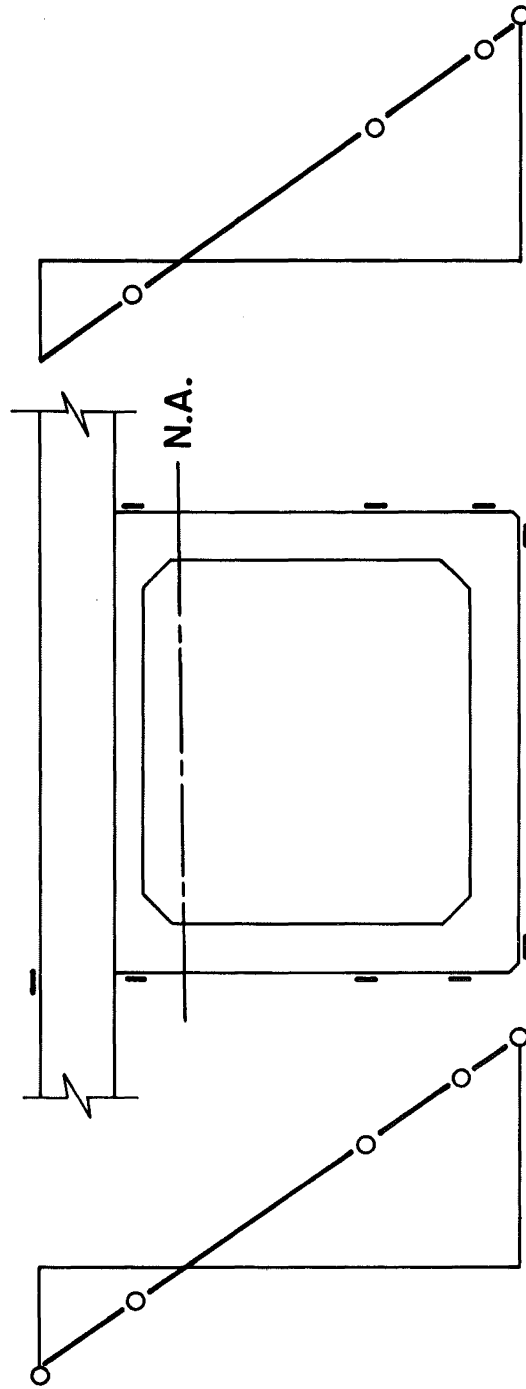


Fig. 29 Typical Strain Distribution in an Interior Beam

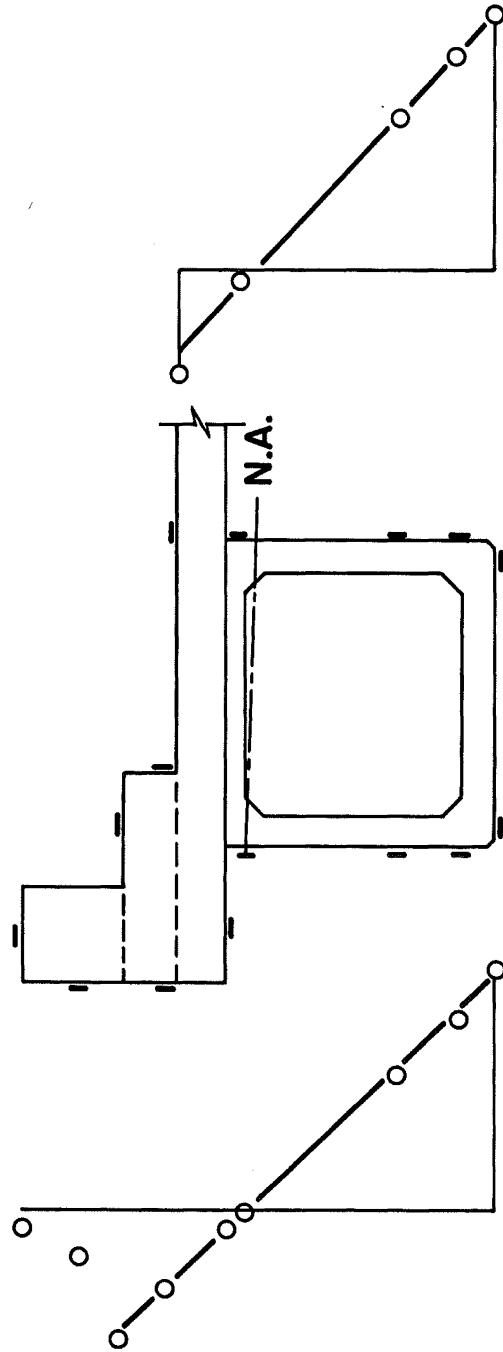


Fig. 30 Typical Strain Distribution in an Exterior Beam

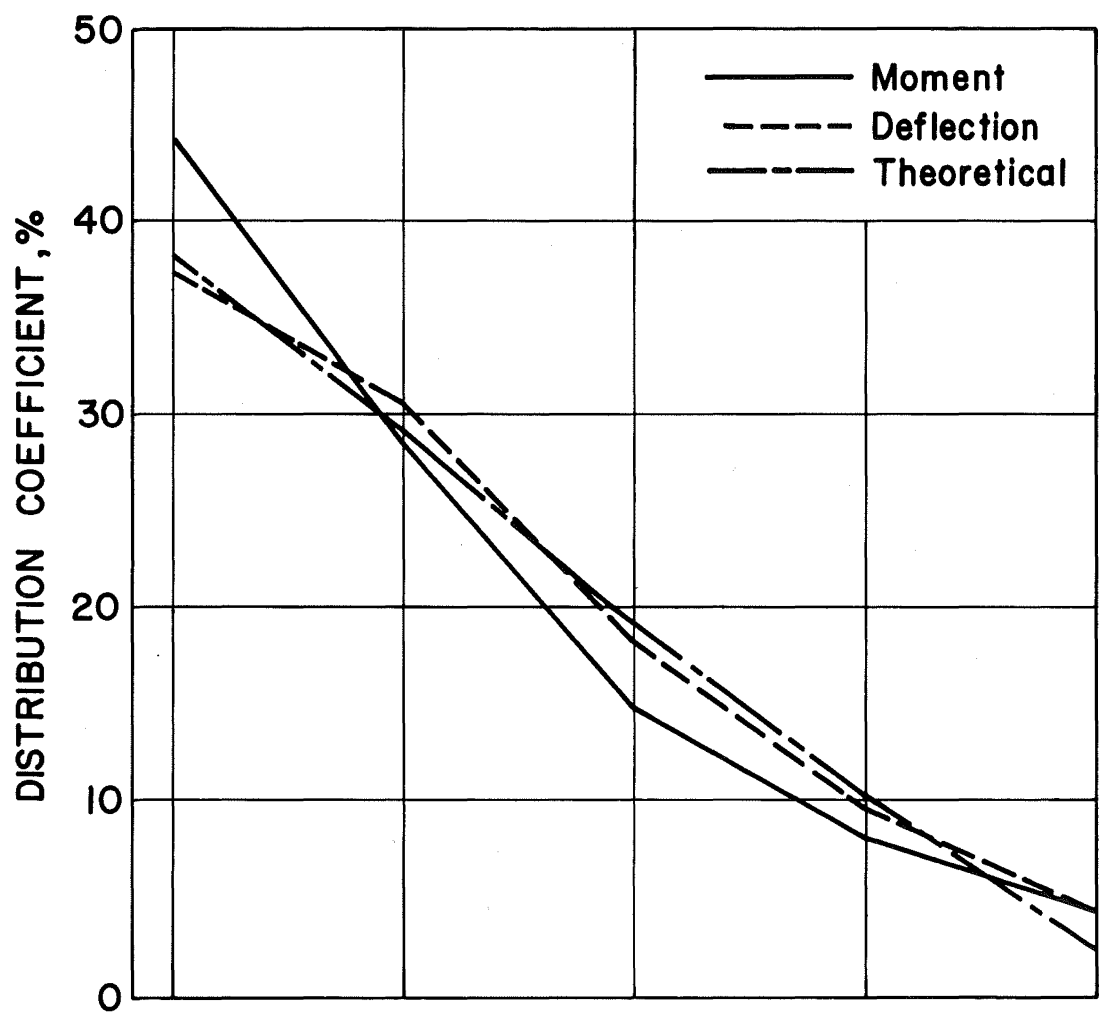
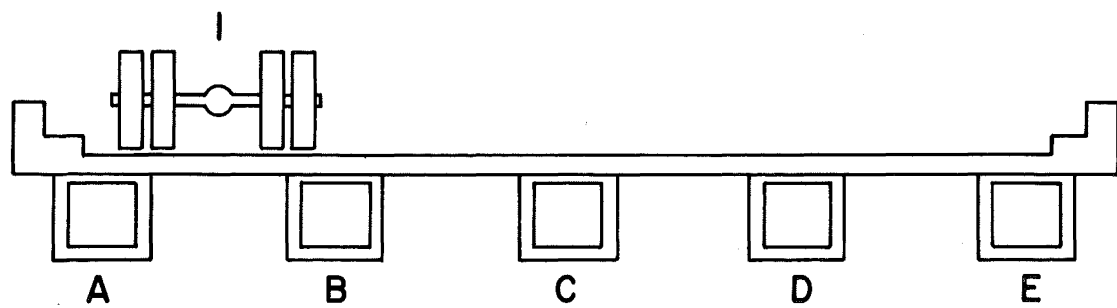


Fig. 31 Comparison of Test Results and Guyon-Massonnet Theory - Distribution Coefficients, With Diaphragms

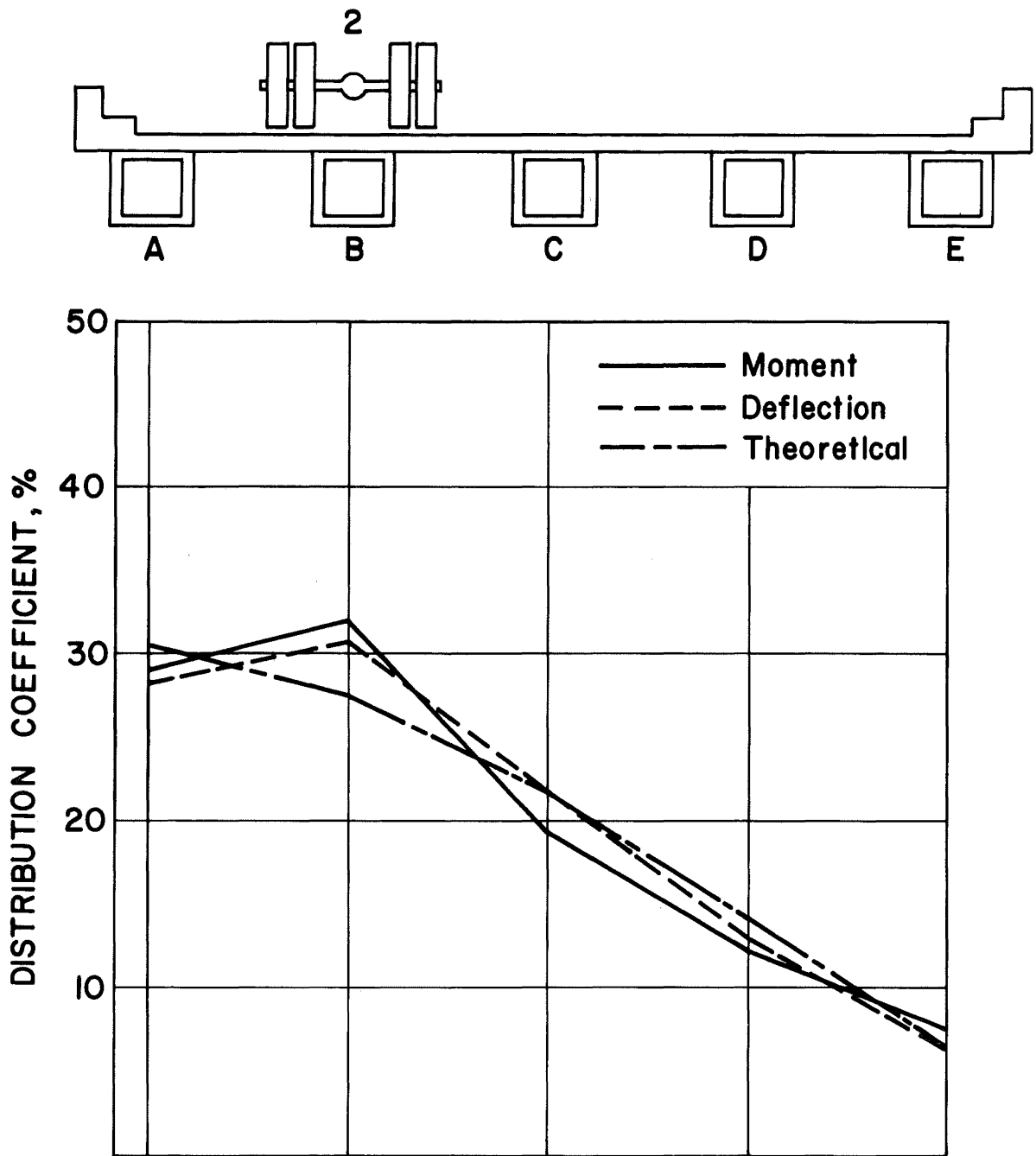


Fig. 32 Comparison of Test Results and Guyon-Massonnet Theory - Distribution Coefficients, With Diaphragms

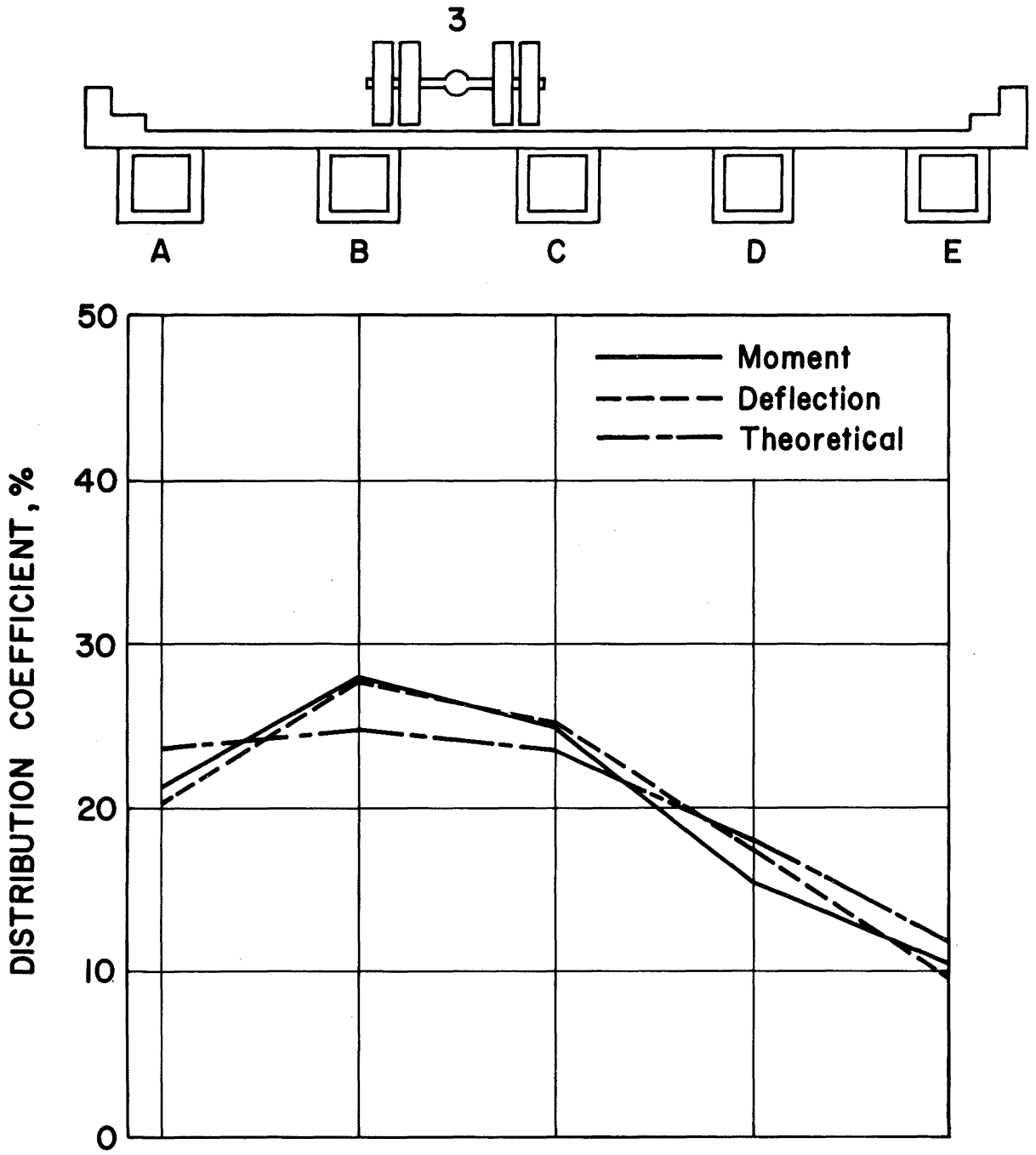


Fig. 33 Comparison of Test Results and Guyon-Massonnet Theory - Distribution Coefficients, With Diaphragms

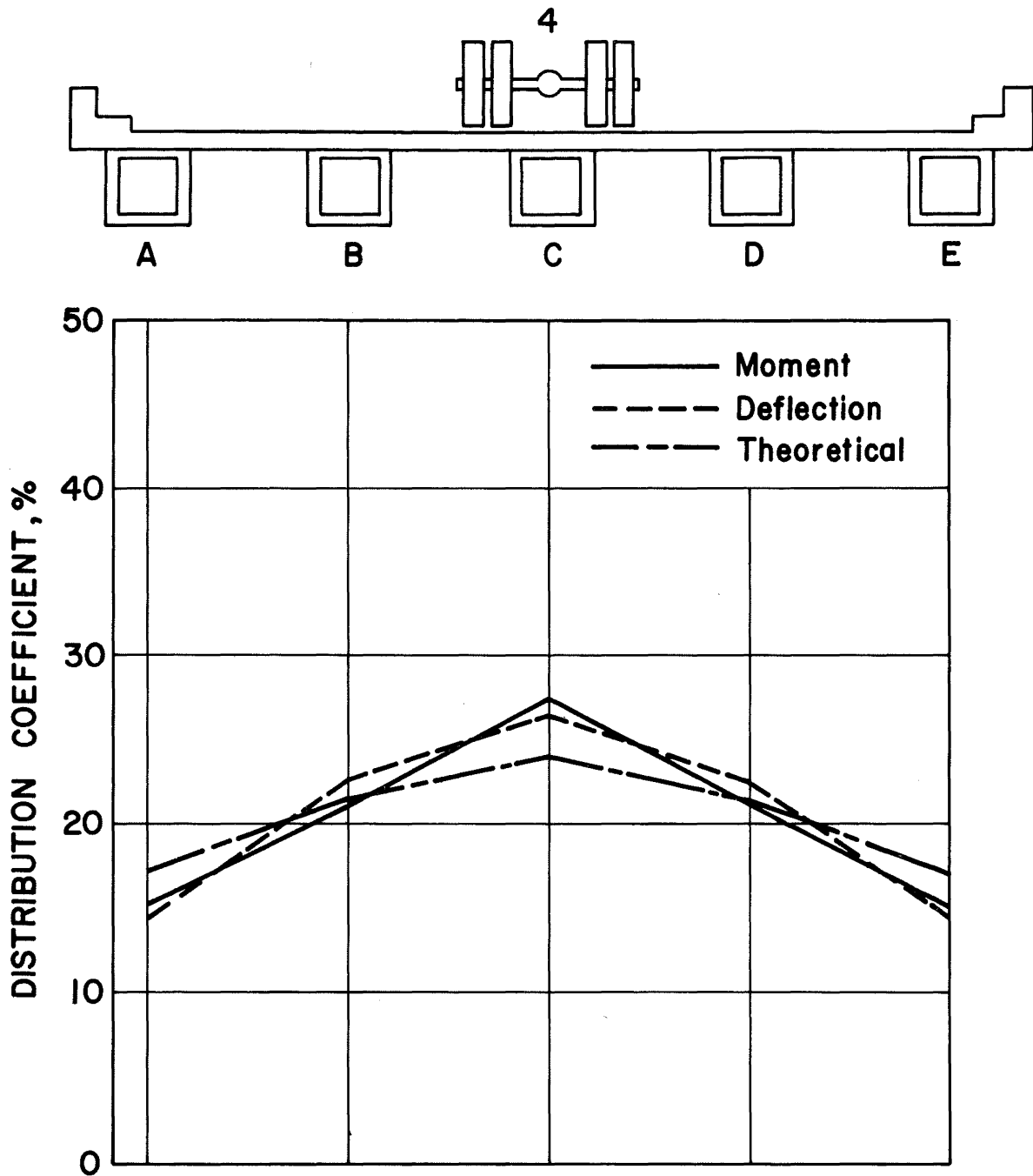


Fig. 34 Comparison of Test Results and Guyon-Massonnet Theory - Distribution Coefficients, With Diaphragms

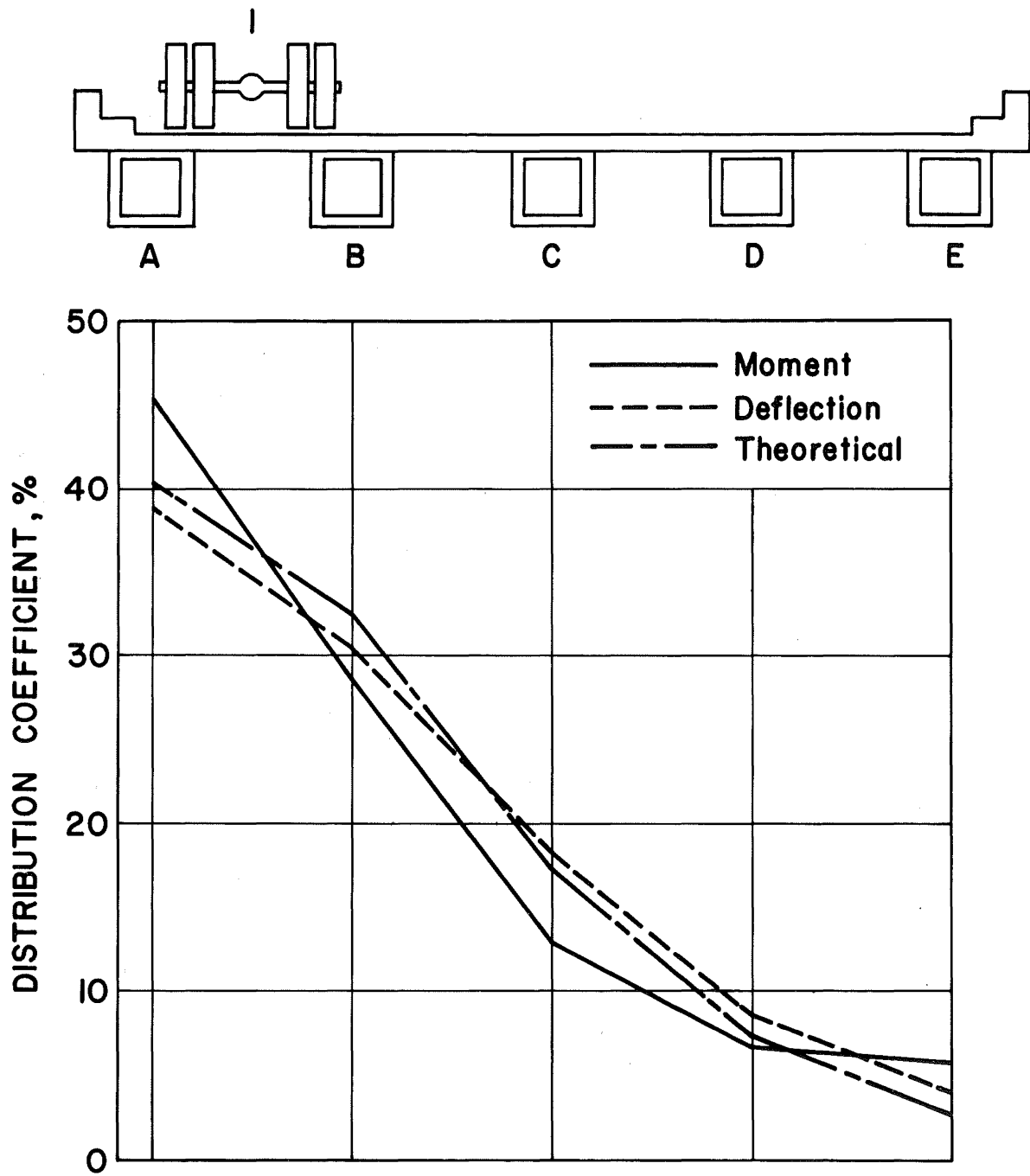


Fig. 35 Comparison of Test Results and Guyon-Massonnet Theory - Distribution Coefficients, Without Diaphragms

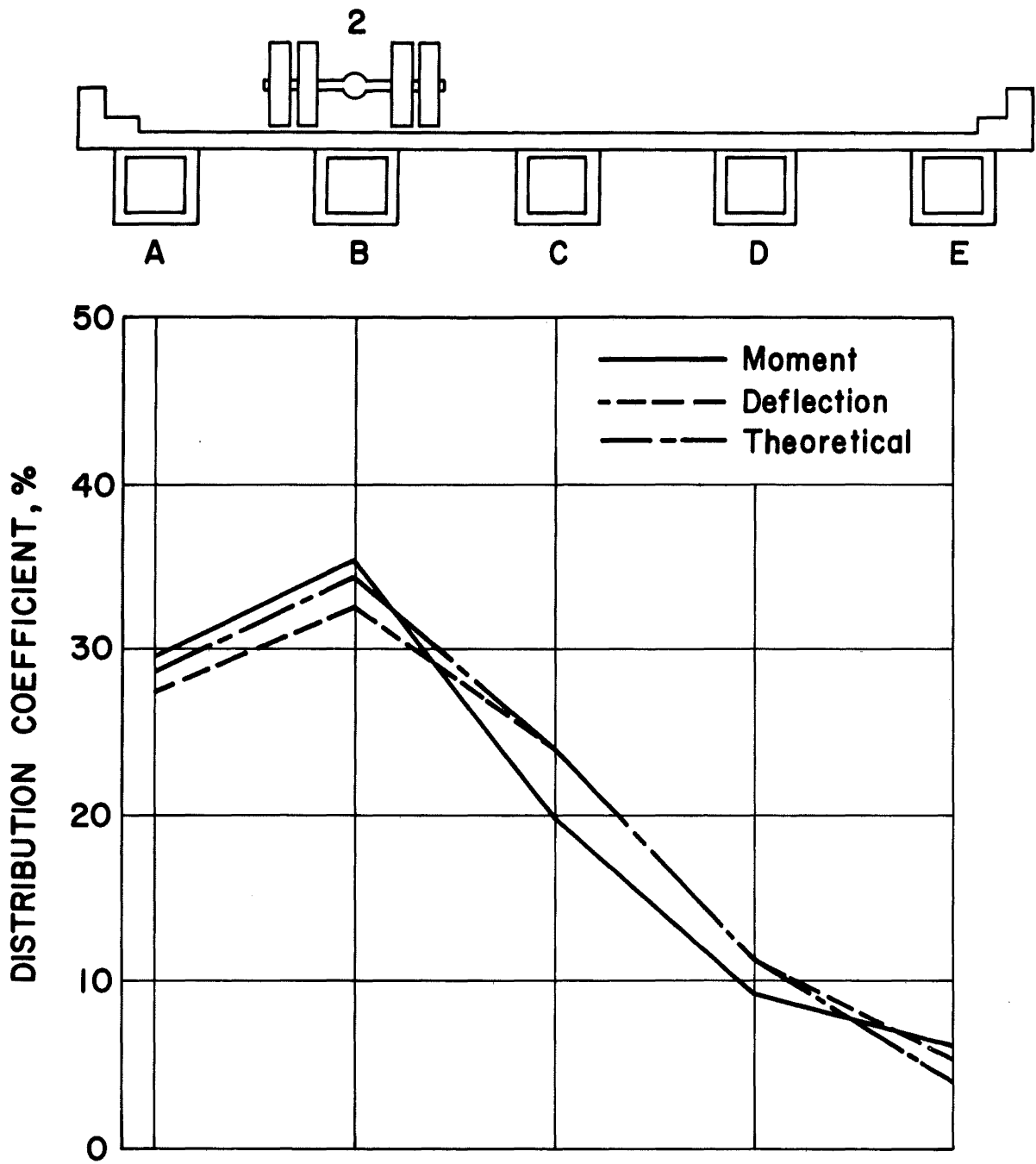


Fig. 36 Comparison of Test Results and Guyon-Massonnet Theory - Distribution Coefficients, Without Diaphragms

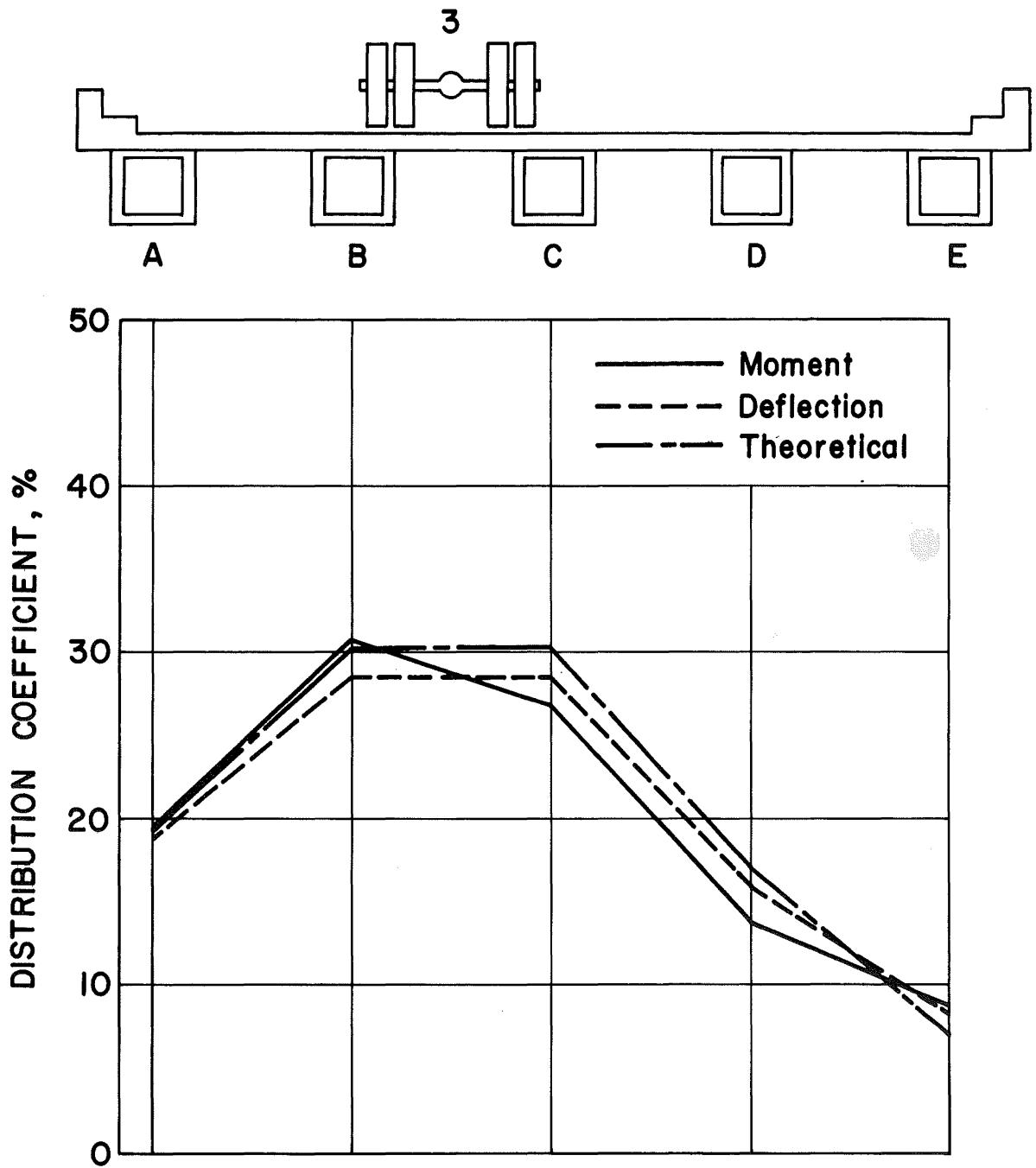


Fig. 37 Comparison of Test Results and Guyon-Massonnet Theory - Distribution Coefficients, Without Diaphragms

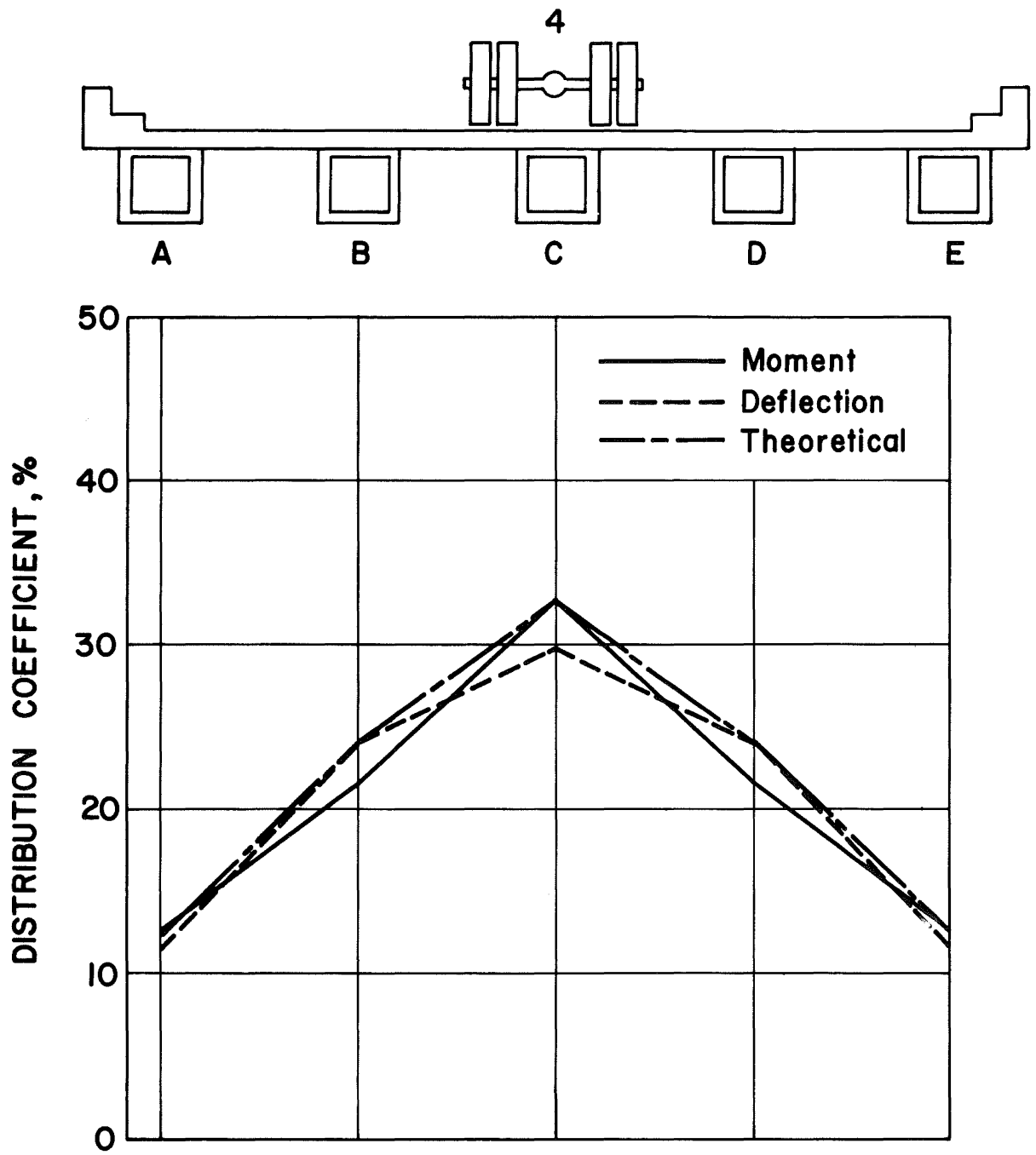


Fig. 38 Comparison of Test Results and Guyon-Massonnet Theory - Distribution Coefficients, Without Diaphragms

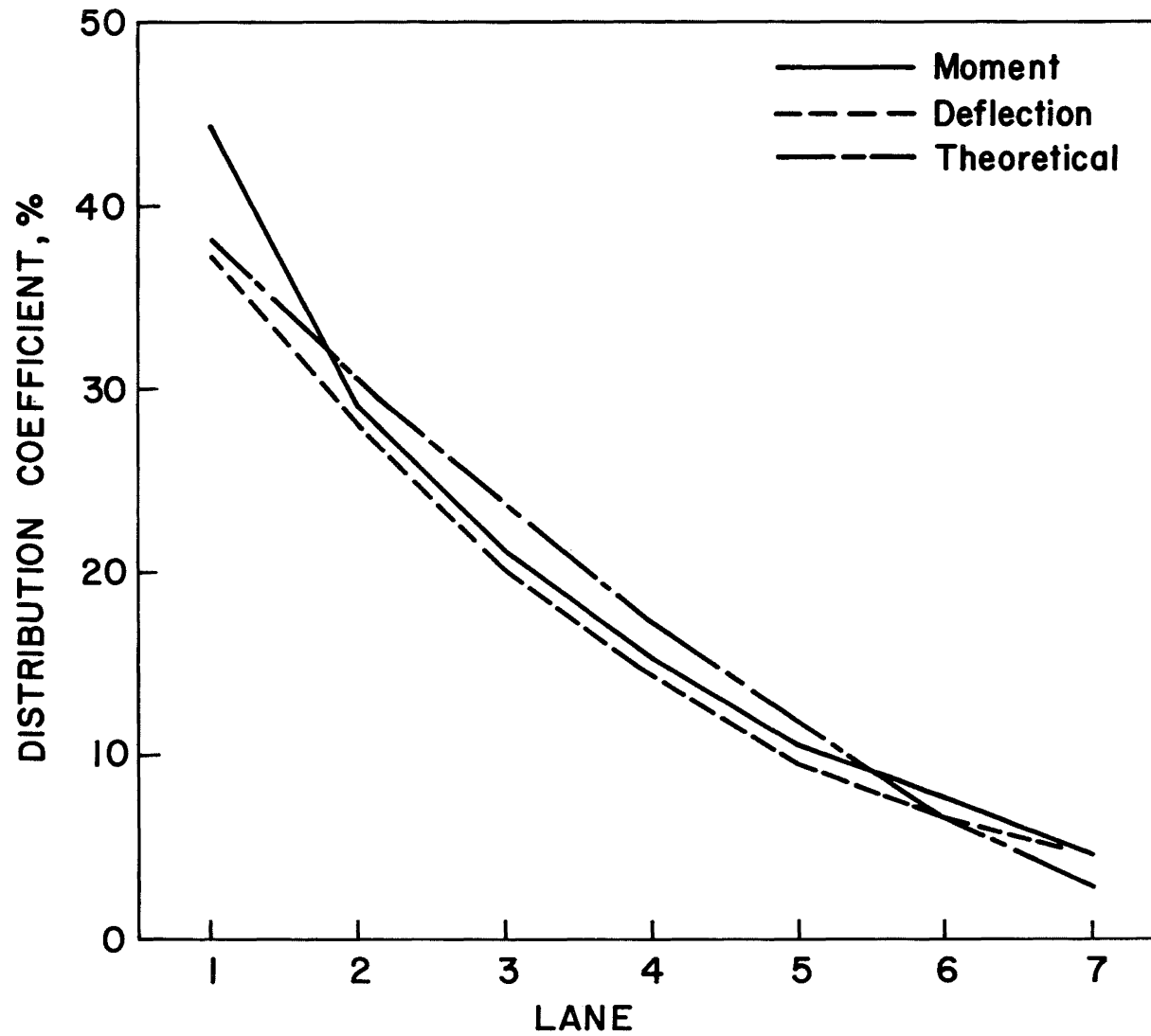


Fig. 39 Comparison of Test Results and Guyon-Massonnet Theory - Influence Line for Distribution Coefficients, Beam A, With Diaphragms

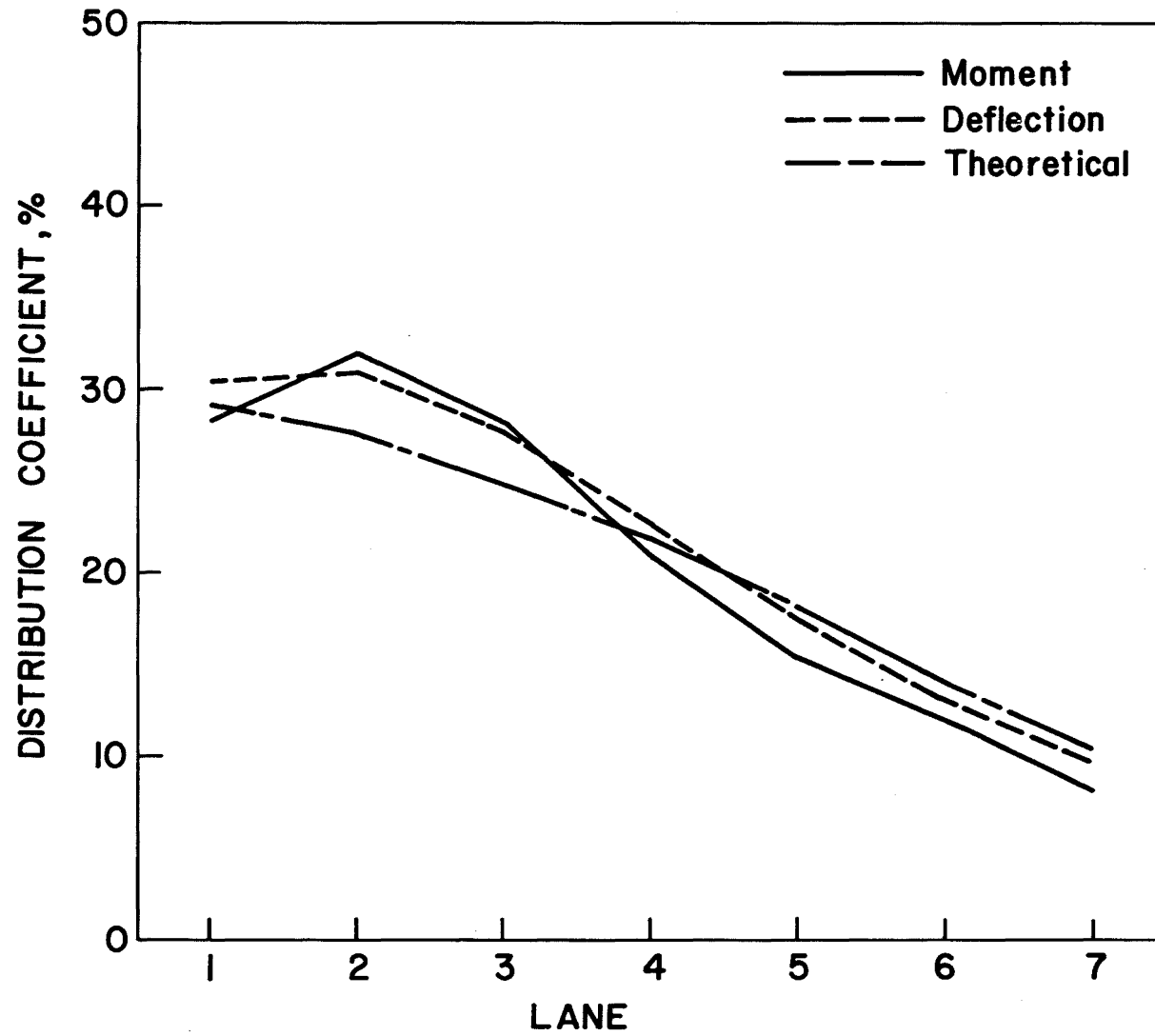


Fig. 40 Comparison of Test Results and Guyon-Massonnet Theory - Influence Line for Distribution Coefficients, Beam B, With Diaphragms

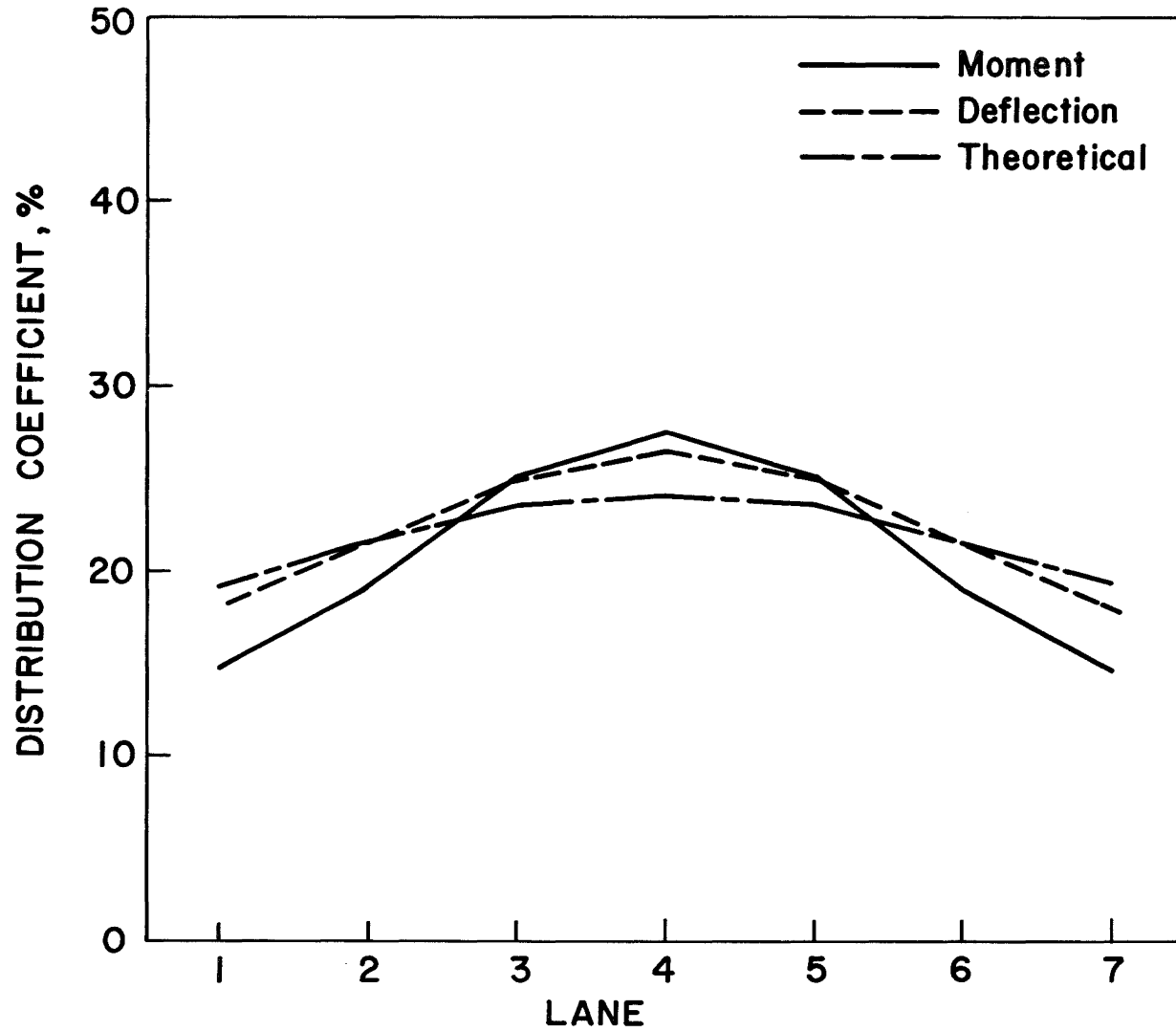


Fig. 41 Comparison of Test Results and Guyon-Massonnet Theory - Influence Line for Distribution Coefficients, Beam C, With Diaphragms

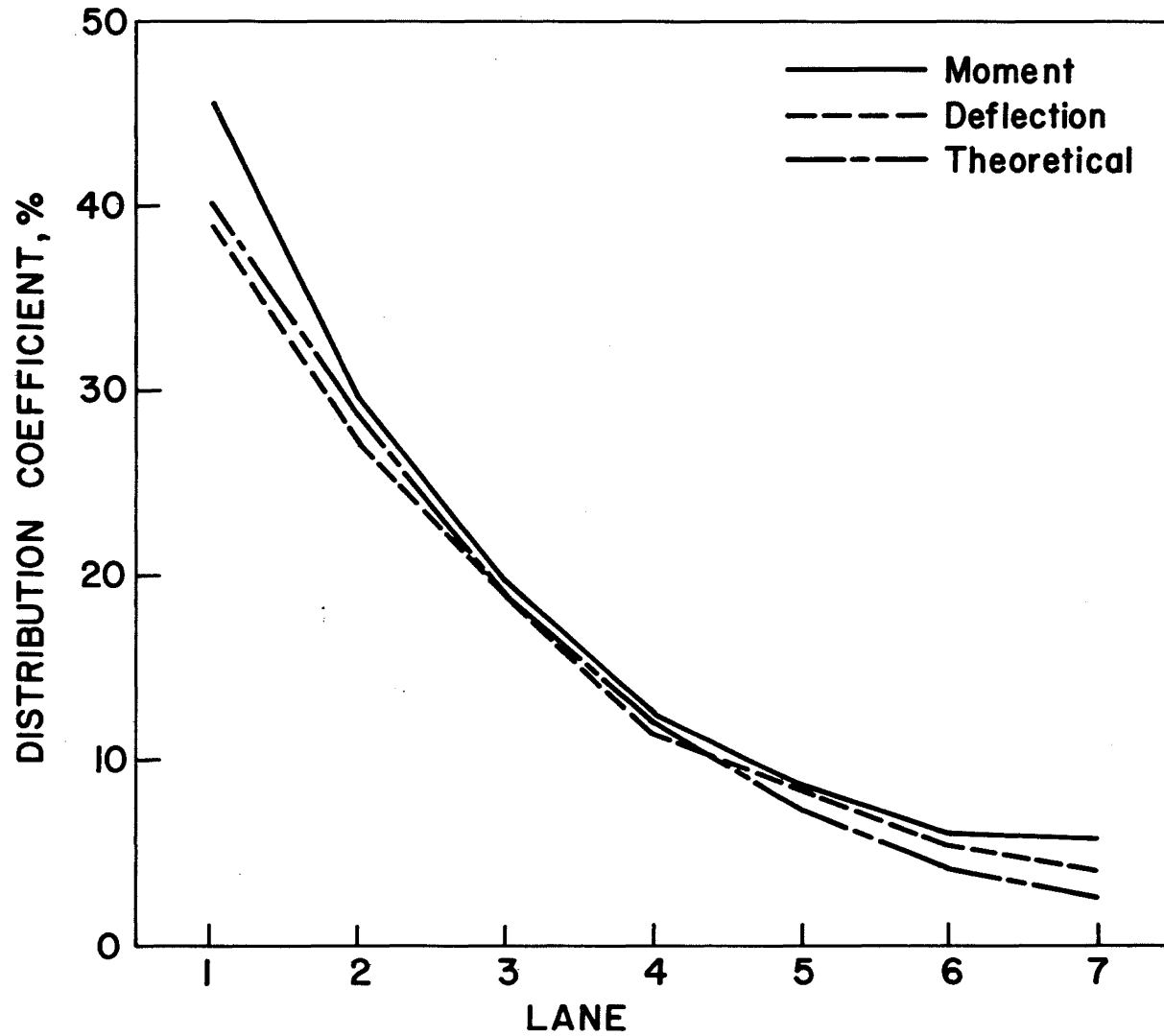


Fig. 42 Comparison of Test Results and Guyon-Massonnet Theory - Influence Line for Distribution Coefficients, Beam A, Without Diaphragms

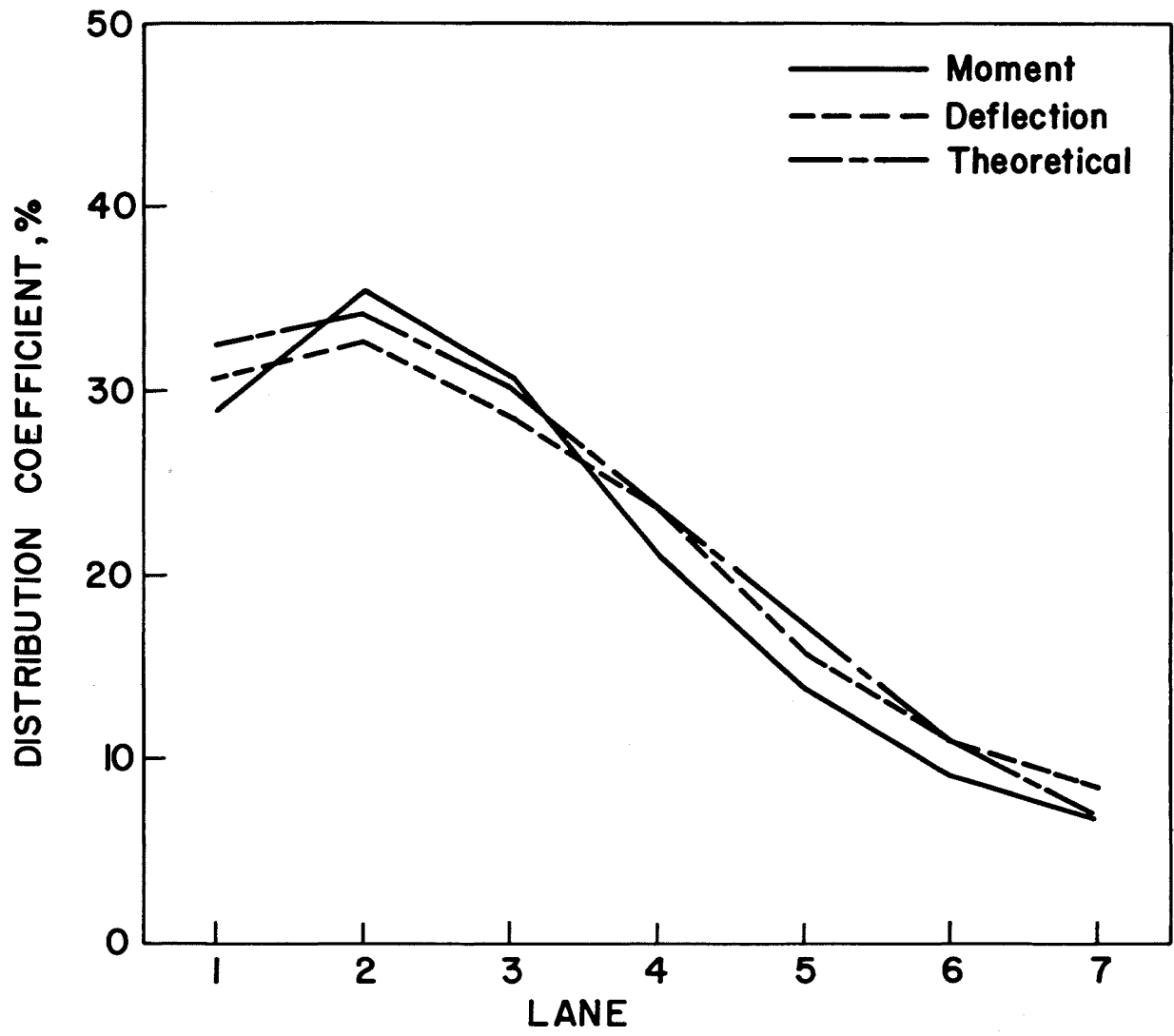


Fig. 43 Comparison of Test Results and Guyon-Massonnet Theory - Influence Line for Distribution Coefficients, Beam B, Without Diaphragms

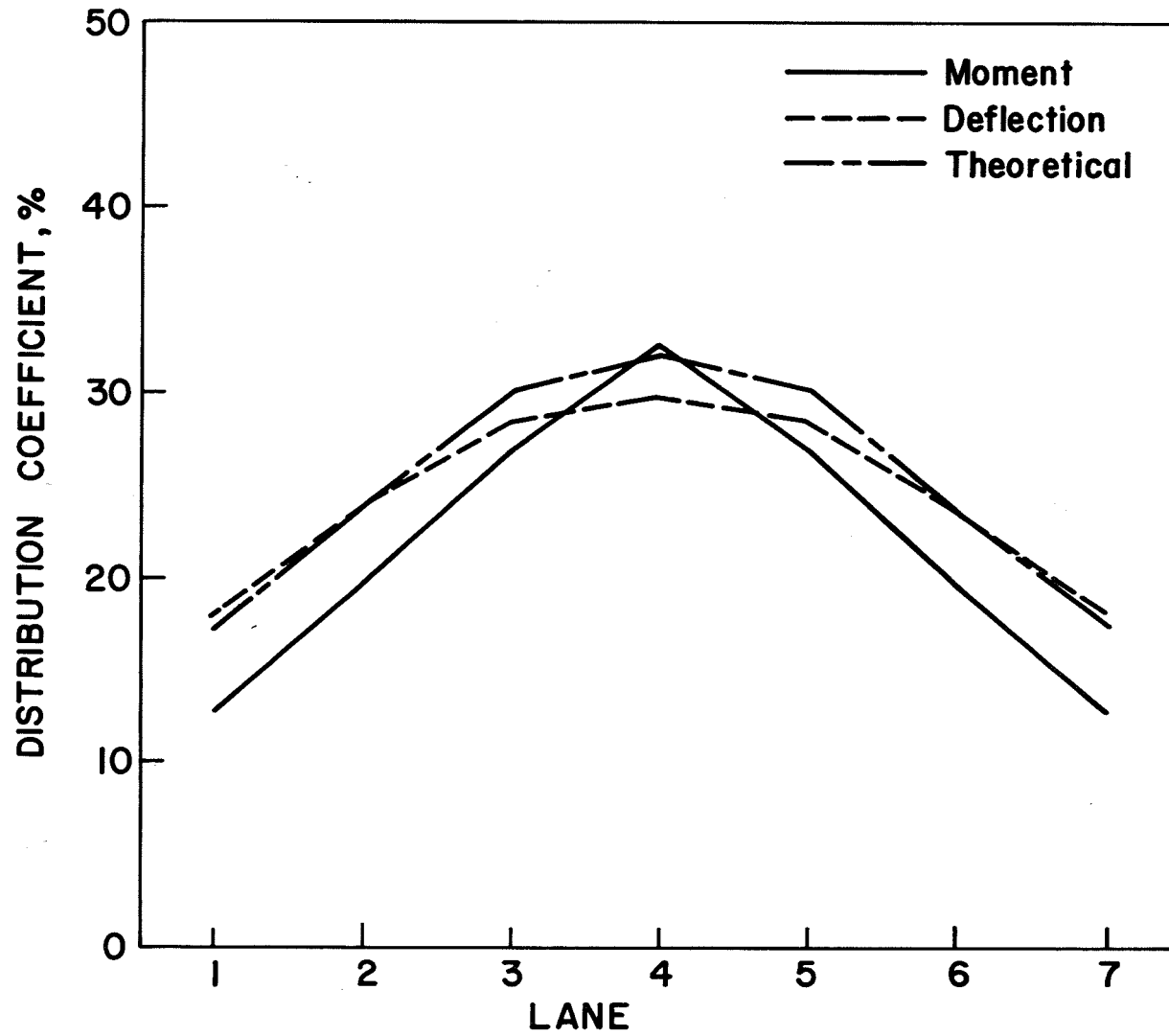


Fig. 44 Comparison of Test Results and Guyon-Massonnet Theory - Influence Line for Distribution Coefficients, Beam C, Without Diaphragms

11. REFERENCES

1. Pennsylvania Department of Highways, Bridge Division
STANDARDS FOR PRESTRESSED CONCRETE BRIDGES, 1960
2. American Association of State Highway Officials
STANDARD SPECIFICATIONS FOR HIGHWAY BRIDGES,
Washington, D. C., 1961
3. Douglas, W. J. and VanHorn, D. A.
LATERAL DISTRIBUTION OF STATIC LOADS IN A PRESTRESSED
CONCRETE BOX-BEAM BRIDGE, Fritz Engineering Laboratory
Report 315.1, August 1966
4. Guilford, A. A. and VanHorn, D. A.
LATERAL DISTRIBUTION OF DYNAMIC LOADS IN A PRESTRESSED
CONCRETE BOX-BEAM BRIDGE - DREHERSVILLE BRIDGE, Fritz
Engineering Laboratory Report 315.2, February 1967
5. Guilford, A. A. and VanHorn, D. A.
LATERAL DISTRIBUTION OF VEHICULAR LOADS IN A PRE-
STRESSED CONCRETE BOX-BEAM BRIDGE - BERWICK BRIDGE,
Fritz Engineering Laboratory Report 315.4, October
1967
6. Schaffer, T. and VanHorn, D. A.
STRUCTURAL RESPONSE OF A 45° SKEW PRESTRESSED CON-
CRETE BOX-GIRDER HIGHWAY BRIDGE SUBJECTED TO VEHICULAR
LOADING - BROOKVILLE BRIDGE, Fritz Engineering Labora-
tory Report 315.5, October 1967
7. Rowe, R. E.
CONCRETE BRIDGE DESIGN, John Wiley and Sons, Inc.,
1962
8. Rowe, R. E.
SUPPLEMENT TO CONCRETE BRIDGE DESIGN, John Wiley and
Sons, Inc., 1962
9. Mattock, A. H. and Kaar, P. H.
PRECAST-PRESTRESSED CONCRETE BRIDGES, 6. Tests of
Half-Scale Highway Bridge Continuous Over Two Spans,
Journal of the PCA Research and Development Labora-
tory, Vol. 3, No. 3, September 1961

10. Guyon, M. Y.
CALCUL DES PONTS LARGE A POUTRES MULTIPLES SOLIDARISES
PAR DES ENTRETOISES, Annales des Ponts et Chaussees,
Paris, September-October 1946
11. Massonnet, C.
METHODE DE CALCUL DES PONTS A POUTRES MULTIPLES TENANT
COMPTE DE LEUR RESISTANCE A LA TORSION, Publications,
International Association for Bridge and Structural
Engineering, Zurich 10, 1950
12. Massonnet, C.
CONTRIBUTION AU CALCUL DES PONTS A POUTRES MULTIPLES,
Annales des Travaux Publics de Belgique, June, October,
and December 1950